9-2003

Kinetic and Analytical Studies on Catalytic and Noncatalytic Oxidative Degradation of Some Hazardous Organic Dyes Using Hydrogen Peroxide

Salem Hmoud Salem Al-Ameri

United Arab Emirates University
Faculty of Science

Kinetic and Analytical Studies on Catalytic and Noncatalytic Oxidative Degradation of some Hazardous Organic Dyes using Hydrogen Peroxide

M. Sc. Thesis

Submitted to

Faculty of Science
United Arab Emirates University

In Partial fulfillment
for the degree of

Master in Environmental Science

By

Salem Hmoud Salem Al-Ameri
B. Sc. Science (Chemistry)
U.A.E University (1992)

September 2003

United Arab Emirates University
Faculty of Science
Department of Chemistry

Title:
Kinetic and Analytical Studies on Catalytic and Noncatalytic Oxidative Degradation of some Hazardous Organic Dyes using Hydrogen Peroxide

Name: **Salem Hmoud Salem Al-Ameri**

Supervisors

Name	Position	Signature
Principal Supervisor **Dr. Alaa Eldin Salem.**	Associate Prof. of Analytical Chemist Chemistry Department, Faculty of Science, UAEU	
Co supervisors **1. Dr. Ibrahim Salem**	Associate Prof. of Physical Chemistry Chemistry Department, Faculty of Science, UAEU	
2. Dr. Ihsan Shehada	Assistant Prof. of Physical Chemistry Chemistry Department, Faculty of Science, UAEU	

The Thesis of Salem Hmoud Salem Al- Ameri for the Degree of Master of Science in Environmental is approved.

.....

Examining Committee Member, Dr. Alaa Eldin Salem

.....

Examining Committee Member, Prof. Fathy Alamri

.....

Examining Committee Member, Prof. Mary Jo Ondrechen

.....

Dean of the Graduate Studies, Dr. Hadef Rashed Al-Owais

United Arab Emirates University
2003/2004

Dedication

I humbly dedicate this dissertation to the greatest woman in my life.

To my Mother **Obaidah Salem**, for her love, care, and prays.

Table of contents

Abstract

Dyes have become a very important part to countless modern applications. As a result of this huge consumption of dyes in manufacturing processes, huge amounts of wastewater contaminated with dyes are released into different natural dumps like rivers and seas. These dyes contaminated wastes have dangerous impacts on the environment and toxic affects. Tw

this environmental task. First, dyes vary in their chemical and physical natures and different waste treatments are needed which sometime are not available. Second, getting rid of these pollutants from its sources is costly, that many manufactures can not afford. As a result, solving these two problems is a hot area for environmental researches.

Different approaches to deal with dyes pollutants have been applied. One of these approaches is the chemical treatment of dyes using the bleaching and oxidation power of hydrogen peroxide. H_2O_2 was used to degrade many organic dyes especially in the presence of some metal ions like Fe^{+2} or Cu^{+2}. This method is effective, has safe clearance outcomes and economically cheap in addition to the availability of its primary materials worldwide.

In this work, two commonly used dyes by many manufacturers haves been chosen for investigation. These are the thionine and methyl violet dyes. The aim of this study was to study the kinetics and mechanisms of catalyzed and noncatalyzed degradation of the two dyes using H_2O_2. Degradation products were identified using different analytical techniques like C, H, N analysis, IR, and HPLC. Cu^{+2} ion was used as catalyst. Due to the difficulty in identifying degradation products by analytical techniques, a computational approach to calculate the potential energy for each fragment was carried out. In the following, a brief description for each chapter of the thesis:

1. Chapter I, introduction, includes a general and updated literature survey on dyes degradation kinetics and mechanisms. Different treatment approaches were also described. An updated survey on thionine and methyl violet dyes was also given.

2. Chapter II, experimental, include a description of experimental procedures, instrumentation used, materials and reagents, preparation of the various standard and buffer solutions and finally a brief description of the computational approach used.

3. Chapter III, result and discussions. In this part the following themes have been studied and discussed.

1. Kinetics of thionine and methyl violet dyes degradation by H_2O_2 were investigated. Oxidation in presence and absence of catalysts was also studied.

2. The oxidation rate for the uncatalyzed reaction was found to increase when concentration of H_2O_2 increases until it reaches a maximum value at high concentrations of H_2O_2. In catalyzed reaction, the rate reached maximum at the beginning and started to declines with increasing concentrations of H_2O_2.

3. The oxidation rate for both uncatalyzed and catalyzed reactions is increased by increasing concentrations of methyl violet dye until high concentrations of dye and then it decreased.

4. The oxidation rates for both uncatalyzed and catalyzed reactions for both dyes increased by increasing concentrations of Cu^{+2}. Strong acceleration by adding Cu^{+2} to the reaction medium is attributed to the induction of free radicals which are highly active in attacking the organic dyes.

5. The oxidation rate for both uncatalyzed and catalyzed reactions is increased by increasing pH values and reaches maximum in pH range of 9.0 – 11.0.

6. The oxidation rate for both uncatalyzed and catalyzed reactions is increased by increasing the ionic strength of the reaction medium.

7. The oxidation rate for both uncatalyzed and catalyzed reactions was found to decrease by increasing the concentration of sodium dodecyl sulphate, SDS, even before reaching the critical micelles concentration, CMC value.

Different analytical methods have been used to identify the degradation products of the two dyes. Elemental analysis, IR, and HPLC analyses were used to identify the degradation products. But due to the difficulties of separating these products, a computerized approach to predict these compounds by predicting the most energetically favorable compounds and reaction rout have been done. The two dyes were found to possibly produce up to four products through different cracking pathways.

Acknowledgement

I would like to express my full gratitude for **Dr. Alaa Salem,** *Associate Prof. of Analytical Chemistry, UAE University,* for suggesting the problem and his continuous support and follow-up during executing the thesis. Without his continuous encouragement, during data acquisition, and thesis preparation, this work would not be possible to be shown as it is now.

I am also so grateful for **Dr. Ibrahim Salem,** *Associate Prof. of Physical Chemistry, UAE University,* for suggesting the problem, continuous support and assistance during the kinetic measurements, and in formulating the kinetic part.

I am also so grateful for Dr. **Ihsan Shihidi,** *Assistant Prof. of Physical Chemistry, UAE University,* for assistening me in preparing the computational part and in revising the introduction part. Without his assistance, some questions to be answered through this work would be still opened.

I am also so grateful for my brothers and sisters for their continuous encouragement and support.

Finally, I do greatly appreciate the helps and support of the Deanship of graduate studies and Faculty of Science, UAE University, for administrative support and lab facilities they offered me during the preparation of this thesis.

List of Figures

List of Tables:

Chapter I

1. *Introduction*

1. Introduction:

Chemical dyes are one of the most important contaminants of waste water. These dyes are produced from a wide range of industrial plants as paper mills, textile factories, food and cosmetic industries ...etc. [1, 2]. Treatment of waste water containing dyes can be monitored by observing colour disappearance of from discharged water. However, the disappearance of colour (decolourization) does not always mean that we are getting cleaner water, since decolourization of the water can occur without actual break of the complex structure of the dyes. As an example, addition of bleach to coloured waste water could decolorize water but the colourless waste could still have some organic compounds that are highly toxic like aromatic amines which are highly hazardous. Therefore, to clean wastewater, we should have ways to degrade the dye with its organic fragments. Public, local and the federal authorities regulation insist on producing colour free and organic free wastewater [2].

Because of its environmental impact, tough regulations are expected to be implemented in the coming years. The chemical and biological treatment of the wastewater is very difficult and expensive since a very wide range of chemicals will be produced by many industries. For example, dyes along with other residual chemical reagents used in processing different operations, impurities from the raw materials, hazardous materials produced during finishing process as polyvinyl alcohol, starches, surfactants, pesticides and biocides will be produced in the textile production [3].

In order to investigate processes to clear colors, the complex structure of the dyes along with their source of toxicity should be thoroughly studied. Dyes can be classified into [4, 5]:

1- Acidic dyes: water soluble anionic compounds bound to a color bearing groups as chromophoric substance of acidic functional group like carboxylic group. Addition of sulfonic group, water insoluble dye is converted water soluble compound.

2- Basic dyes: are cationic dyes where the chromophore is basic functional group such as amino group.

3- Direct dye: Sulfonic acids salts of azodye (phenylazobenzene group). They are water soluble dyes.

4- Reactive dyes: Water soluble dyes that have a high affinity to bound to wet textile through a covalent bonding.

5- Disperse dyes: Water insoluble dyes used in hydrophobic fibers. The ability of these dyes to bound to fibers are highly dependent on the pH of the solution.
6- Metal complex dyes: like chromium azomethane, copper in phthalocyanine ..etc. Because of the transition metal modify the surface chemistry between molecule and fabric, they exhibit superior light and strongly resist washing [5].

To clear out and degrade dyes with their colors from waste water, the following processes are used: Physical, electrochemical and chemical processes.

1.1 Physical processes:

Physical processes are baseed on using physical means to separate dyes before reaching the waste water without a chemical treatment. Collected dye waste is then treated or shipped to treatment plants. Membranes can be used to filter out dye molecules. Efficiency is dependent on the sizes of dye molecule and pores of the membrane. For example, the cut off molecular weight is <1000 MWCO for reversed Osmosis. Membrane modules could be modified by adding powdered activated carbon to an activated sludge unit. This is usually used in the domestic waste [6, 7].

1.2. Electrochemical processes:

These methods are widely used to treat wastewater from industries as Kraft mill, textile, and tannery. The basic principle of the electrochemical technique is to discharge an electric current through electrodes in the wastewater and hence inducing different redox chemical reactions [8]. Oxidation will occur at the anode where chlorine gas will be collected and reduction will occur at the cathode where oxygen gas will be collected. The insoluble metal of the anode will migrate into the solution and it will act as coagulating agent [9]. The production of hydrogen gas will act as an excellent floating agent where it will float to the surface carrying colloids and suspended partials to the surface. Sometimes ozone and chlorine gas are produced at the anode and they will oxidize some organics. Sometimes, a precipitate will occur due to presence of certain ions (e.g. magnesium, calcium,...) and results in increasing the pH of the wastewater. Reactions occurs during electrochemical treatment could be referred to as electro-coagulation, electro-flotation, electro-oxidation and electro-reduction [10].

It was shown that the electrochemical treatment of wastewater was successful in removing, two acid dyes, from solution, used in the carpet industry on the surface of iron electrode [11]. These dyes namely are, Acid Red 337 (azo) and Acid Blue 40 (anthraquinone). Both degradation and adsorption mechanism are contributing to removal of Acid Red 337 whereas adsorption appears to be the primary mechanism responsible for removal of Acid Blue 40. Addition of sodium meta-bisulfite was shown to enhance removal of both dyes. It was postulated that the dithionite and/or sulfoxylate radical anion that may be formed during the reduction of bisulfite is responsible for the more efficient cleavage of the azo linkage in Acid Red 337. The mechanism for enhanced removal of Acid Blue 40 by addition of meta-bisulfite is most probably due to reduction of the anthraquinone dye to a hydroquinone, which in one of its form adsorbs better to the iron solids generated in the electrochemical treatment process.

Recent studies have been done on the cathodic reduction of some important dyes such as Vat Yellow 1, Acid Red 27, Acid Yellow 9, Reactive Red 4, Reactive orange 4, and Reactive Black 5 [4, 12]. The stoichiometry of the dyestuffs reductions were studied with redox titrations using a Fe(II)-TEA complex as the reducing agent [12, 13]. Acid Red 27 was reduced to the corresponding amines at room temperature, while full reduction of Reactive Black 5 was observed at elevated temperatures [12]. In potentiostatic reduction experiments, Acid Red 27 was decolorized with an uptake of 4 electrons. Reactive Black 5 could be readily decolorized by cathodic electron transfer. The reaction proceeds via relatively stable hydrazo intermediates.

Investigations with cyclic voltammetry and galvanostatic batch electrolysis experiments indicate that the rate of decolourization with Reactive Black 5 depends somewhat on transport processes in the diffusion layer of the cathode. The absorbance of the investigated dyestuff solutions could be decreased to below 20% of the initial value. For a 50% decrease in absorbance, electrical energy of about 6 kWh m^{-3} was consumed [13].

1.3 Chemical processes:

In chemical processes, decolourization, demineralization and degradation of dyes occur by chemical reactions. Chemical treatment could be classified to coagulation, flocculation, adsorption, chlorination, reduction and bleaching with hydrogen peroxide

1.3.1 Coagulation and flocculation

The addition of a coagulant or a flocculent to dye solution has the effect of neutralizing the surface charges of suspended materials. Cationic polymers, aluminum salts and alum were commonly used [14-16]. Alum has been one of the most effective coagulants used. More recently, other aluminum salts that are more basic such as polyaluminum chloride, (PAC) and polyaluminum sulfate, (PAS) have been used and shown to be more effective in dye water treatment than alum and aluminum sulfate [17, 18]. The coagulation of the four reactive dyes: turquoise DG, red DB-8, orange OGR and black DN using PAC revealed dye removal dependent on pH and dosage of coagulant [17, 18]. The highest degree of color removal was obtained for turquoise DG in both acid and neutral media. For the other three dyes, the order of efficiency was pH dependent [17]. The amount organic substances that were removed (measured by the reduction in chemical oxygen demand (COD) did not exceed 75% regardless of sample pH [18].

1.3.2. Reduction

Water soluble dyes were reduced chemically by a variety of reducing agents such as dithionite, formamidinesulfinic acid (FAS), tin chloride, iron(II)-triethanolamine and either hydrosulfite or bisulfite --catalyzed borohydride [19, 20]. However, sodiumborohydride which is one of the strongest water-soluble reducing agents has not been extensively employed in dye wastewater decolorization due to its rapid reaction with water at pH ≤ 8.0 and its tendency to be reduced via a hydride transfer mechanistic pathway.

$$BH_4^- + 8\,OH^- \rightarrow B(OH)_4^- + 4\,H_2O + 8\,e^- \quad E^o 298 = 1.24V$$

$$BH_4^- + 3H_2O + H^+ \rightarrow B(OH)_3 + 4H_2\uparrow$$

$$\Delta F^o{}_{298} = -88.8 kcal/mol \quad BH_4^-$$

This drawbacks have been overcome by employing hydrosulfite in conjunction with borohydride. The latter rapidly reduces hydrosulfite to dithionite in pH range of 5-8

$$BH_4^+ + 8\,HSO_3^- + H^+ \xrightarrow{pH\,5-8} 4\,S_2O_4^{2-} + B(OH)_3 + 5\,H_2O$$

Although the exact mechanism of this reaction was not well confirmed, it is believed that both [BH_5] and [$SO_2^{-\bullet}$] are the likely intermediates: [19-20].

$$BH_4^- + H^+ \rightarrow [BH_5]$$

$$[BH_5] + 8HSO_3^- \rightarrow 8[SO_2^{-\bullet}] + B(OH)_3 + 5H_2O$$

The $[SO_2^{-\bullet}]$ radical anion is also a very strong single electron reducing agent whose oxidation product is hydrosulfite;

$$[SO_2^{-\bullet}] + H_2O \rightarrow HSO_3^- + H^+ + e^-$$

Therefore, the overall borohydride- hydrosulfite chemistry can be viewed as involving hydrosulfite as a catalyst:

$$BH_4^- + 8HSO_3^- + H^+ \rightarrow 8[SO_2^{-\bullet}] + B(OH)_3 + 5H_2O$$

$$8[SO_2^{-\bullet}] + 2R_1R_2Ar{=}NArR_3R_4 + 4H^+ + 8H_2O \rightarrow 8HSO_3^- + 2R_1R_2ArNH_3^+ + 2R_3R_4ArNH_3^+$$

$$BH_4^- + 2R_1R_2Ar{=}NArR_3R_4 + 5H^+ + 3H_2O \xrightarrow{\text{bisulfit,pH=6}} 2R_1R_2ArNH_3^+ + 2R_3R_4ArNH_3^+ + B(OH)_3$$

On the other hand, it has been found that sodium bisulfite can also catalyzes borohydride reduction. In case of copper-metallized dyes, reduction was achieved by a bisulfite-catalyzed borohydride treatment.

In a field study, industrial effluents containing a mixture of azodyes were treated using a bisulfite – catalyzed borohydride reduction followed by precipitation with a cationic coagulant. Where more than 90% of color reduction was possible. In these field studies, effective treatment was achieved at pH 5-6 with preaddition of bisulfite (ca. 200-500 mg $Na_2S_2O_3$/L) followed by addition of a caustic solution of sodium borohydride. The borohydride solution was then added to slight excess relative to the requirements of the dye solution [19].

An improved method of treatment employing sodium bisulfite catalyzed sodium borohydride with a cationic agent has been reported by Cook, et al [21]. Another improved method employing flocculation with a cationic polymer followed by treatment with sodium hydrosulfite reducing agent was been patented by Weber [16]. Several problems associated with all previous methods. These are:

a- Large volumes of solids are produced.

b- The floc produced settles slowly.

c- The effluent from some types of treatments still retains a yellow color resulting in staining of the cloth when the water is reused in dyeing.

The need to recycle makes the yellow color undesirable or unacceptable while the large volumes of solids produced create their own disposal problems and slow settling of solids create the need to have very large and expensive settling basins. Most of these problems have been resolved, by Sheppered et al. [14], using a multi-step process for decolorizing dye-waste effluent. The process can be summarized as follows

a- treating the effluent with a sodium hydrosulfite at a concentration of 50-100 ppm of a reducing agent per 1000 ADMI units of color.

b- reducing the pH of the liquid effluent to a value in the range of 2.0-7.0

c- treating the liquid effluent with a coagulant to neutralize the surface

d- charge on suspended materials, wherein said neutralization mixture comprises in a ratio of 30-70 to 70-30 percent by weight (i:ii):

(i) at least one aluminum salt selected from the group consisting of aluminum hydroxy-chloride, aluminum polyhydroxychloride, alum, aluminum chloride, and sodium aluminate; and

(ii) a cationic polymer selected from the group consisting of: (A) at least one water soluble cationic polymer selected from the group consisting of (A) a copolymer of acrylamide with a cationic monomer such as methacryloylethyltrimethyl ammonium[X^-].or acryloylethyltrimethyl-ammonium[X^-], where X^- is selected from the group consisting of chloride, bromide, iodide, SO_4^{2-} . and $CH_3SO_4^{2-}$; (B) polyamines of Formula I or (C) poly quaternary ammonium compounds of Formula II:

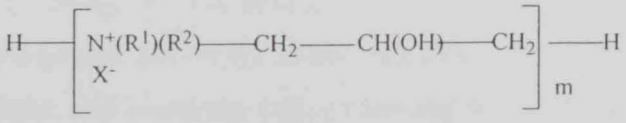

Formula I

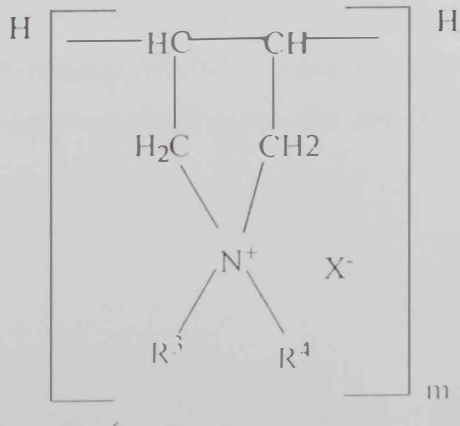

Formula II

e- adjusting the pH of a mixture thus formed to be ≥ 5.0

(e) subjecting the mixture to a flocculating process by adding from 1-5 ppm of at least one compound selected from the group consisting of:

(i) anionic polymers selected from the group consisting of acrylic acid/acrylamide copolymers in excess of 2 million molecular weight; and

(ii) nonionic polymers selected from the group consisting of polyacrylamides greater than 2 million molecular weight;

this will bind the flocs formed in step c into large, dense, easily-settled particles. This prescribed procedure reduced the colored effluent efficiently and also reduced its final flocculation volume [14].

Decolourization of 20 selected azodyes by granular sludge containing sulfide was reported [22]. All azodyes tested, were completely reduced yielding colorless products. Although all reactions followed first-order kinetics, reaction rates varied greatly between dyes. Half-life times resulted ranged from 1 - 100 h. The slowest reaction rate found for reactive dyes with triazine reactive groups. No correlation obtained between a dye's half-life time and its molecular weights, indicating that cell penetration was probably not an important factor. Since granular sludge contains sulphide, eight dyes were also monitored for direct chemical decolorization by sulphide. All these dyes were reduced chemically albeit at slower rates than in the presence of sludge at comparable sulphide levels. Increasing sulphide concentrations, was shown to stimulate the azo reduction rate.

Nicotinamide adenine dinucleotide, NADH, has been found to reduce a variety of azodyes by four electrons to generate the corresponding aromatic amines [23]. These dyes are Orange I, Orange II, 4-hydroxybenzene, Alura red, Sunset yellow FCF, 4-(4-sulfophenyaazo)-phenol and 2-(4-sulfophenyaazo)-phenol derivatives. The reduction is a pH dependent and increased with increasing pH. Reduction of 4-(4-sulfophenyaazo)-phenol and 2-(4-sulfophenyaazo)-phenol, specifically substituted with methyl, methoxy, halo, and nitro groups, was studied to determine the susceptibility of azodyes to reduction by NADH. Except for the nitro- substituted azodyes , all other azodyes were reduced. NADH is highly selective and its selectivity toward the dye reduction is strongly dependent on the dye structure [23].

The reduction of azodyes by zero-valent iron metal (Fe-0) at pH 7.0 was studied in aqueous, anaerobic batch systems [24]. Orange II was reduced by cleavage of the azo linkage, as evidenced by the production of sulfanilic acid (a substituted aniline). Adsorption of the dyes on iron particles was less than 4% of the initial concentration, and > 90% mass balance was achieved by summing aqueous concentrations of dye and product amine. All of the azodyes tested were reduced with first-order kinetics. Correlation analysis using k_{obs} for all of the azodyes, estimates of their diffusion coefficients, and calculated energies of their lowest unoccupied molecular orbitals (E-LUMO), gave no strong trends that could be used to derive structure-activity relationships [25-27].

1.3. 3. Adsorption

Adsorption is an effective method for lowering concentration of dissolved organics in effluents. Many adsorbents were used for adsorbing different classes of dyes [19, 28-52]. These adsorbents comprise activated carbon [19, 28-32, 34-36, 53], bone char [28], clays [37-39], alumina [40, 41], silica [42, 43], silica gel [44], natural sediment [54, 55], Fullerene C-60 hydrosol [47], chitosan beads [48], polymers [49], bagasse pith [50], rice husk ash [51], coir pith [52], magnesium hydroxide [56] and iron oxides [57]. Of these, activated carbon has been evaluated extensively for the waste treatment of the different classes of dyes, that is, acid, direct, basic, reactive, disperse and so forth [19, 28-31, 34, 36, 53].

Commercial activated carbon prepared from lignite and bituminous coal, wood, pulp mill residue, coconut shell and blood, have a surface area ranging from 500-1400 m^2/g. The feasibility of adsorption on carbon for the removal of dyes has been demonstrated by adsorption isotherms. For a group of basic and disperse dyes, it was shown that dyes of the same application class exhibit similar adsorption characteristics. However, within each class, differences in chemical structures (e.g. oxazine, methine, thiazine, azo, or anthraquinone) influence the affinity of specific dyes for the activated carbon. In case of basic dyes, the relative affinity was correlated to the basicity of dye molecules. Disperse dyes did not show much differences in adsorption properties between dyes of different chemical structures. The presence of a dye-carrier increased the adsorption efficiency of disperse yellow and disperse red 73. Higher carrier concentrations increased the solubility of disperse dye which

reduces the repulsive forces between the dye and the carbon surface, allowing adsorption to take place [19].

Anionic azodyes are not readily adsorbed by activated carbon, due to the sulfonic groups, which make the dyes water soluble and polar. Therefore, such dyes are not readily adsorbed onto the non-polar carbon surface. The dyes were first degraded (reduced), and its reduction products (aromatic amines) then adsorbed. The individual degradation products of reactive dyes have much better absorbability on carbon than the parent dyes themselves [17-19]

In general, anionic dyes adsorbability was found to be enhanced by increasing molecular size and aromaticity, and by decreasing solubility, polarity and carbon chain branching. Dyes of high molecular weight are adsorbed into the transitional pores of an activated carbon, whereas smaller molecular weight dyes penetrate into the micro pores. Besides temperature, pH, contact time and carbon dosage, the choice of the type of carbon is of a great importance. The adsorption of Acid blue 277 onto four different types of activated carbon; Calgon virgin and regenerated filtersorb F 400 (manufactured from litumous coal); Norit Darco (made from wood) and Westvaco Nuchar (made from pulb mill residue), gave maximum capacity of 36.6 mg/g for virgin Calcon F400, 58.0 mg/g for regenerated carbon F400 , 93.0 mg/g for Nuchar and 117 mg/g for Norit Darco. The fact that Acid blue 277 is better adsorbed onto regenerated carbon rather than virgin one was ascribed to the reduced surface area of the micro pores as a result of thermal regeneration. This will prevent the penetration of relatively large molecules (Acid blue 277 has a molecular weight of 546) [20, 27].

In more recent studies, the removal of acid dyes, Tectilon Blue 4R,-Tectilon Red 2B and Tectilon Orange 3G, from single solute, bisolute and trisolute solutions by adsorption on activated carbon (GAC F400) and from single solute onto bone char have been investigated in isotherm experiments [28, 32]. It was found that the activated carbon had a much higher specific surface than the bone char. Calculations involving the pore size distribution data indicate that only 14% of the total specific surface of the activated carbon is available for adsorption due to the high molecular area and aggregation of the dye. The equilibrium data indicate that dye aggregation takes place in the solid phase of both adsorbents with higher solid phase aggregation numbers found using the bone char, which is indicative of multilayer adsorption [28].

Experimental results were modeled using the Langmuir and Freundlich adsorption isotherm theories with the Langmuir model proving to be the more suitable. The Ideal Adsorbed Solution (IAS) model was coupled with the Langmuir isotherm to predict binary adsorption on the dyes [32]. A similar study was performed using granular activated carbon filtrasorb 400 to treat a ternary solution of acid dyes and the process plant dye-effluent from a nylon carpet printing plant in a fixed-bed column system and the results were compared with a single dye adsorption [36]. The adsorption capacity, in milligrams of adsorbate per gram of adsorbent, decreased by 12-25% in the ternary system compared to the single component system. This reduction has been attributed to competitive adsorption occurring in the ternary component system. Dye adsorption from a process plant effluent showed approximately 65% decrease in adsorption capacity compared to the ternary solution system. A chemical oxygen demand analysis on these components indicated that the dyes accounted for only 14% of the total oxygen demand [36].

The adsorption of 23 organic molecules, including a number of polyaromatic dyes, from aqueous solution to kaolinite and amorphous alumina was investigated at pH 9 [40]. Strong preferential adsorption to kaolinite was observed over the whole pH range, and at pH 9 the dyes also adsorbed much more to kaolinite than to gibbsite or silica. The basal spacing of kaolinite crystals, measured by X-ray diffraction, did not change when 3,6-diaminoacridine was adsorbed, indicating that the dye molecules were not intercalated between the crystalline layers. It is suggested that the negatively charged, flat silica faces of kaolinite crystals may serve as templates for pi-stacking association of the positively-charged polyaromatic molecules [55].

The equilibria and kinetics of the sorption of fluorescein and sulforhodamine B fluorescent dyes were investigated with two oppositely charged, consolidated aquifer materials by sandstone and limestone [55]. Magnesium hydroxide, on the other hand, was found to be an active adsorbent for acid, direct and basic dyes [56]. However, magnesium hydroxide precipitated from aqueous solution of magnesium sulfate was much better than that from magnesium chloride. It was also demonstrated thermodynamically that, acid and direct dyes were readily adsorbed onto magnesium hydroxide rather than basic dyes [56].

Extensive work was done on the adsorption of azodyes (Orange II, Orange I, and Orange G) on α-Fe_2O_3 and α-FeOOH has been carried out [57]. Adsorption of

azodye was less favored when the sulfonic groups were on the naphthalene ring in Orange G, suggesting an inner sphere mechanism of complex formation between the dye and α-Fe_2O_3 [57]. The crystalline face of the oxide and the appropriate metal-metal atomic distance rather than the density of surface sites (surface area) seem to control the extent of the adsorption. The adsorption of Orange II was found to be decreased with increasing solution pH.

Modeling of the adsorption processes was carried out taking into account the number of adsorption sites, the equilibrium constants, and the surface area of different azodyes. The most favorable condition for adsorption was the closest matching of the M-M atomic distance of the oxide to the O-O bond distance in the sulfonic group: -O-S-(O-O) of Orange II. This explained why Orange II showed a higher adsorption on α-Fe_2O_3 than on α-FeOOH and Al_2O_3. The adsorption of Orange II was unaffected by the presence of chloride or nitrate anions. However, the adsorption of the same dye decreased dramatically when sulfate or sulfite anions were added in solution along with the azodye. This indicates the competitive nature of these anions with dye during adsorption process, suggesting that the sulfonic group of Orange II is the binding site for this dye on α-Fe_2O_3 and α-FeOOH. Fig. 1a the formation of dye-bidentate bridging complex with α-Fe_2O_3, (Fig. 1b) is the most probable adsorption mechanism. However, the ligand exchange with α-FeOOH led to the possibility of unidentate complex formation (Fig. 1c) [57, 58]

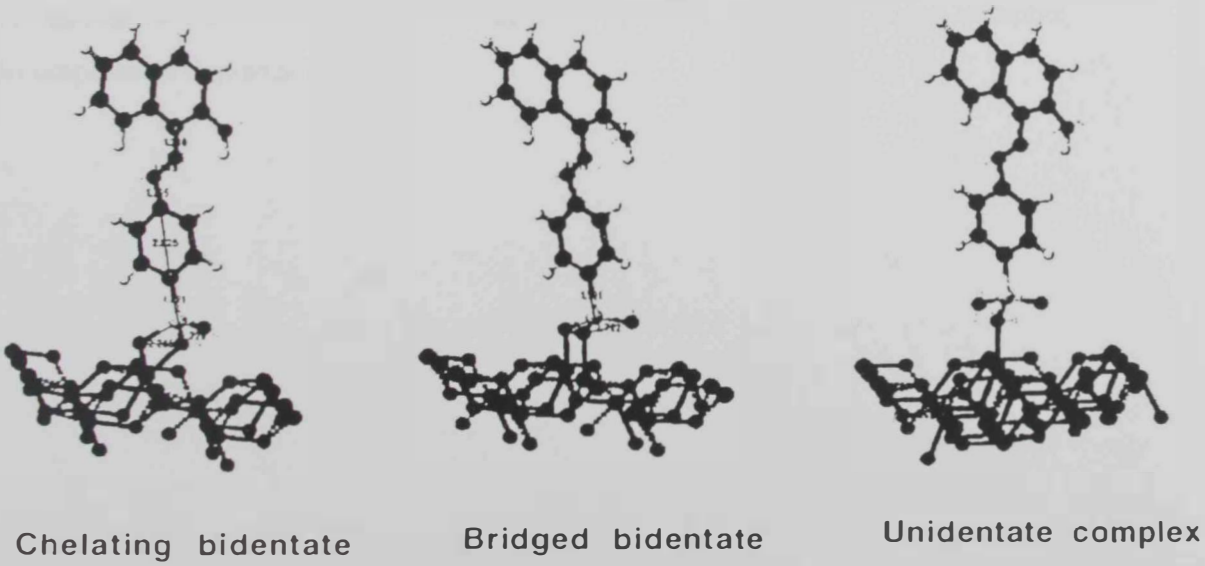

Figure 1.1. The molecular structure of chelating bidentate (a), bridged bidentate (b) and the unidentate (c) complexes.

1.3.4 Bleaching with hydrogen peroxide

Hydrogen peroxide, and other peroxy compounds which yield hydrogen peroxide in aqueous solution, have been used in fabric and surface bleaching. However, peroxy compounds, such as sodium perborate (monohydrate or tetrahydrate), sodium percarbonate, and the like, have relatively mild bleaching performance at low temperatures (below 100°C) [58].

Transition metal chelates, especially manganese and iron, were used as bleaching catalysts for peroxy compounds [58-61]. These transition metal chelates can be used, for example, in laundering fabrics with an appropriate peroxy compound, for example, sodium perborate monohydrate. Transition metal chelates improve the oxidizing power of peroxy compounds, they sometimes damage fabrics when used as bleaching activators.

Macrocyclic tetraamido ligands [62] has been used as novel and unusually effective bleach activators for peroxy compounds. Additionally, it has not been taught, disclosed or suggested that these types of compounds will be unusually advantageous in the areas of dye transfer inhibition, anti-soil redeposition and stain removal. Collins et al [63, 64] have used an oxidative stable bleach activator, macrocyclic tetraamido compounds, having the structure below in conjunction with an effective amount of a source of peroxy compound [63, 64].

These compounds form robust, long-lived oxidation catalysts. Robust oxidation catalyst means that when the catalyst is added to a solvent in the presence of an oxidant, such as a peroxide, the half-life of the activated form of the metal complex is 30 seconds or more. The half-life is the time in which half of the metal complex decomposes or degrades [63].

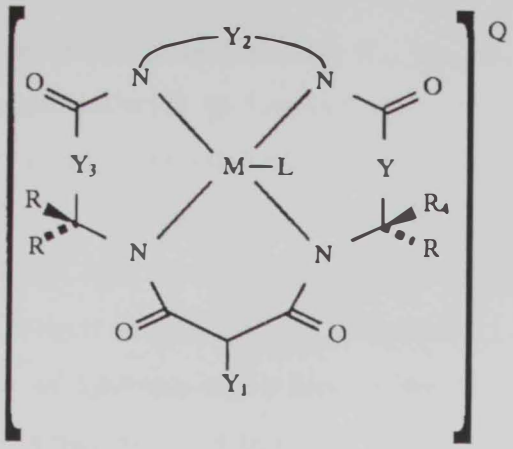

Figure 1.2: Molecular structure of the tetraamido compound

Y_1, Y_2, Y_3 and Y_4 represent a bridging groups. R = H, alkyl, cycloalkyl, cycloalkenyl, alkenyl, aryl, alkynyl, alklaryl, halogen, alkoxy, phenoxy, CH_2CF_3, or CF_3. M is a transition metal with oxidation state of I, II, III, IV, V, or VI. Q counterion balances the charge of the compound (generally, negative; preferably -1) on a stoichiometric basis. L labile ligand which can attach to M.

Peroxy compound can be an organic or inorganic compound containing the --O--O-- peroxide linkage. include hydrogen peroxide, hydrogen peroxide adducts, compounds capable of producing hydrogen peroxide in aqueous solution, organic peroxides, persulfates, perphosphates, and persilicates. Hydrogen peroxide adducts include alkali metal (e.g., sodium, lithium, potassium) carbonate peroxyhydrate and urea peroxide. Compounds capable of producing hydrogen peroxide in aqueous solution include alkali metal (sodium, potassium, lithium) perborate (mono- and tetrahydrate).

Alternatively, an alcohol oxidase enzyme and its appropriate alcohol substrate can be used as a hydrogen peroxide source. Organic peroxides examples include benzoyl and cumene hydroperoxides. An effective amount of peroxy compound is an amount sufficient to generate at least 0.001 ppb active oxygen (A.O.) [64].

These macrocyclic tetraamido complexes were used effectively as activators in bleaching of dyes, dye transfer inhibition, and in stain removal. The macrocyclic tetraamido complexes possess superior dye transfer inhibitory (DTI) performance, compared to polyvinyl pyrrolidone, a known effective DTI compound. Collin et al., found that tetraamide complexes in conjunction with hydrogen peroxide are able to oxidize and degrade trichlorophenol effectively [65].

Manganese complexes with the general formula $[L_n Mn_m X_p]^z Y_q$ were used as bleach catalysts with hydrogen peroxide to remove stain from clothes [66]. In mixtures thereof and wherein n and m are independent integers from 1-4; X represents a coordinating or bridging species, such as H_2O, OH^-, O_2, S^{2-}, N^{3-}, HOO^-, O_2^{2-}, O_2^{1-}, $R-COO^-$, with R being H, alkyl, aryl, optionally substituted Cl^-, SCN^-, N_3^- etc. or a combination thereof; p is an integer from 0-12; Y is a counter-ion, the type of which is dependent on the charge z of the complex; z denotes the charge of the complex which can be positive, zero or negative. If z is positive, Y is an anion, such as Cl^-, Br^-, I^-, NO_3^-, ClO_4^-, NCS^-, PF_6^-, RSO_4^-, OAc^-, BPh_4^-, $CF_3SO_3^-$, RSO_3^-, RSO_3^-, etc. If z is negative, Y is a cation, such as an alkali metal, alkaline earth metal or (alkyl) ammonium cation and L is a ligand being a macrocyclic organic molecule [66]

A preferred commercial example is manganese complex (IV) with 1,4,7-trimethyl-1,4,7-triazacyclononane, (abbreviated as Me_3TACN), namely $[Mn^{IV}(\mu\text{-}O)_6(Me_3TACN)_2](PF_6)_2$. This complex in conjunction was very efficient in removing stain (tea, fruits and win) from clothes. However, the addition of MnO_2 generally causes the enhancement of bleach activity of Me_3TACN, but the extent of enhancement greatly depends on the amount of manganese dioxide added in bleach experiment. The bleach activity reaches the highest value, when the ratio of Me_3TACN to MnO_2 ranges from 1:25 to 1:39. More MnO_2 results in the decline of bleach activity, but it still reveals a significantly higher bleach activity than Me_3TACN alone. On the other hand, soluble manganese salts such as $MnSO_4$, $MnCl_2$, $Mn(NO_3)_2$ and $Mn(OAc)_2$ in 1:1 ratio reduce the bleach activity of Me_3TACN. When $MnCl_2$, $Mn(NO_3)_2$ and $Mn(OAc)_2$ are used, the bleach activity dramatically decreases. Also, the results indicated that Fe_2O_3, Fe_3O_4, $Fe(OH)_3$, Cu_2O, CuO, $Cu(OH)_2$ and CeO_2 do not give enhanced bleaching activity with Me_3TACN [66].

1. 4. Aim of the present work

The aim of this work is to study the chemical kinetics of degradation process of Methyl violet and thionine dyes using H_2O_2 in the presence and the absence of Cu^{2+} as catalyst. The rate laws and degradation mechanisms will be evaluated and inferred. Structure of the proposed intermediate compounds will be investigated spectroscopically using, C , H , N analysis, HPLC and IR, analyzing methods. A computational approach will be adopted to confirm degradation mechanism of the dye and to show the probable intermediates by calculating total energy of different expected fragments.

Chapter II

2. *Experimental*

2. Experimental

2.1 Materials and Reagents

Different concentrations of hydrogen peroxide solutions, different buffer values made from 0.1M Na_2HPO_4 and 0.1M KH_2PO_4, thionine dye, methyl violet dye, different concentration of $CuSO_4$, 5% KI, ammonium molybdate solution, H_2SO4 solution, $Na_2S_2O_3$ solution, starch drops were used. All chemicals used were of analytical reagent grade. H_2O_2 solutions were prepared by direct dilution and were standardized iodometrically using sodium thiosulphate. Phosphate buffer (KH_2PO_4 + Na_2HPO_4) was used throughout for adjusting the pHs.

2. 2 Apparatus

UV-VIS. spectrophotometic measurements were recorded on a Shimadzu 2101 PC UV-VIS. Spectrometer supplied with Shimadzu data acquisition system. The pH measurements were made on a Mettler Delta 320 pH-meter. The UV/vis. For identifying degradation products, an HPLC, WATER ALLIANCE, Model 2695 with UV-VIS detector Model 486 and software package Millenium 32, USA, was used. The column used was C18 with internal diameter of 4 mm, length of 150 mm and the particle size was 4 μm. For IR measurements , DTGS KBr was used as a detector and the beamsplitter was KBr.

2. 3 standard solutions

2. 3. 1 Standard sodium thiosulphate solution

0.5 M sodium thiosulphate was prepared by dissolving 24.8 g into 1000 ml CO_2-free doubly distilled water. Few drops of chloroform were added. The thiosulphate solution was standardised against 5% standard potassium iodate solution [67].

2. 3. 2 Standard hydrogen peroxide solution

Stock 30% hydrogen peroxide solution (purchased from Merk, Schuchardt, München, Germany) was used. Several initial concentrations of the hydrogen peroxide solutions were obtained by mixing definite volumes of standard (freshly prepared) stock solution of hydrogen peroxide with doubly distilled H_2O. The initial concentration of hydrogen peroxide was determined by transferring the diluted

hydrogen peroxide solution to a conical flask and adding 50 ml of H_2SO_4 (1M) followed by 5 ml of 30% potassium iodide solution and 3 drops of 3% ammonium molybdate solution. The liberated iodine (equivalent to hydrogen peroxide concentration) was titrated immediately with a standard sodium thiosulphate solution [67]. No thermal decomposition occured for H_2O_2 solution within the concerned concentrations in the temperature range 30-45°C.

2. 3. 3. Standard dye solution

A 10^{-3} M thionine and methyl violet dyes solutions were prepared by dissolving 0.0263 g and 0.0394 g, respectively, into CO_2-free doubly distilled H_2O to prepare stock solution of 10^{-4} M by dilution several concentrations of both dyes. Prepared solutions were kept in dark bottles placed in refrigerators to avoid either thermal or photolytic transformations.

2. 3. 4. Standard copper (II) solution

A 0.1 M stock standard $Cu(NO_3)_2.3H_2O$ was prepared by dissolving 6.04 g in CO_2-free doubly distilled H_2O. several concentrations of copper nitrate were prepared by dilution and standardized [68].

2. 3. 5. Buffer solution

Phosphate buffers ($KH_2PO_4 + Na_2HPO_4$) having pHs of 5.0, 5.5, 6.0, 6.5, 7.0, 7.5, 8.0, 8.5, 9.0, 10.0, 10.5, 11.0 were prepared and used throughout. For attaining high pHs, few drops of sodium hydroxide solution were added [69-71].

2. 4 Procedures

2. 4. 1 Kinetic measurements

In a typical kinetic run, 1.00 mL of standard dye solution together with 1.00 mL buffer solution were placed in a thermostated quartz UV/Vis. cell. The reaction was started by injecting 1.00 mL of H_2O_2 of a known concentration and monitoring the course of reaction by observing the decay in absorbance at λ_{max} = 600 or 584 nm for thionine and methyl violet, respectively. The rate change in the initial absorbance, $(dA/dt)_o$, was determined from the slope of the first part of the absorbance-time curves. The initial rate values were obtained by dividing $(dA/dt)_o$ values over the absorbitivity of the substrate dye [69, 70, 72, 73]. ε values of 5.1×10^4 $L^1mol^{-1}cm^{-1}$ and 4.1×10^4 $L^1mol^{-1}cm^{-1}$ at λ_{max} = 600 and 584 nm for thionine and methyl violet,

respectively were used. The ionic strength was controlled by the addition of sodium chloride prior to the addition of hydrogen peroxide.

On the other hand, the kinetics of the decomposition reaction of hydrogen peroxide with copper nitrate in the absence and in the presence of t-butanol was monitored iodometrically by titrating aliquots at different time intervals. The initial reaction rates were determined from $d[H_2O_2]/dt$ versus $[H_2O_2]$ plots.

2. 4. 2 Product analysis

One experiment was carried for each dye by dissolving 2 g of thionine or methyl violet dye into 150 ml distilled water. An excess of 10 M H_2O_2 is added and the pH was adjusted with buffer to pH = 7.0. The mixture was thermostated at 35 °C. When complete color removal occurred solution was evaporated. The solid residues of the two experiments were collected and subjected to C,H,N elemental analysis, IR analyses.

2. 4. 3 HPLC Analysis

In another experiment, excess KI was added to colorless solutions to remove excess H_2O_2 in solution. Produced I_2 was removed by adding $Na_2S_2O_3$ till no blue color was produced as indicated by starch indicator. Degradation products were extracted into dichloromethane using separating funnel. Resultant oxidation products were identified using HPLC. Using polarity method HPLC machine column Mobile phases consists of 80:20 or 60: 40 water:acetonitrile were used.

2.5. Computational treatment for the products proposed by the degradation reaction of both methylene blue and Thionine

The z matrices for all products were obtained from the protein data bank files generated after molecular mechanics calculations were performed using the 3-D ChemDrawe software [74]. The steepest descent and the conjugate gradient methods were used to optimize the geometrical shape of the designed molecules[75-78]. The Hartree-Fock calculations were done by using the Guassian 98 software with Gaussian basis sets [79]. Along with the output files for all the runs are submitted in appendix 1.

CHAPTER III

3. RESULTS AND DISCUSSION

3. 1. Kinetic measurement

3. 1. 1. Absorption spectra

When thionine dye was mixed with hydrogen peroxide at pH= 7.0, the rate of reaction was very slow. However, when a small amount of copper (II) nitrate solution was added, the rate of reaction increased considerably, (Fig. 1). On the other hand, the rate of reaction with methyl violet dye in absence and presence of copper (II) ions was much faster compared to that of thionine, (Fig. 2). Since the color of both dyes decays with time, the progress of the reaction was followed by monitoring the absorbance change at λ_{max} = 600 and 584 nm for thionine and methyl violet respectively. The reaction followed a first-order dependence as indicated in the inserts in Fig. 3. 1 and Fig. 3. 2.

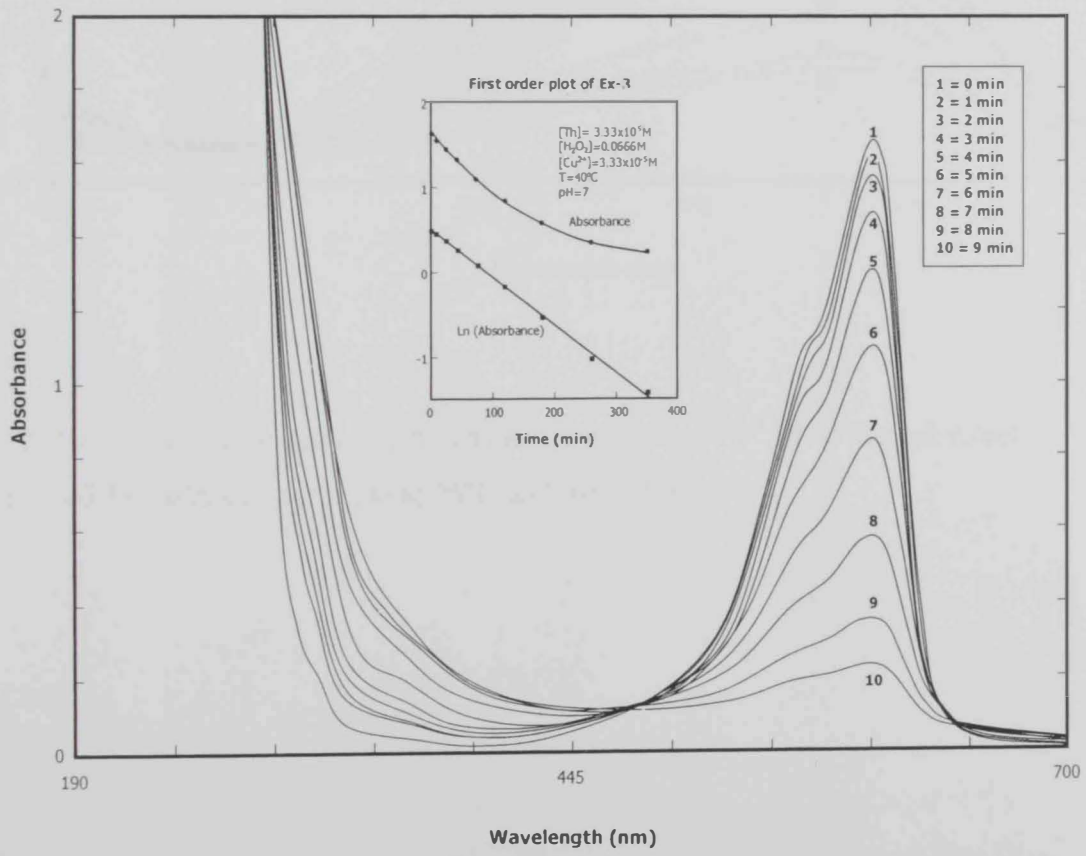

Fig. 1. Time resolved spectra for the oxidation of 3.34 x 10^{-5} M of thionine with 0.067 M hydrogen peroxide in presence of 3.34 x10^{-5} of Cu^{+2} at 40°C and pH = 7.0.

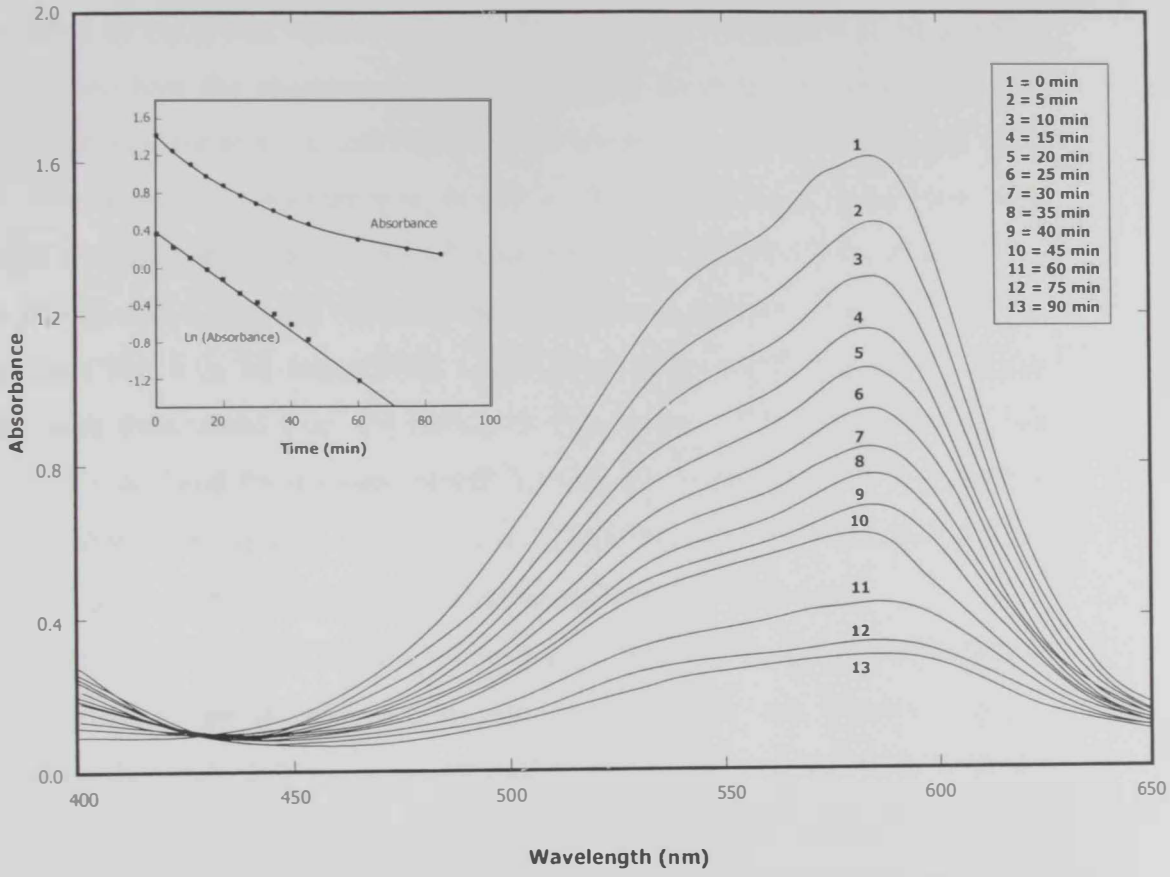

Fig. 2. Time resolved spectra for the oxidation of 3.34 x 10^{-5} M of methyl violet with 0.142 M hydrogen peroxide at 25°C and pH = 7.0.

3. 1. 2. Effect of hydrogen peroxide

The effect of hydrogen peroxide concentration on the non-catalyzed oxidation reaction rate for thionine dye was examined at 3.34 x 10^{-5} M. Constant temperature 40°C for thionine dye and 25°C for methyl violet dye at pH = 7.0 while the concentration of H_2O_2 was varied from 0.03 M to 2.493M. Figures 3 (a, b) and 4 (a, b) demonstrate how the absorbance decays with time at different concentrations of hydrogen peroxide for thionine and methyl violet respectively. [The two figures show that by increasing the concentration of H_2O_2, the rate of dyes degradation also increase]. For the copper (II)- catalyzed reactions, where cupper nitrate solution of a 3.34 x 10^{-5} M and 2.00 x 10^{-5} M was added to thionine mixture, Fig. 5 (a, b), and methyl violet Fig. 6 (a, b), respectively. The values of the initial absorbance change $(dA/dt)_0$ were determined from the curves in figures 3-6. The initial reaction rate values were calculated by dividing $(dA/dt)_0$ over the absorbitivity of dye studied. The latter values were equal to 5.1 X 10^4 $L^1mol^{-1}cm^{-1}$ at λ_{max} = 600 nm and 4.1 X 10^4 $L^1mol^{-1}cm^{-1}$ at λ_{max} = 584 nm for thionine and methyl violet respectively.

The initial rate values were then plotted versus the initial concentration of hydrogen peroxide, for thionine and methyl violet, respectively Figures 7 and 8. These figures demonstrated that in the absence of copper (II) ions, the rate of reaction increased gradually with increasing initial peroxide concentration $[H_2O_2]_0$; reaching a maximum ≥ 0.8 M and ≥ 2.0 M for thionine and methyl violet respectively. This means that the order of reaction changes from one at lower concentrations to zero at a higher ones. Similar behavior was reported earlier for the oxidation of quinoldine red dye with hydrogen peroxide [72].

For the catalyzed reactions, however, the rate of reaction increased with increasing $[H_2O_2]_0$ reaching a maximum at ≅ 0.4 and 2.0 for thionine and methyl violet respectivly and thereafter decreased. This behavior was described earlier by the formation of an intermediate species through the interaction between hydrogen peroxide and copper (II) ions [80-82]. These species, however, have an inhibiting effect on the reaction. The concentration of such species increase the inhibitory effect with the increase of the concentration of either hydrogen peroxide or copper (II) ions. However, the rate of catalyzed reactions was always higher compared to the uncatalyzed reactions. The catalyzing effect of copper (II) ions was attributed to the

formation of the highly active and non-selective hydroxyl radicals generated from the interaction of hydrogen peroxide with copper (II) ions [80-84].

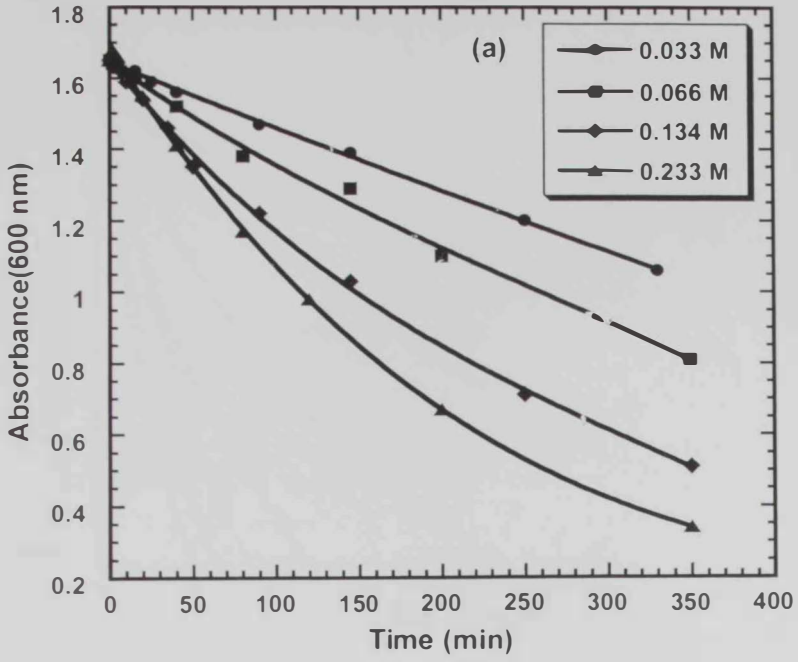

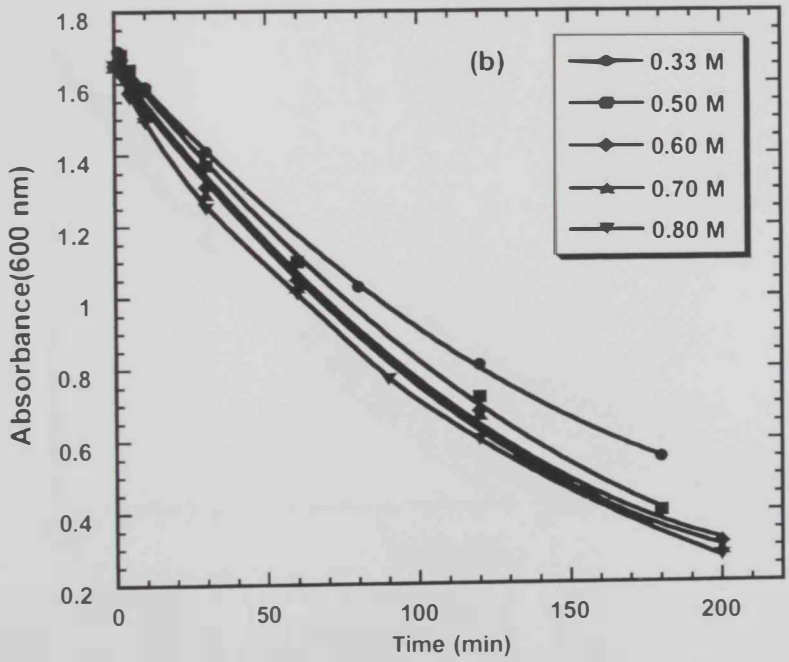

Fig. 3. 3 (a, b). Absorbance – time curves for the reaction of 3.34×10^{-5} M thionine with different concentrations of H_2O_2 at pH = 7.0 and 40°C.

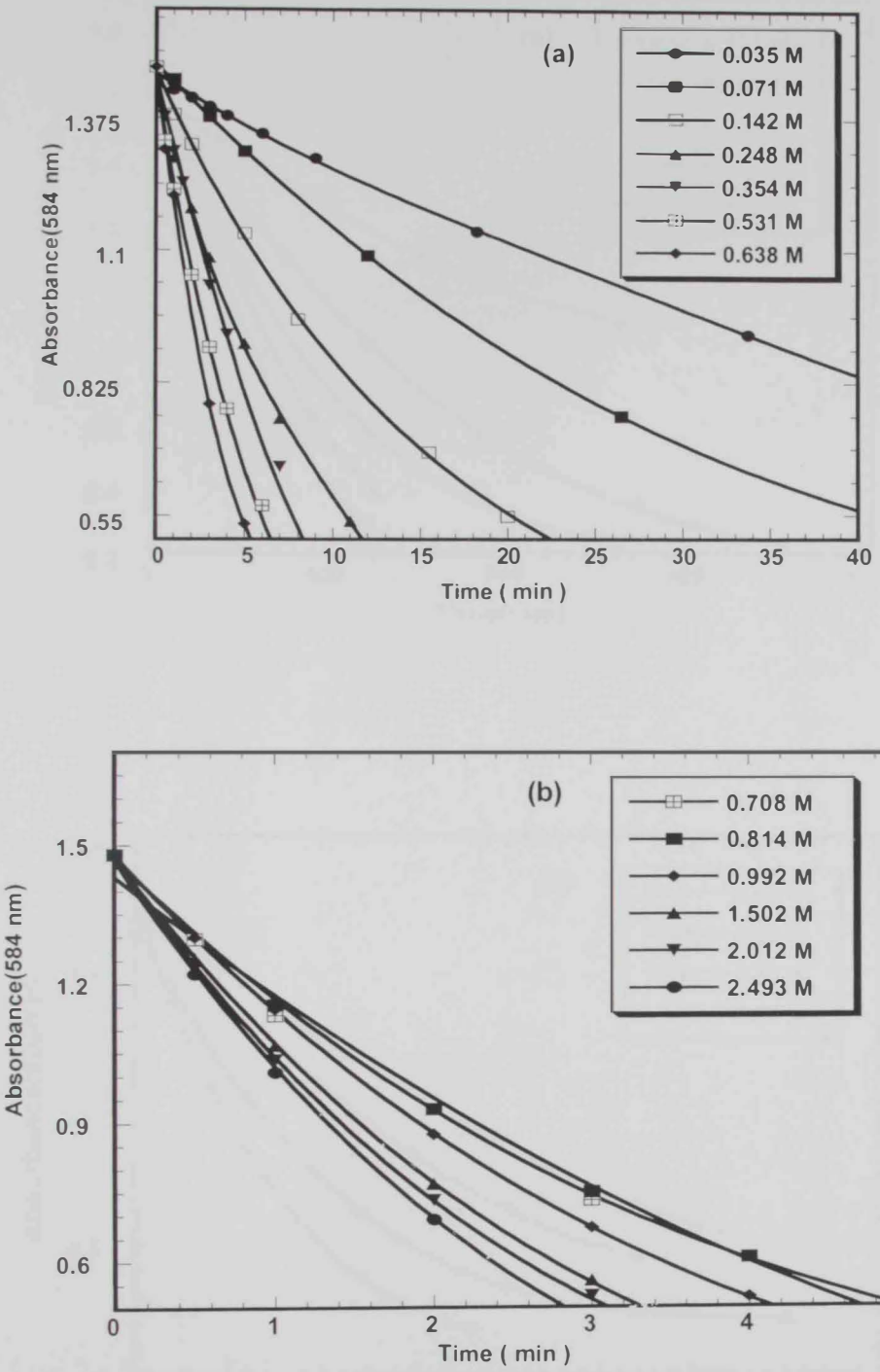

Fig. 3. 4 (a, b). Absorbance – Time curves for the reaction of 3.34×10^{-5} M methyl violet with different concentration of H_2O_2 at 25°C and pH = 7.0

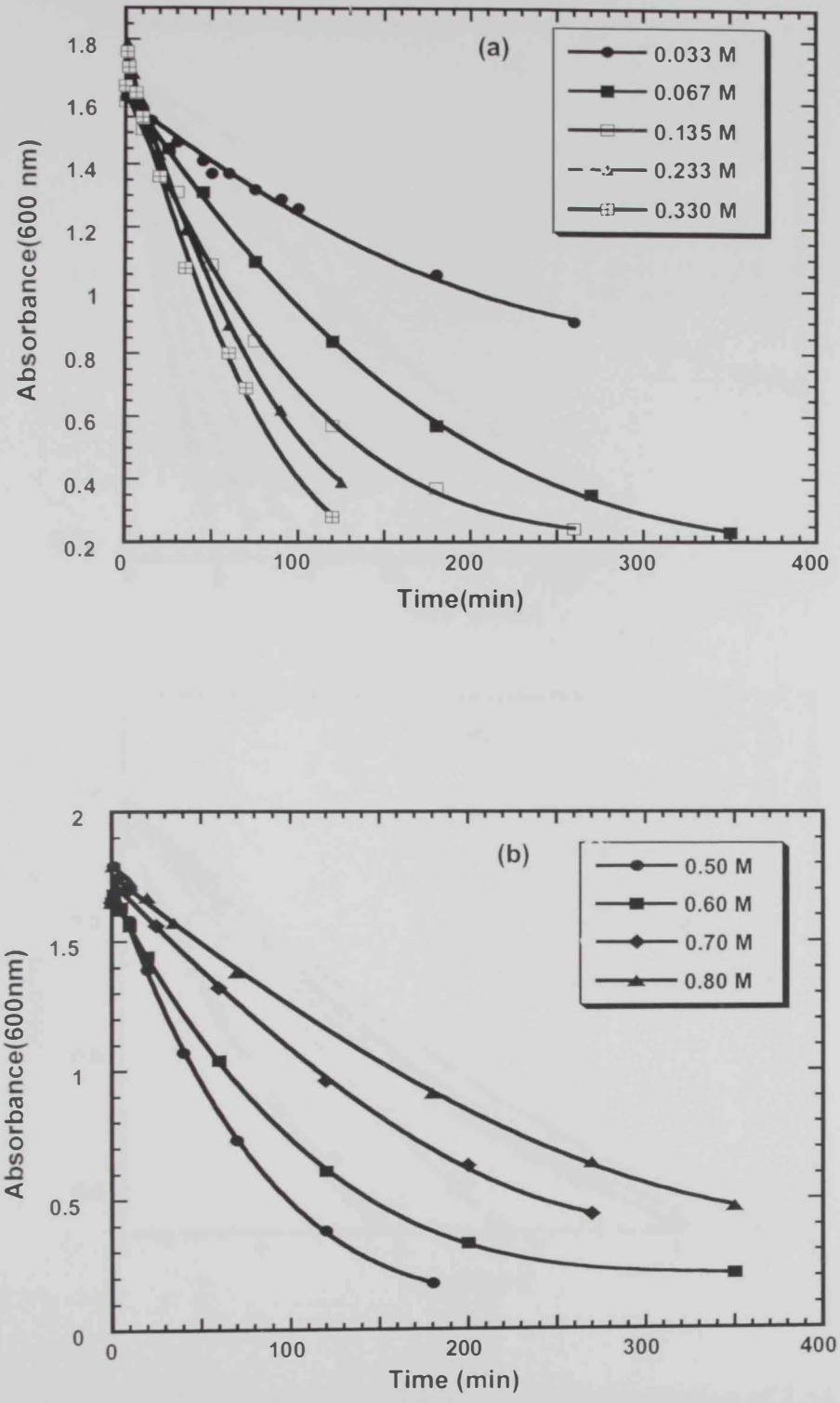

Fig. 3. 5 (a, b). Absorbance – Time curves for the reaction of 3.34 x 10^{-5} M thionine with different concentrations of H_2O_2 at 40°C and pH = 7.0 catalyzed by 3.34 x 10^{-5} M Cu^{+2}.

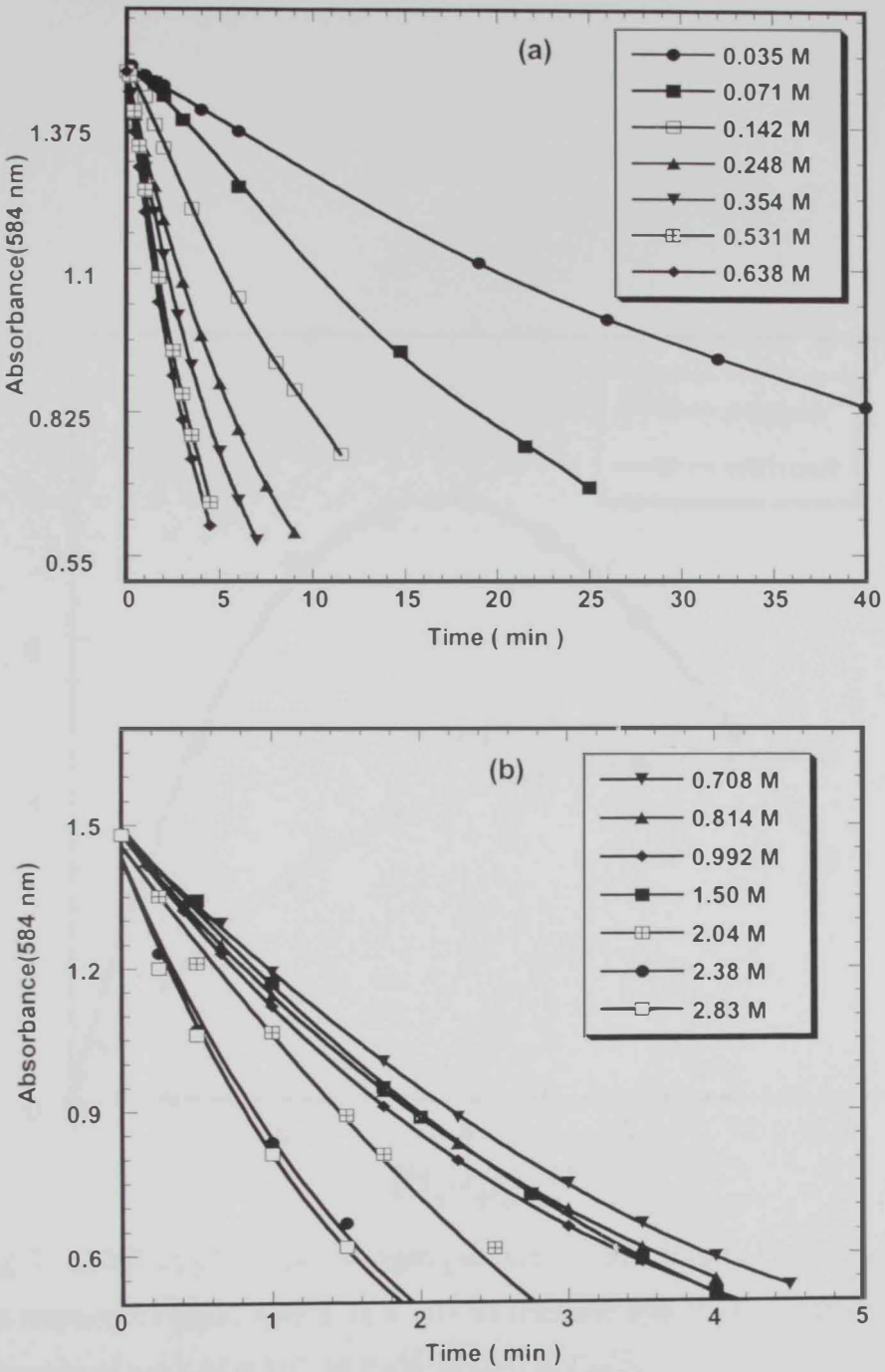

Fig. 3. 6 (a, b). Absorbance – Time curves for the reaction of 3.34×10^{-5} M methyl violet with different concentration of H_2O_2 at 25°C and pH = 7.0 catalyzed by 2.0×10^{-5} M Cu^{+2}.

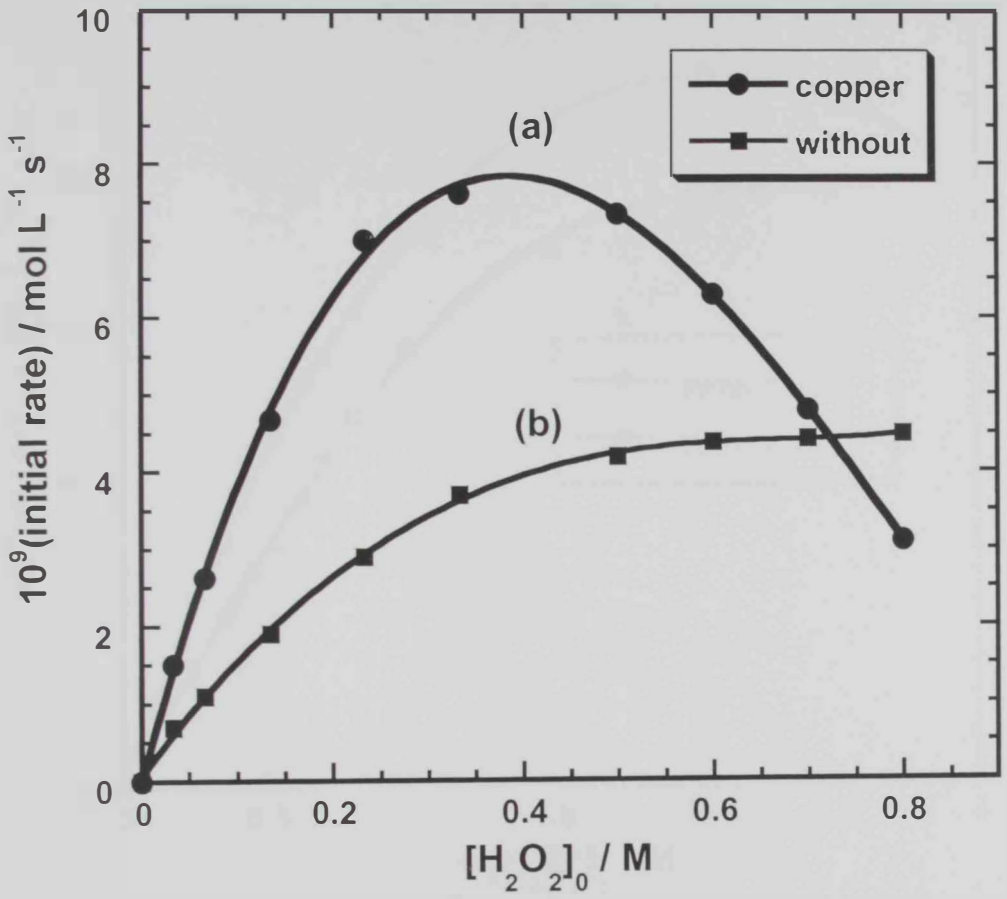

Fig. 3. 7. Effect of initial hydrogen peroxide conc. on initial reaction rate form the reaction of H_2O_2 with 3.34 x 10^{-5} M thionine dye at pH = 7.0, 40°C and in presence of (a) 3.34 x 10^{-5} M Cu^{+2} (b) 0.0 M Cu^{+2}.

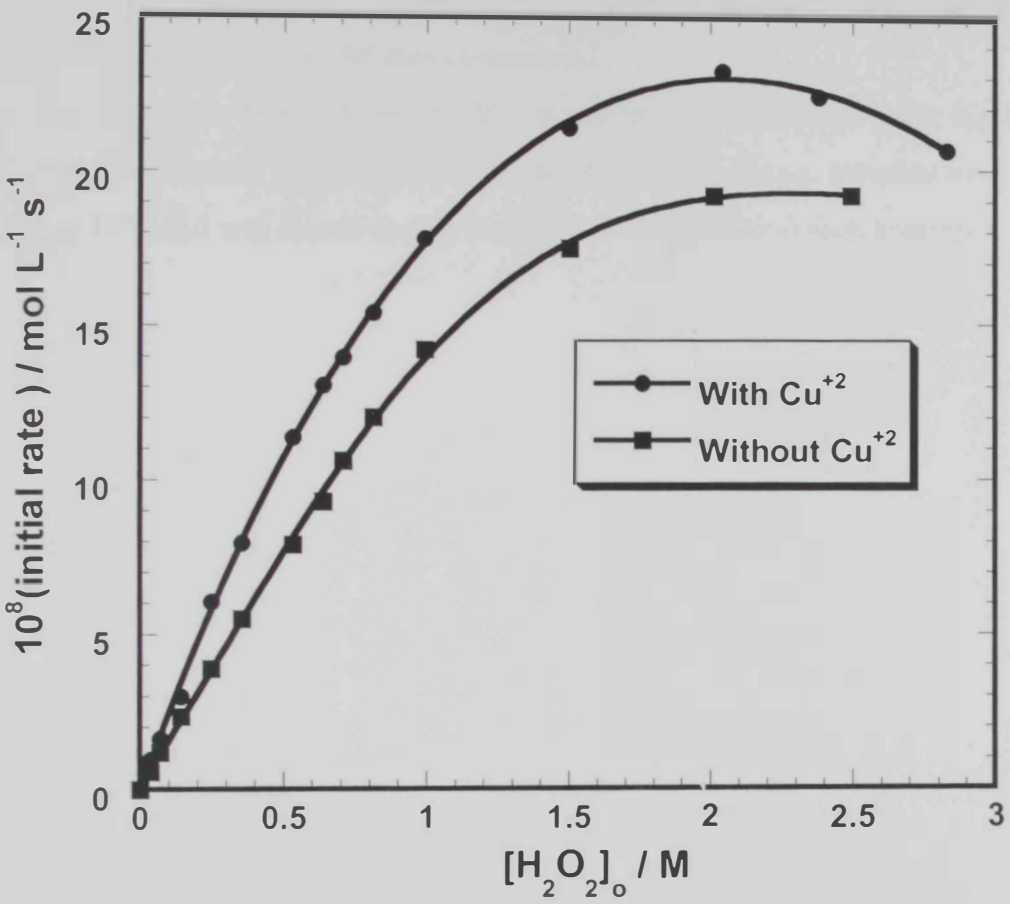

Fig. 3. 8. Effect of initial hydrogen peroxide conc. on initial reaction rate for the reaction of H_2O_2 with 3.34 X 10^{-5} M methyl violet dye at pH = 7.0, and in presence of (a) 2.0 X 10^{-4} M Cu (b) 0.0 M Cu^{+2}.

3. 1. 3. **Effect of the initial dye concentration**

The effect of the initial concentration of the dye on the reaction rate was examined for both dyes, thionine and methyl violet, at a constant pH = 7.0, (Figures 9 and 10). The plots of the initial reaction rate versus the initial concentration of the dye, (Figures 11 and 12), showed that the rate of reaction attained a first order dependence on the initial dye concentration. However, using high concentrations of methyl violet decreased both the rate and the order of reaction. The latter became zero-order at high methyl violet concentrations.

With thionine, however, we could not run more experiments using higher dye concentrations because of the greater absorbance of thionine i.e. thionine has an ε of 51,300 at 25°C and was shown to give high initial absorbance at high concentration.

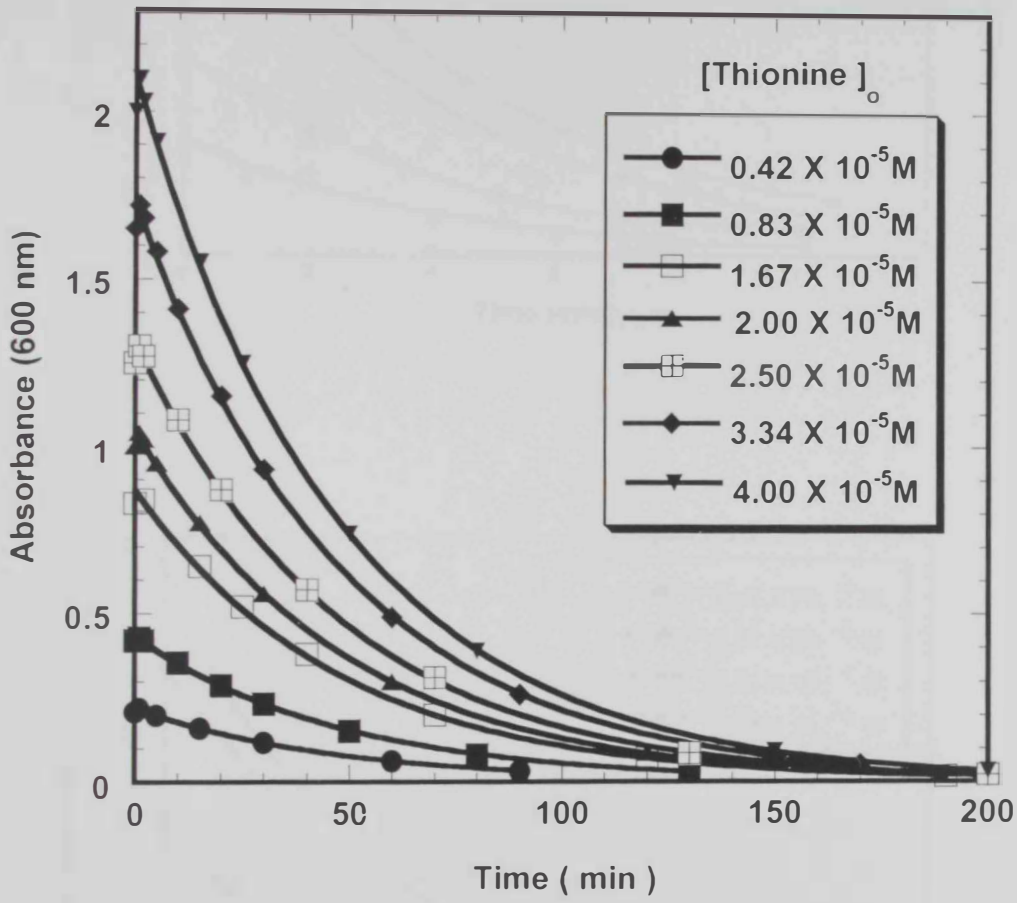

Fig. 3. 9. Decay of absorbance with time at various initial concentrations of thionine dye for its reaction with 0.20 M hydrogen peroxide catalyzed by 5.50×10^{-5} M copper (II) ions at 45°C and pH = 7.0.

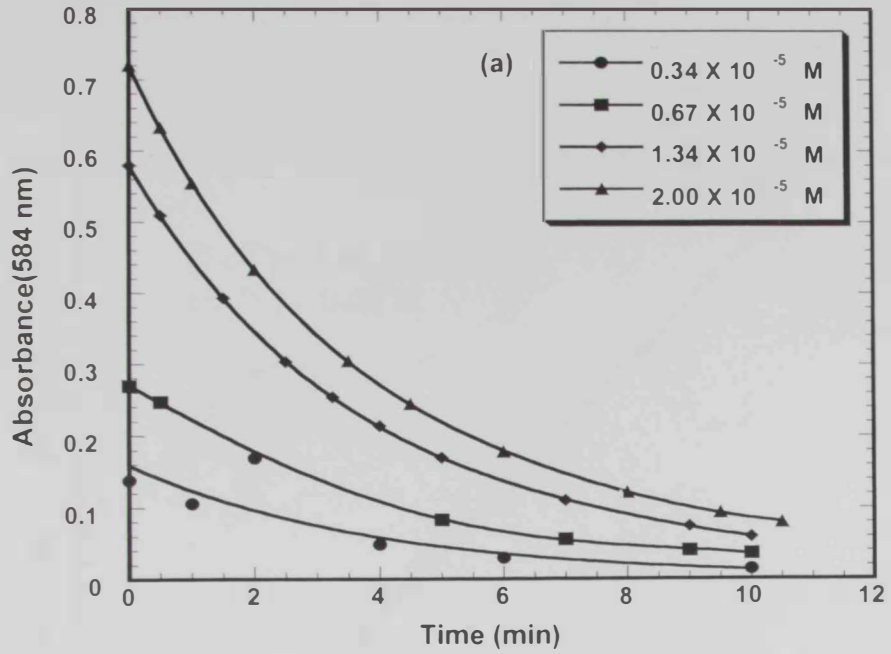

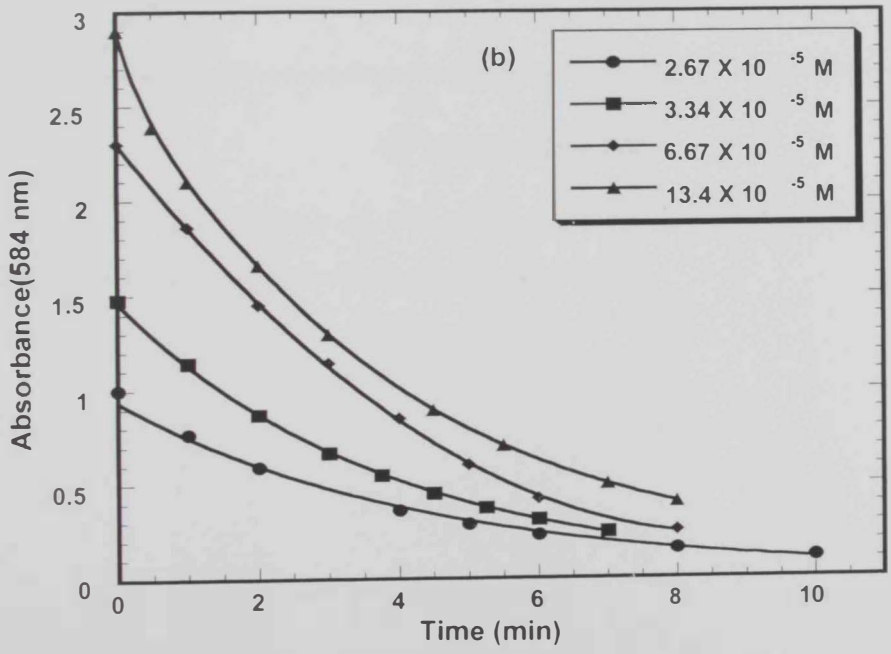

Fig. 3. 10 (a, b). The decay of absorbance with time at various initial concentrations of methyl violet dye for its reaction with 0.992 M H_2O_2 at 25°C and pH = 7.0.

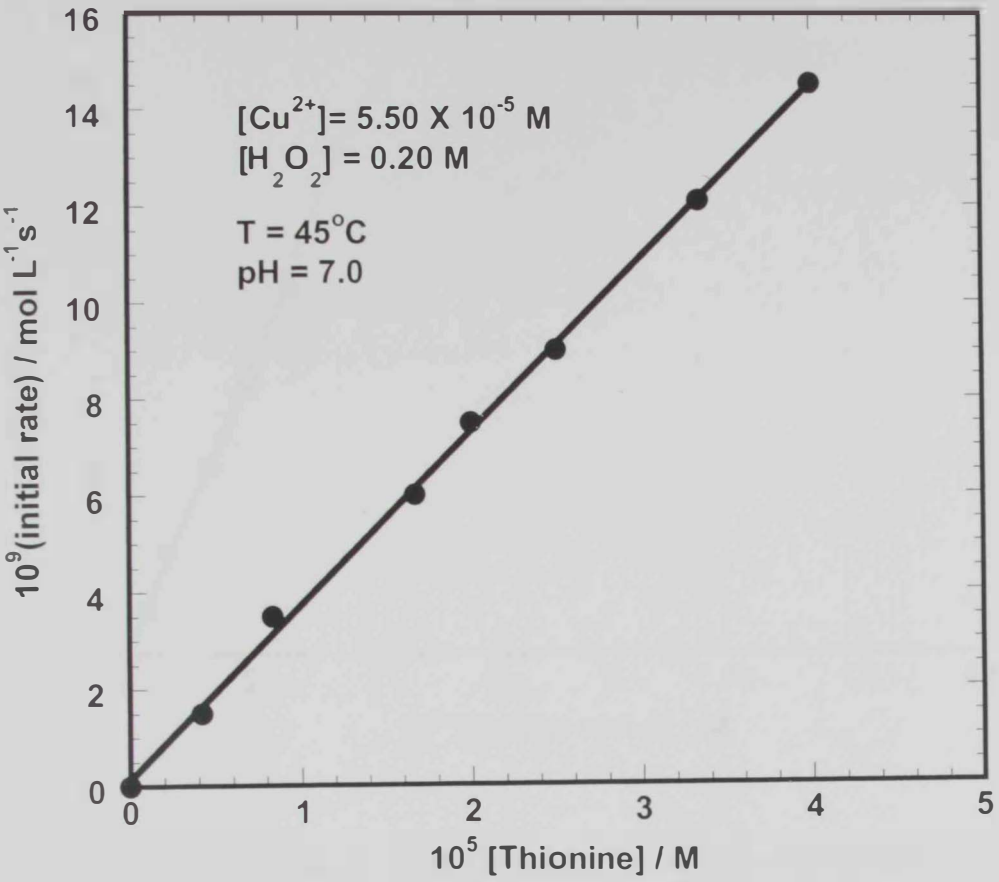

Fig. 3. 11. Dependence of the initial rate on the initial concentration of thionine for its reaction with hydrogen peroxide.

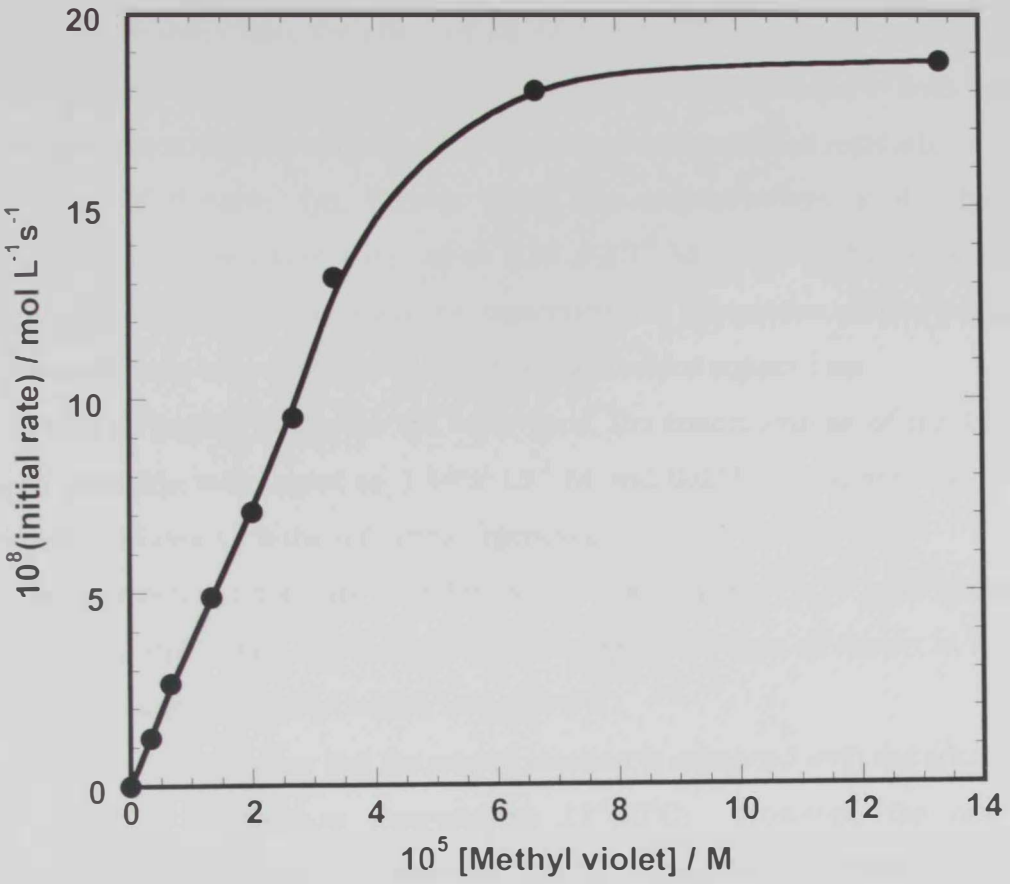

Fig. 3. 12. Dependence of initial rate on the initial concentration of methyl violet for its reaction with H_2O_2 at pH = 7.0 and T= 25°C.

3. 1. 4. Effect of copper (II) ions

In order to investigate the effect of added copper (II) ions on the reaction rate, experiments were carried out at pH= 7.0 using constant concentrations of both the dye and hydrogen peroxide whereas copper(II) concentration was varied regularly.

In case of thionine dye, Figures 13-16, the concentrations of the dye and hydrogen peroxide were kept constant at 3.34×10^{-5} M and 0.20 M, respectively. Experiment in Figure 13 is the reference experiment i.e. experiment carried out under the same conditions as in figures 14-16, but, without added copper ions.

In case of methyl violet, on the other hand, the concentrations of the dye and hydrogen peroxide were equal to 3.34×10^{-5} M and 0.035 M respectively. Also, experiment in Figure 17 is the reference experiments.

Initial reaction rates were then determined from Figures 13-17 and Figures 17-21 and then plotted versus the concentration of copper (II) ions as shown in Figures 22 - 23 for thionine and methyl violet, respectively.

In Figure 22, it is clear that the rate of reaction is enhanced with the addition of copper (II) ions at different temperatures 25°-40°C. However, the order of enhancement was gradually decreased by the increase in copper (II) ions concentration.

With methyl violet, the rate was enhanced, had a maximum, and thereafter decreased, Fig. 23, clearly shows that the rate of reaction was much more enhanced in case of thionine than that with methyl violet. This may be attributed to the differences in hydrogen peroxide concentration used with both dyes. The concentration of hydrogen peroxide used with thionine was 5.7 times greater than that used with methyl violet. Therefore, more hydroxyl radicals are expected to by generated in case of thionine compared to methyl violet. The decreased rate at higher copper (II) concentration can be ascribed to the formation of an inhibitory intermediate formed from the interaction of hydrogen peroxide with copper (II) ions [80-83].

The curves in Figures 22 and 23 are representing both the uncatalyzed and the catalyzed reactions and they elucidate that the contribution of the catalyzed reaction is low in case of methyl violet compared to thionine. In other words, in case of methyl violet, the uncatalyzed reaction constitutes the main contribution to the total rate. Experiments carried out to investigate the effect of ionic strength on the reaction rate (will be discussed in details) revealed that the rate of uncatalyzed reaction decreased

with increasing ionic strength. Therefore, the decreased rate observed at higher copper (II) concentrations in case of methyl violet could be ascribed to the increased ionic strength.

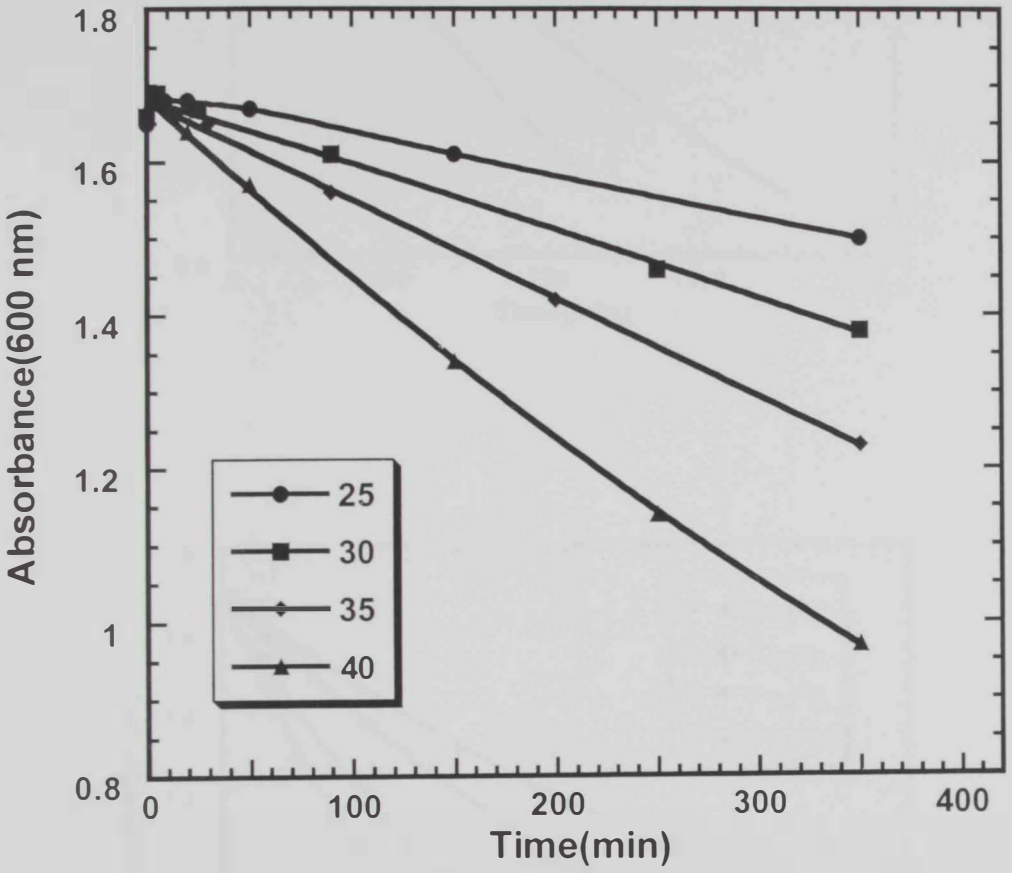

Fig. 3. 13. Absorbance – time curves for the reaction of 3.34 x 10^{-5} M thionine with 0.20 M H_2O_2 at pH = 7.0.

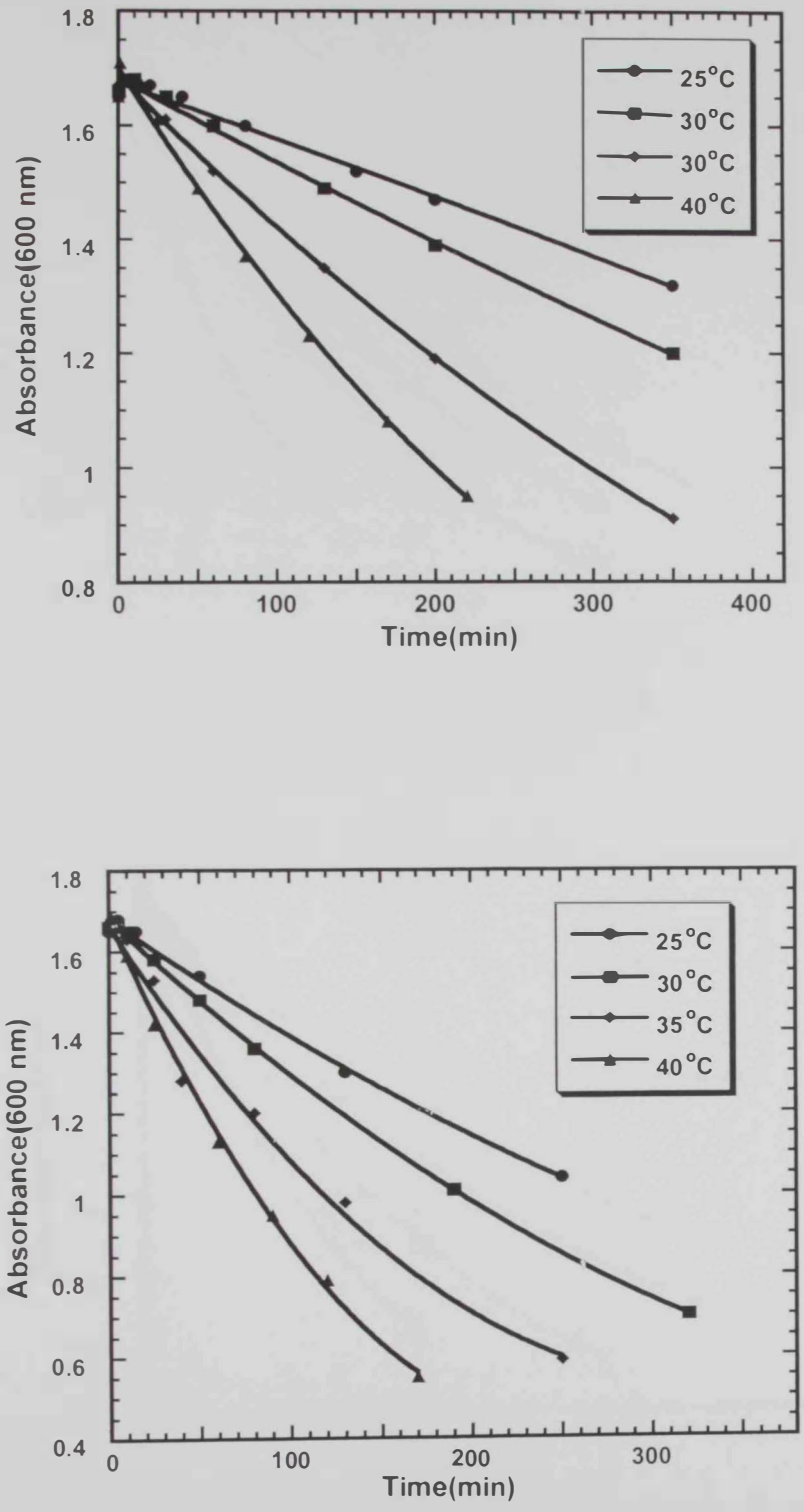

Fig. 3. 14. Absorbance – time curves for the reaction of 3.34 x 10^{-5} M thionine with 0.2 M of H_2O_2 at pH = 7.0 catalyzed by 0.334 x 10^{-5} M (above) and 1.34 X 10^{-5} (down) of Cu^{2+} ions.

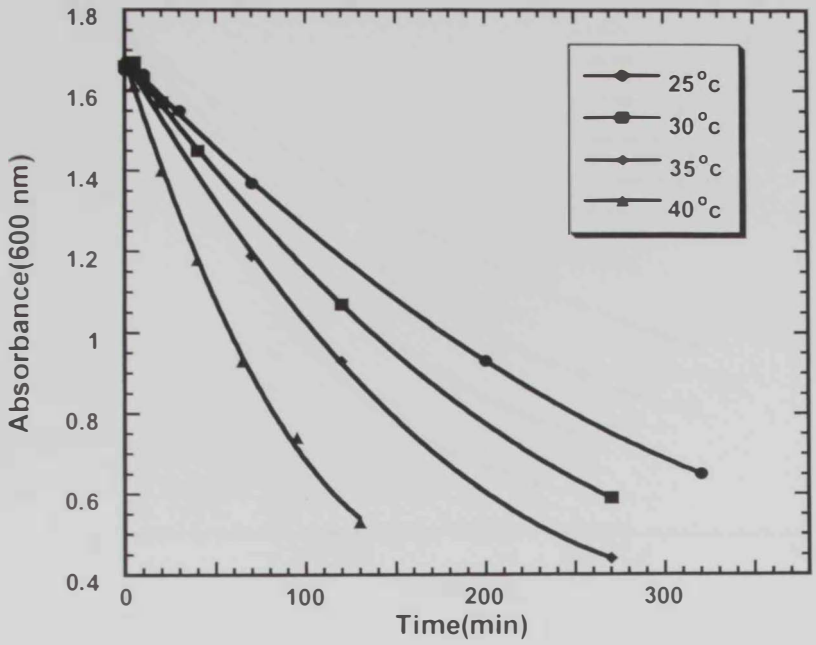

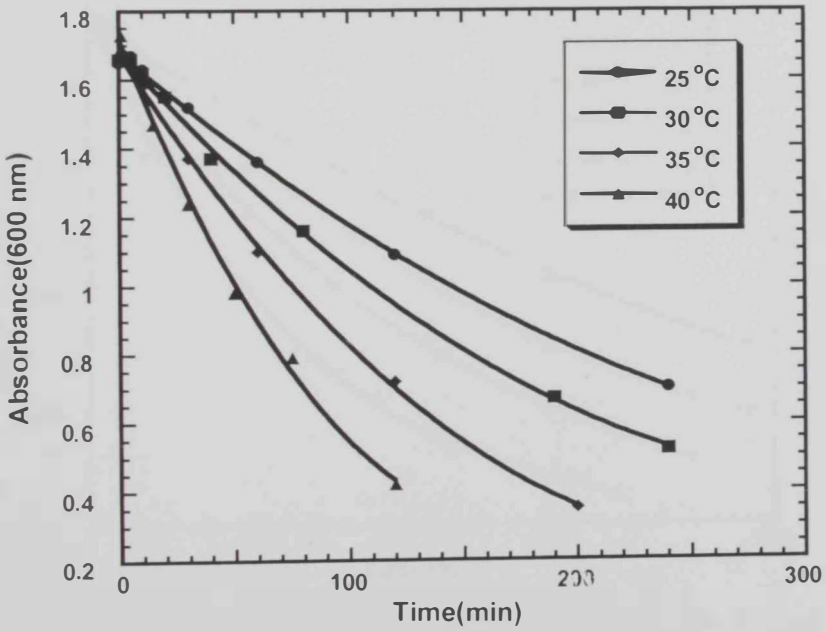

Fig. 3. 15. Absorbance – time curves for the reaction of 3.34 x 10^{-5} M thionine with 0.2 M of H_2O_2 at pH = 7.0 catalyzed by 2.0 x 10^{-5} M (above) and 2.67 X 10^{-5} M (down) of Cu^{2+} ions.

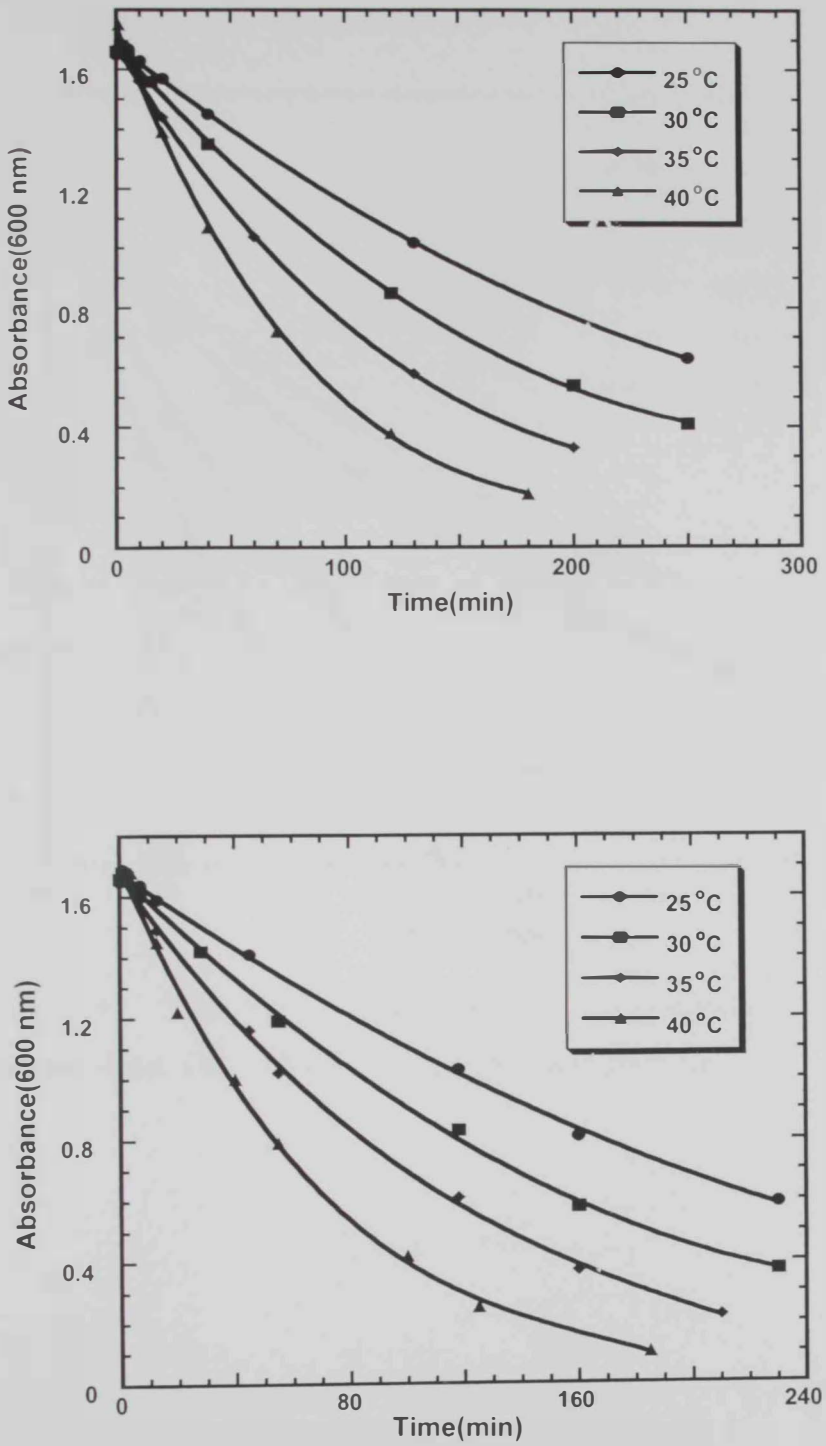

Fig. 3. 16. Absorbance – time curves for the reaction of 3.34 x 10^{-5} M thionine with 0.2 M of H_2O_2 at pH = 7.0 catalyzed by 3.34 x 10^{-5} M (above) and 5.50 x 10^{-5} (down) of Cu^{2+} ions.

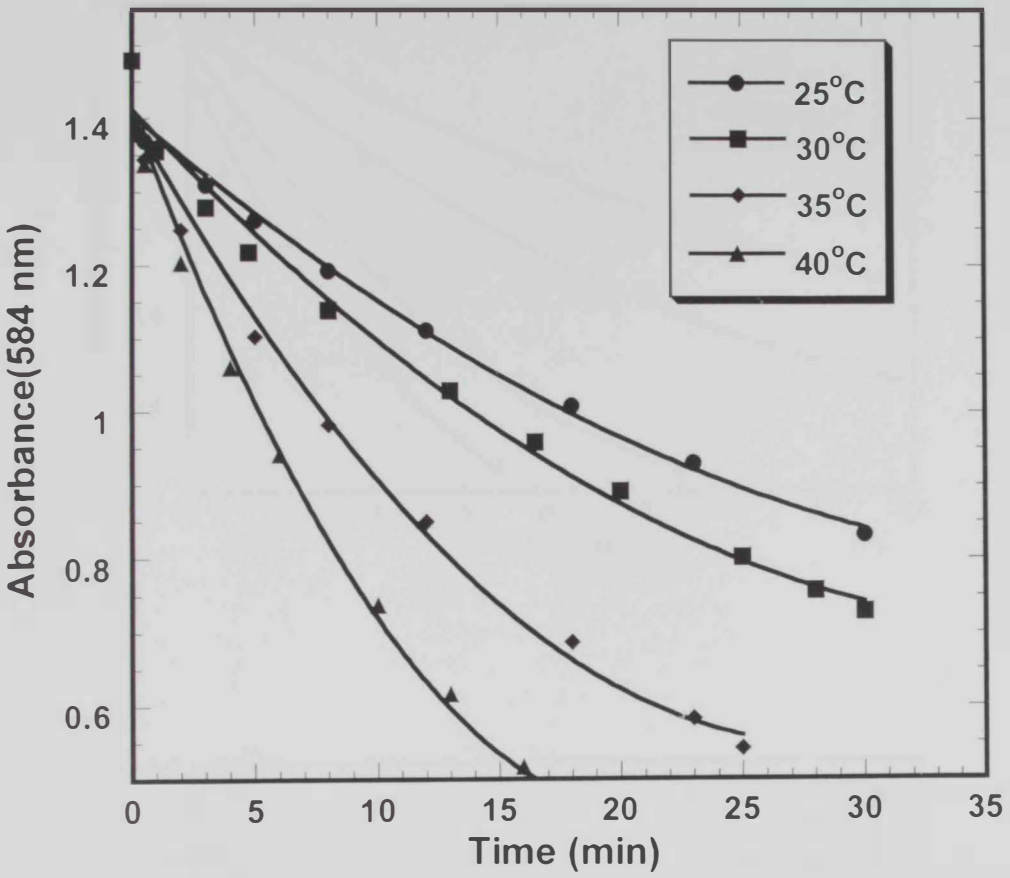

Fig. 3. 17. Absorbance – time curves for the reaction of 3.34 x 10^{-5} M methyl violet with 0.035 M H_2O_2 at 25°C and pH = 7.0.

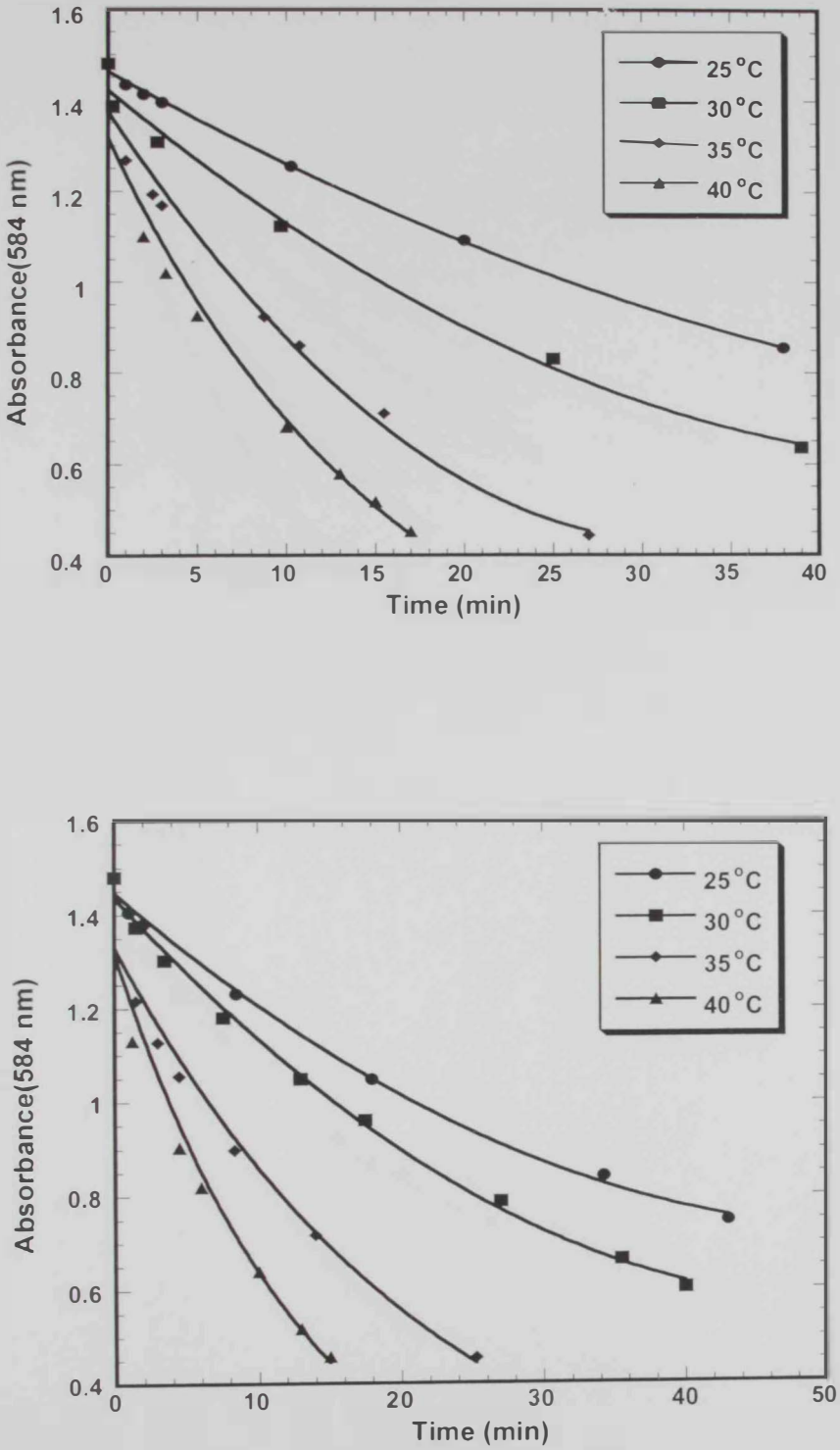

Fig. 3. 18. Absorbance – time curves for the reaction of 3.34 x 10^{-5} M methyl violet with 0.035 M H_2O_2 at 25°C and pH = 7.0 catalyzed by 0.34 x 10^{-5} M (above) and 0.67 X 10^{-5} M (down) of Cu^{2+} ions.

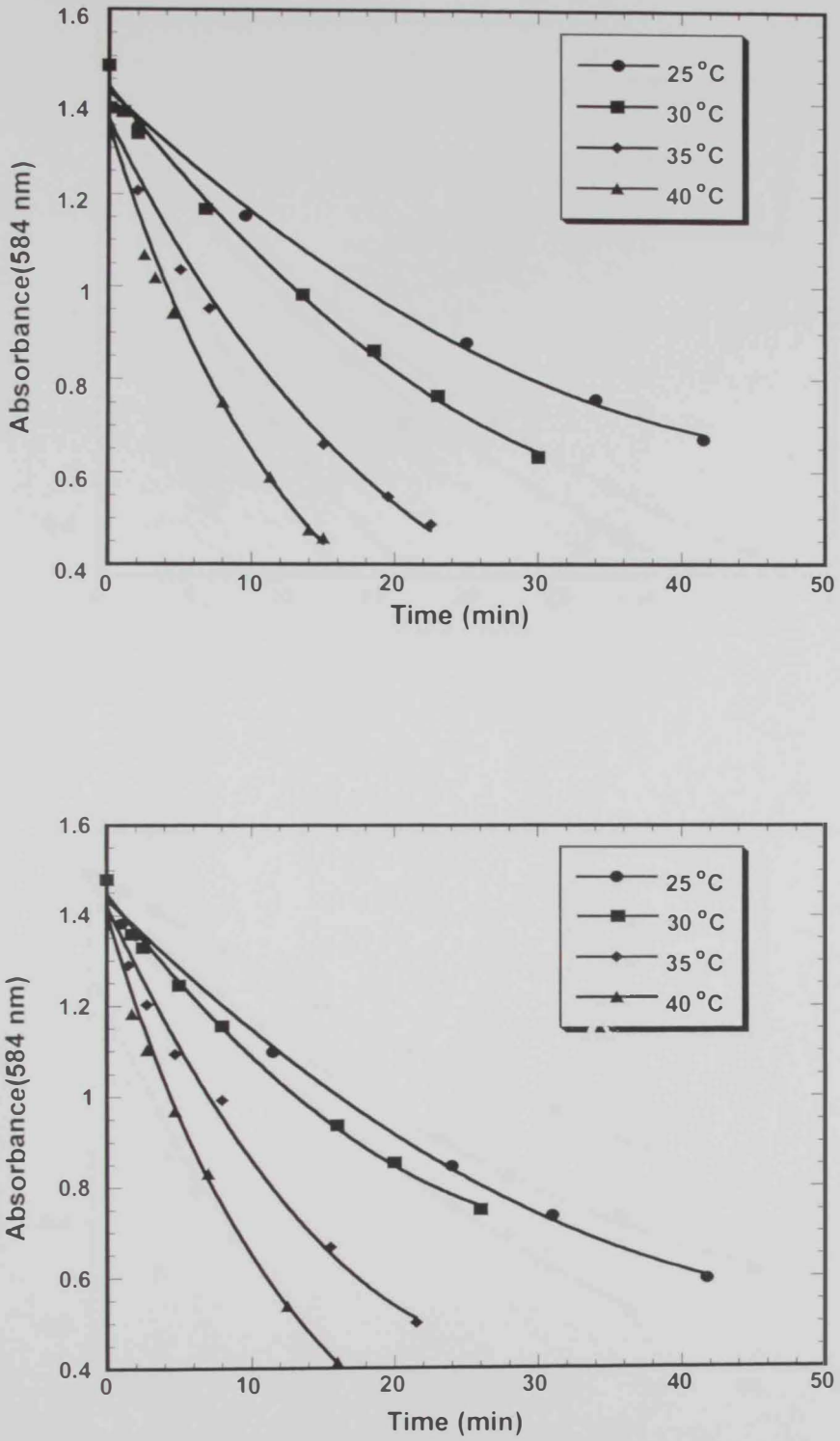

Fig. 3. 19. Absorbance – time curves for the reaction of 3.34 x 10^{-5}M methyl violet with 0.035 M H_2O_2 at 25°C and pH = 7.0 catalyzed by 1.34 x 10^{-5}M (above) and 2.00 x 10^{-5}M (down) of Cu^{2+} ions.

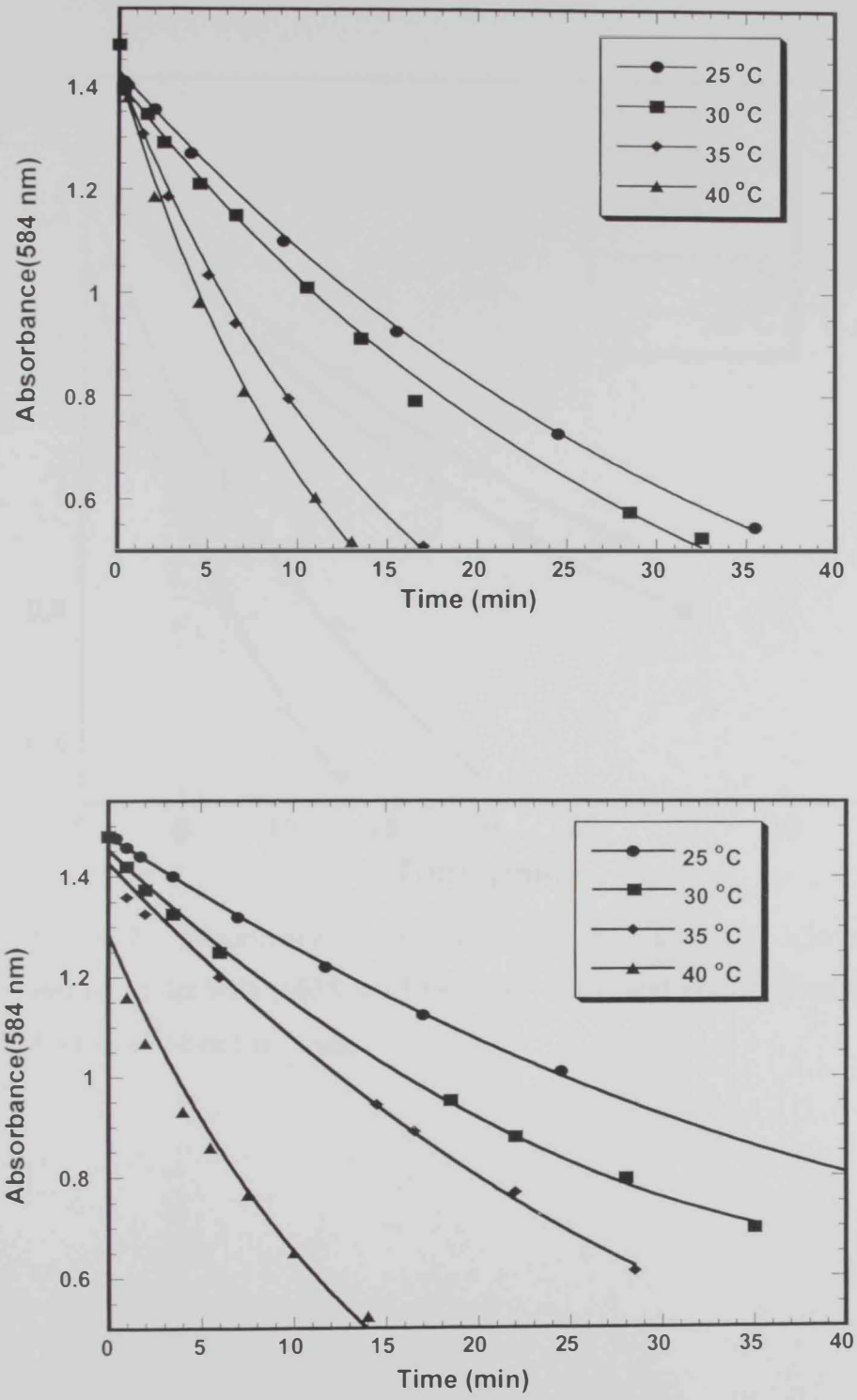

Fig. 3. 20 Absorbance – Time curves for the reaction of 3.34 x 10^{-5} M methyl violet with 0.035 M H_2O_2 at 25°C and pH = 7.0 catalyzed by 2.67 x 10^{-5} M (above) and 4.00 x 10^{-5} M (down) of Cu^{2+} ions.

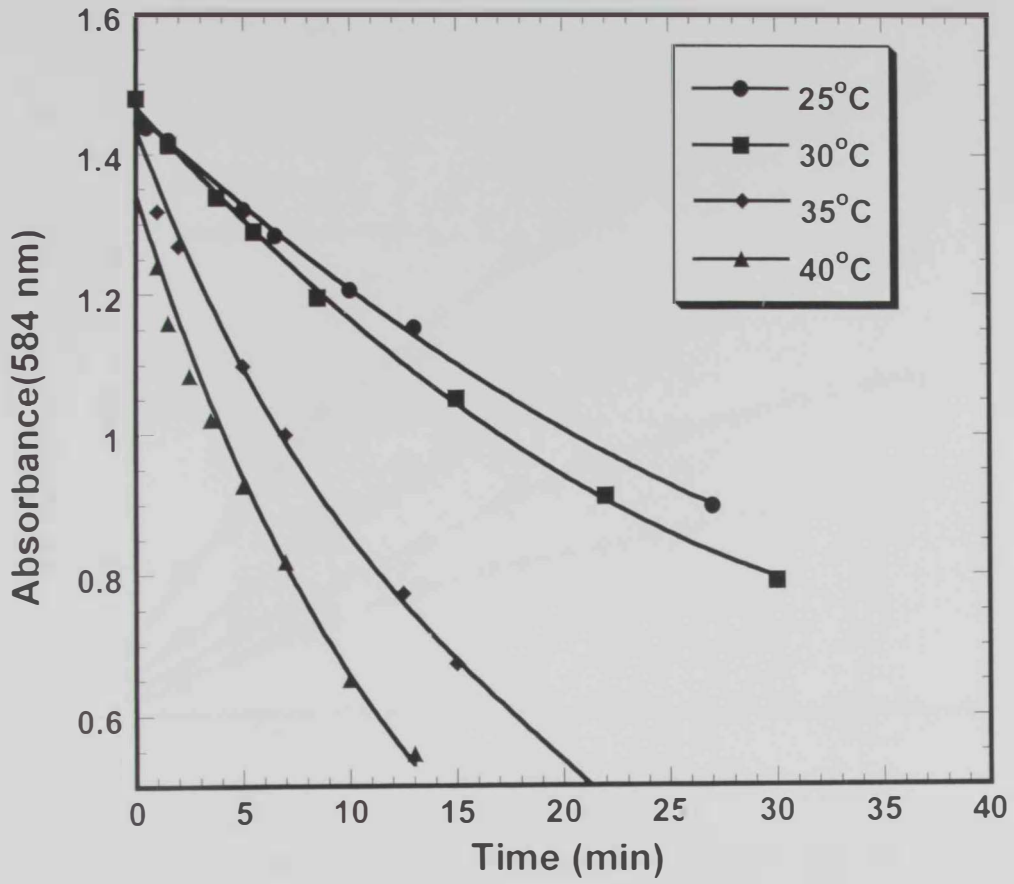

Fig. 3. 21. Absorbance – Time curves for the reaction of 3.34 x 10^{-5} M methyl violet with 0.035 M H_2O_2 at T = 25°C and pH = 7.0 catalyzed by 5.34 x 10^{-5}M of Cu^{2+} ions.

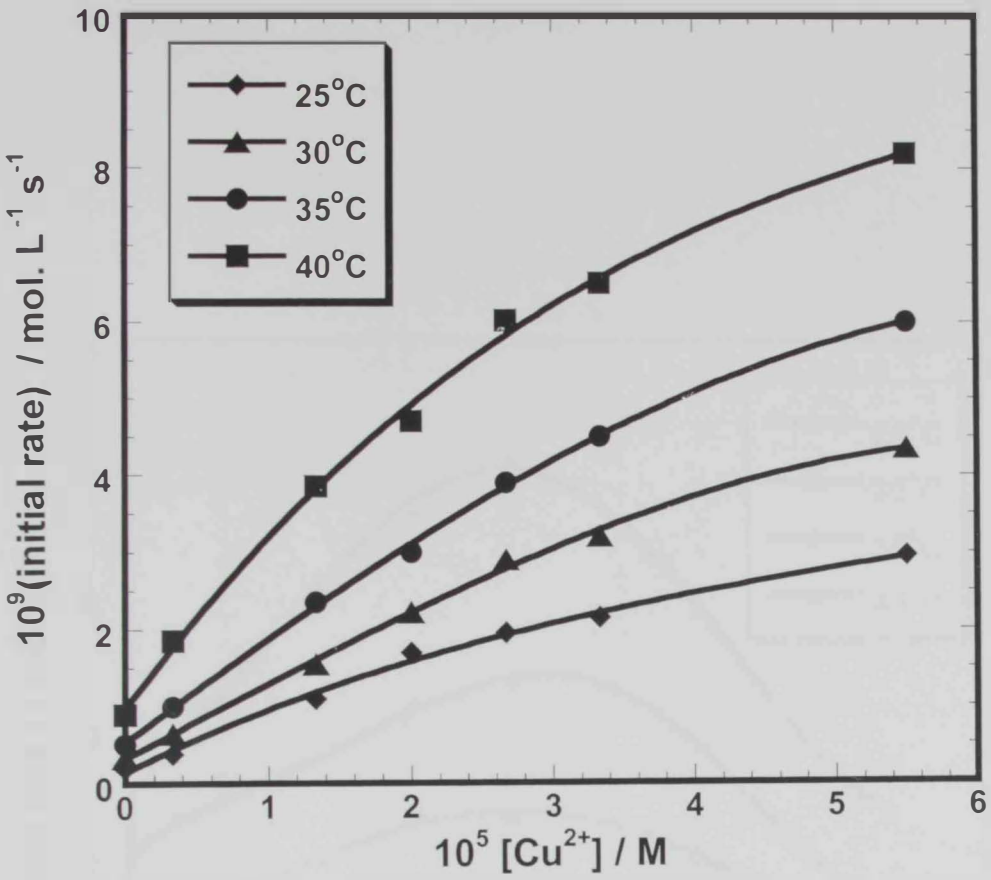

Fig. 3. 22. Dependence of the initial reaction rate on the initial concentration of Cu^{+2} for the reaction of 0.20 M H_2O_2 with 3.34 x 10^{-5} M thionine at pH = 7.0 and at different temperatures.

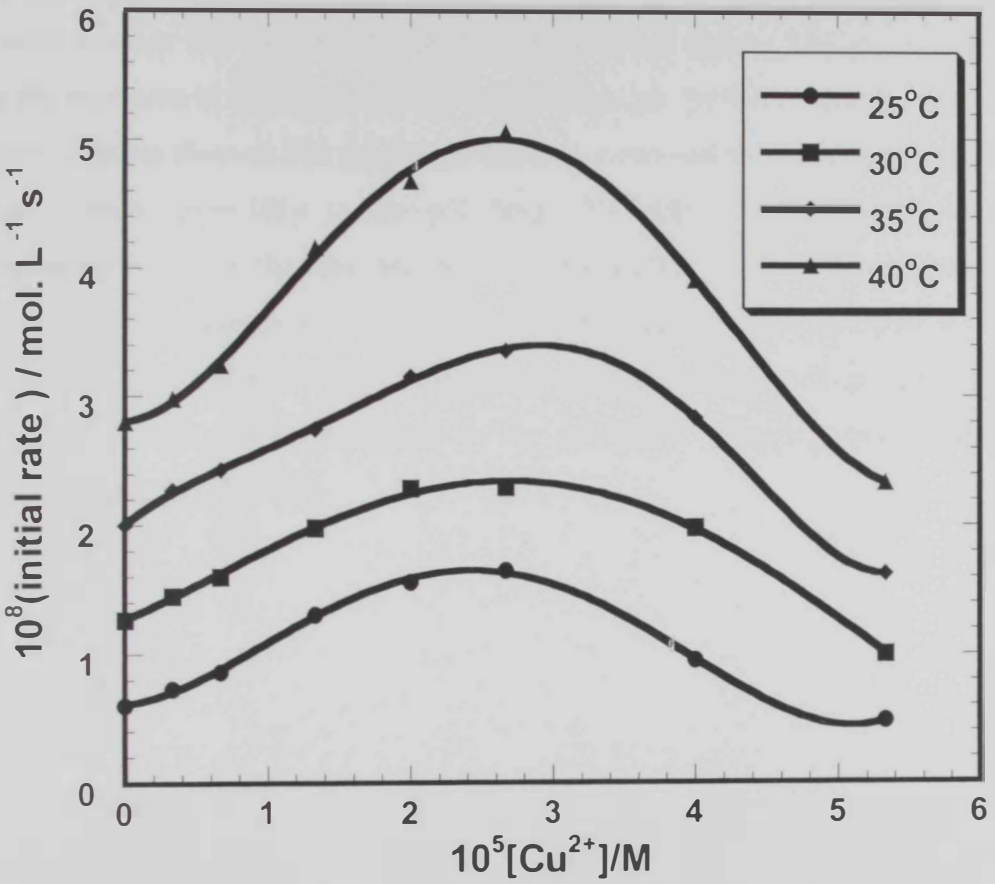

Fig. 3. 23. Dependence of the initial reaction rate on the initial concentration of Cu^{2+} for the reaction of 0.035 M H_2O_2 with 3.34 x 10^{-5} M methyl violet at pH = 7.0 and different temperatures.

3. 1. 5. **Effect of pH**

The effect of pH on the reaction rate was studied for both investigated dyes, thionine and methyl violet. Phosphate buffers of pH values 5-11 was used at constant concentration of hydrogen peroxide (0.14 M or 0.992 M) and 3.34 x 10^{-5} M dye.

Figures 24 and 25 show the variation of absorbance with time at different pHs for the reaction of hydrogen peroxide with thionine and methyl violet respectively. The initial reaction rate values calculated from curves on figures (24-25) were plotted versus pH as shown in figures 26 and 27 for thionine and methyl violet, respectively.

Both figures showed that the rate of reaction increased with increasing pH of the reaction medium especially in the pH range 9.0-11.0. No discernible reaction occurred at pH $\leq$ 6.0 for thionine and pH $\leq$ 5.0 for methyl violet. This suggested that the basic form of hydrogen peroxide, HOO^-, and the unprotonated forms of both dyes are the most reactive species [69]. This means that the rate of reaction was enhanced at higher pH which can be attributed to the formation of hydropeorxide anion in alkaline solutions [69, 85, 87]

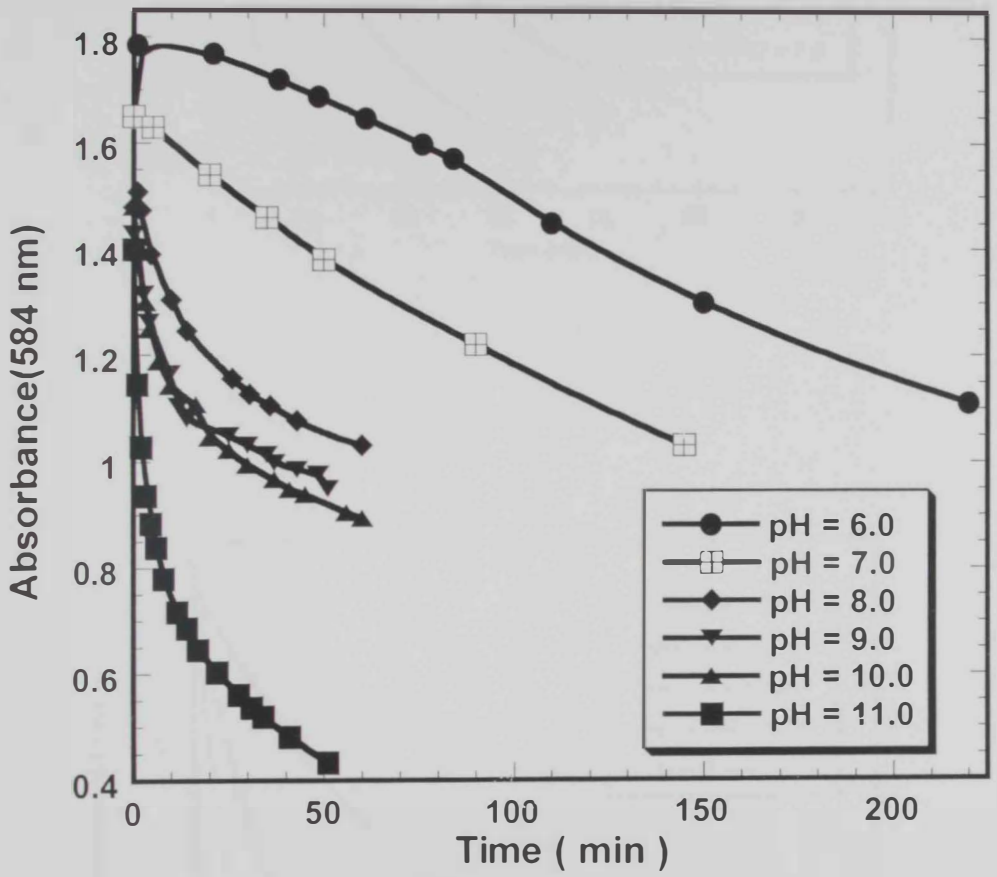

Fig. 3. 24. Absorbance – time curves for the reaction of 3.34 x 10^{-5} M thionine with 0.14 M H_2O_2 at 40°C.

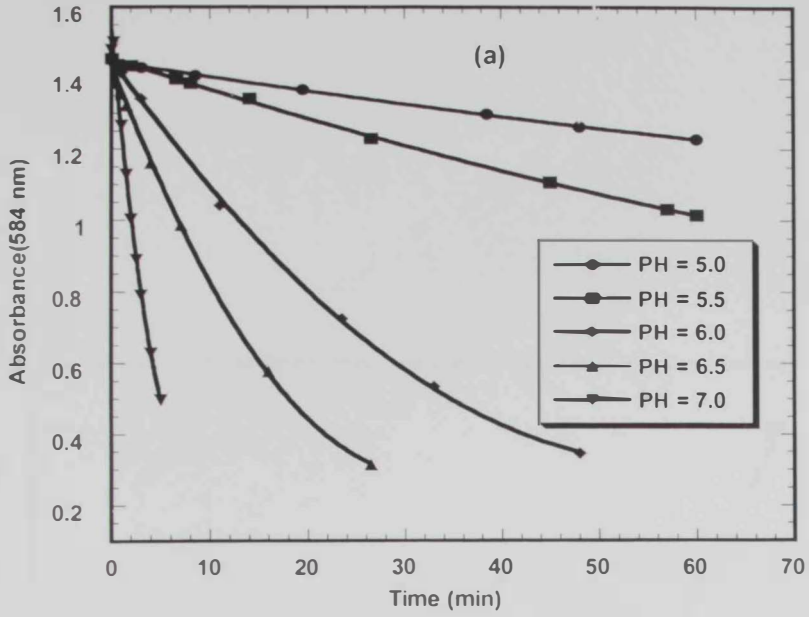

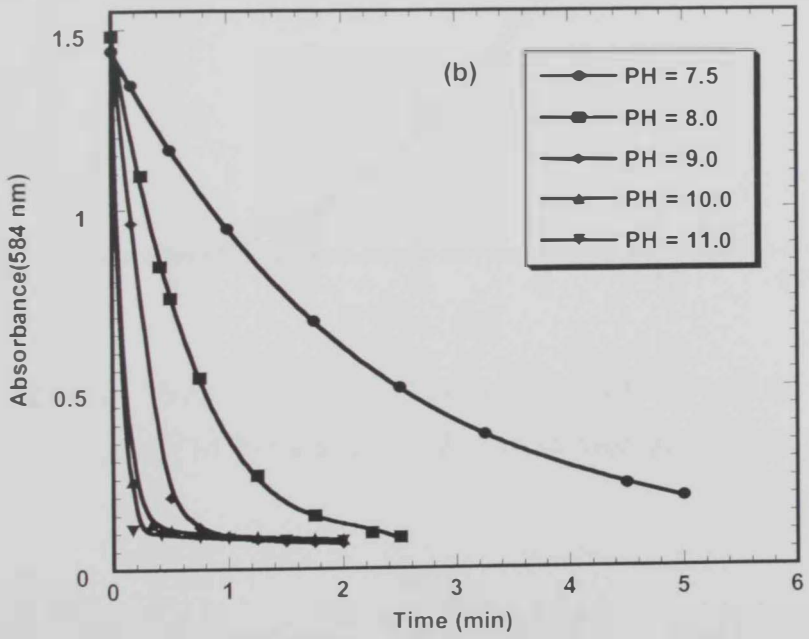

Fig. 3. 25 (a, b). Absorbance – time curves for the reaction of 3.34 x 10^{-5} M methyl violet with 0.992 M of H_2O_2 and 25°C at different pHs

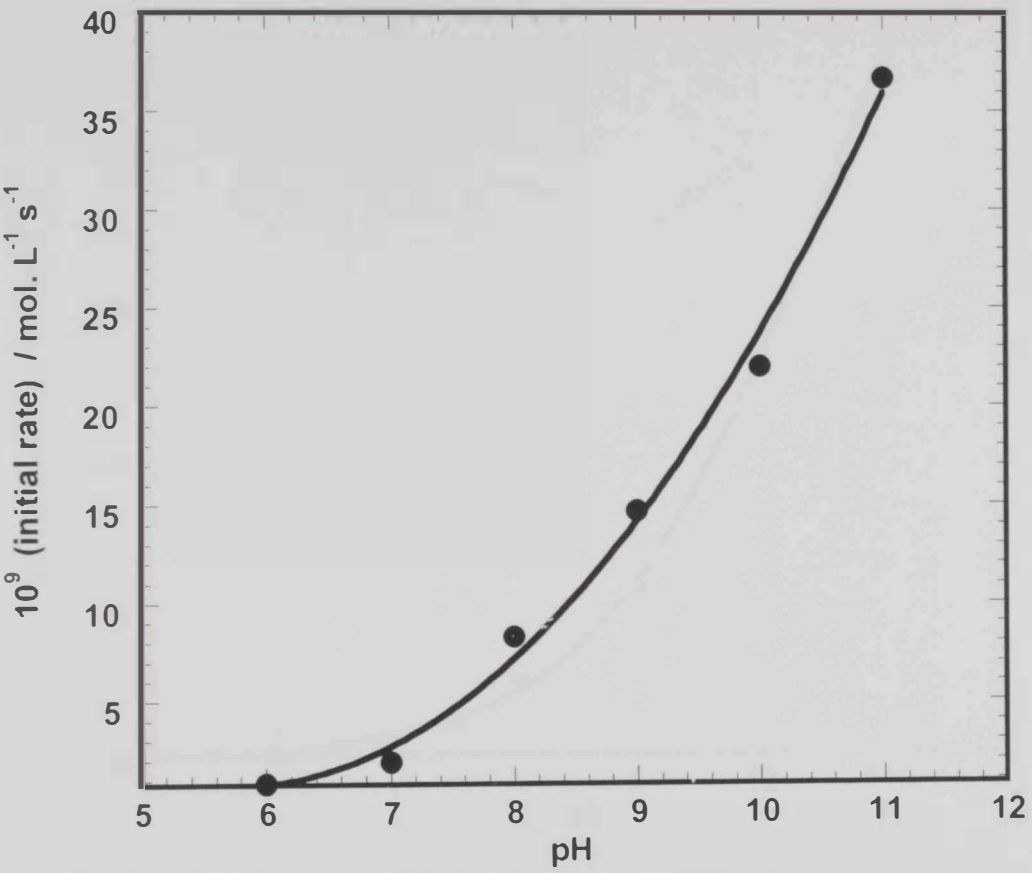

Fig. 3. 26. Variation of the initial reaction rate with pH for the oxidation of 3.34 X 10^{-5} M thionine dye with 0.14 M hydrogen peroxide at 40°C.

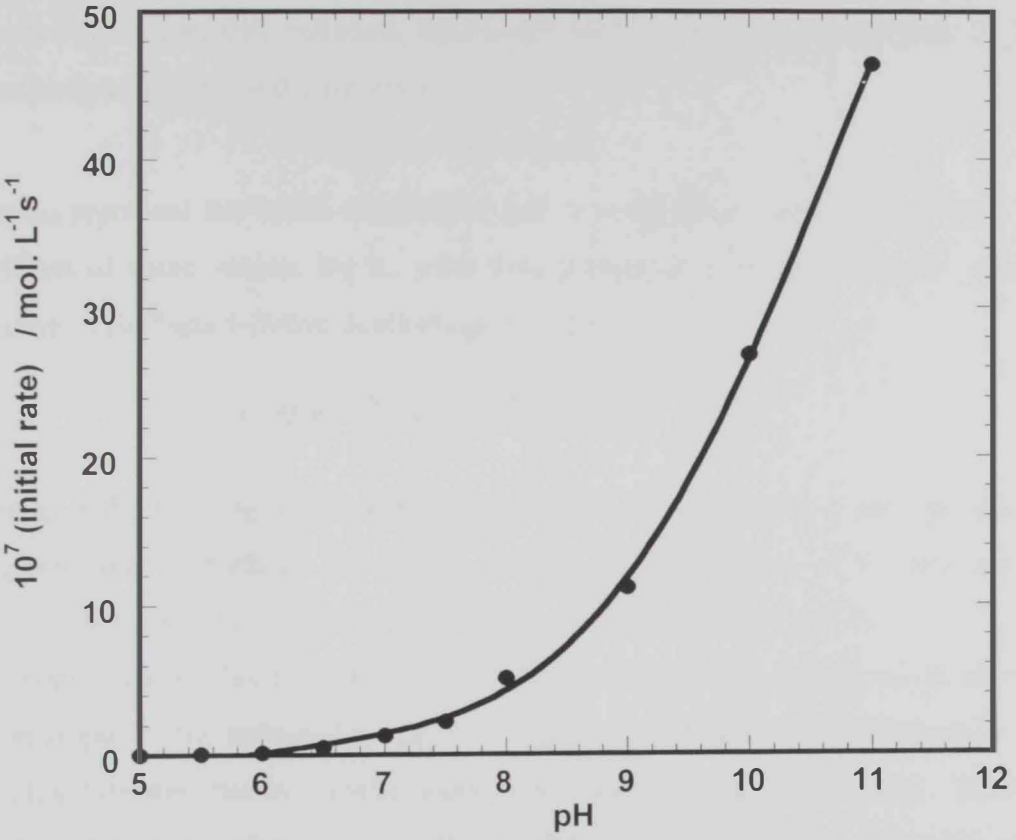

Fig. 3. 27. Variation of the initial reaction rate with pH for the oxidation reaction of 3.34 x 10^{-5} M methyl violet with 0.992 M H_2O_2 at pH = 7.0 and 25°C.

3. 1. 6. **Effect of ionic strength**

The effect of ionic strength on reaction rate was investigated in order to get information about the number charges on the reacting species that constitute the activated complex. The ionic strength was varied by the addition of sodium chloride as an inert salt to 3.34 x 10^{-5} M and 0.067 M concentrations of the thionine and hydrogen peroxide, respectively at pH = 7.0.

At different ionic strength the rate constants, k, were determined using the integrated first-order rate equation, figures 28 and 29 for thionine and methyl violet, respectively according to the equation:

$$\ln A = - kt + \ln A_o$$

where A_o represent the initial absorbance and A is the absorbance at any time t. The logarithms of these values, log k, were then plotted as a function of ionic strength according to BrØnsted-Debye-Huckel equation [16]:

$$\text{Log } k = \log k_o + 2\, AZ_AZ_B \,.\, \frac{\sqrt{\mu}}{1+\sqrt{\mu}}$$

Where k_o is the limiting rate constant at zero ionic strength and k is the rate constant at a given ionic strength μ. Z_A and Z_B are the charge numbers of the two reacting species. The constant A has a value of 0.509 at 25°C and 0.492 at 40°C.

Application of this equation to our systems, thionine and methyl violet, revealed that the slopes of the straight lines are – 1.1 and – 1.15 ,respectively (Figures 30 and 31). This indicates that two single oppositely charged ions are interacting. Since the rate of oxidation of either thionine or methyl violet with hydrogen peroxide under these conditions conformed to second- order kinetics. Therefore, one of the reacting species should be the positively charged substrate and the other one is the hydropeorxide anion, HOO^-, and not H_2O_2. This also explains the rate enhancement found with increasing pH due to the increase in concentration of the hydropeorxide anion [69].

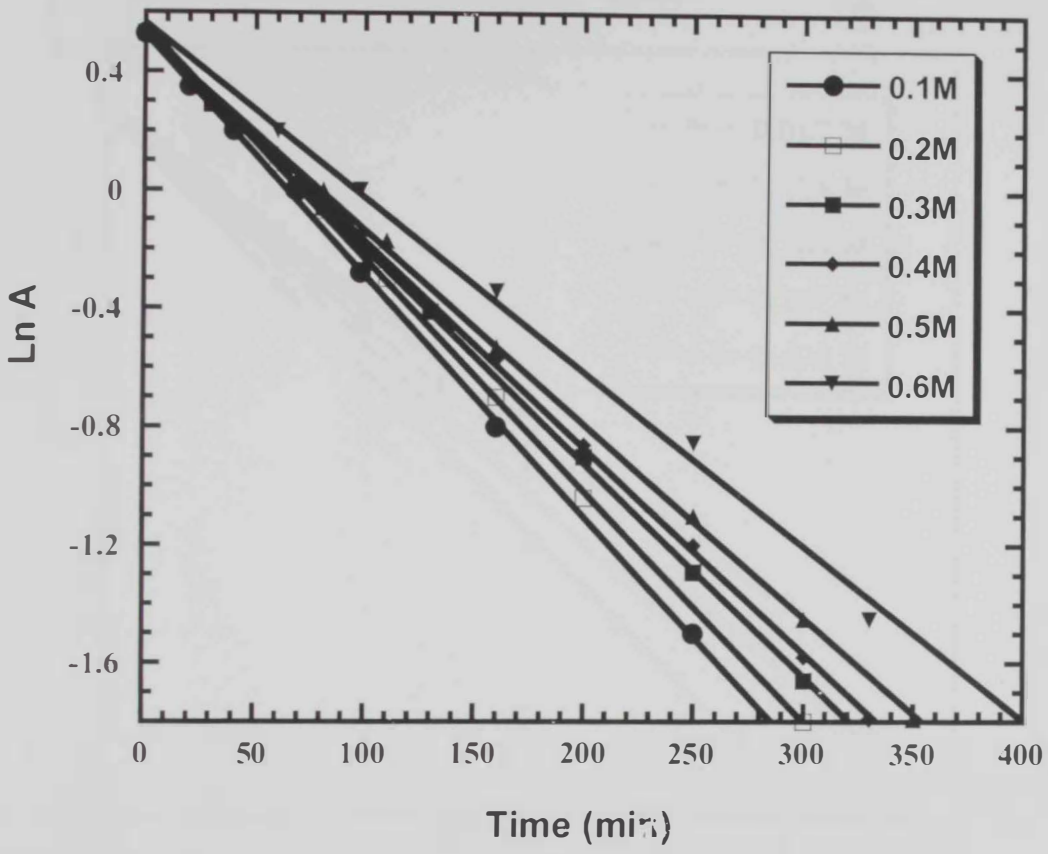

Fig. 3. 28. First order plot for the oxidation of 3.34 x 10^{-5} M of thionine with 0.067M of H_2O_2 in the presence of 3.34 x 10^{-5} M Cu^{+2} at 40°C and pH = 7.0.

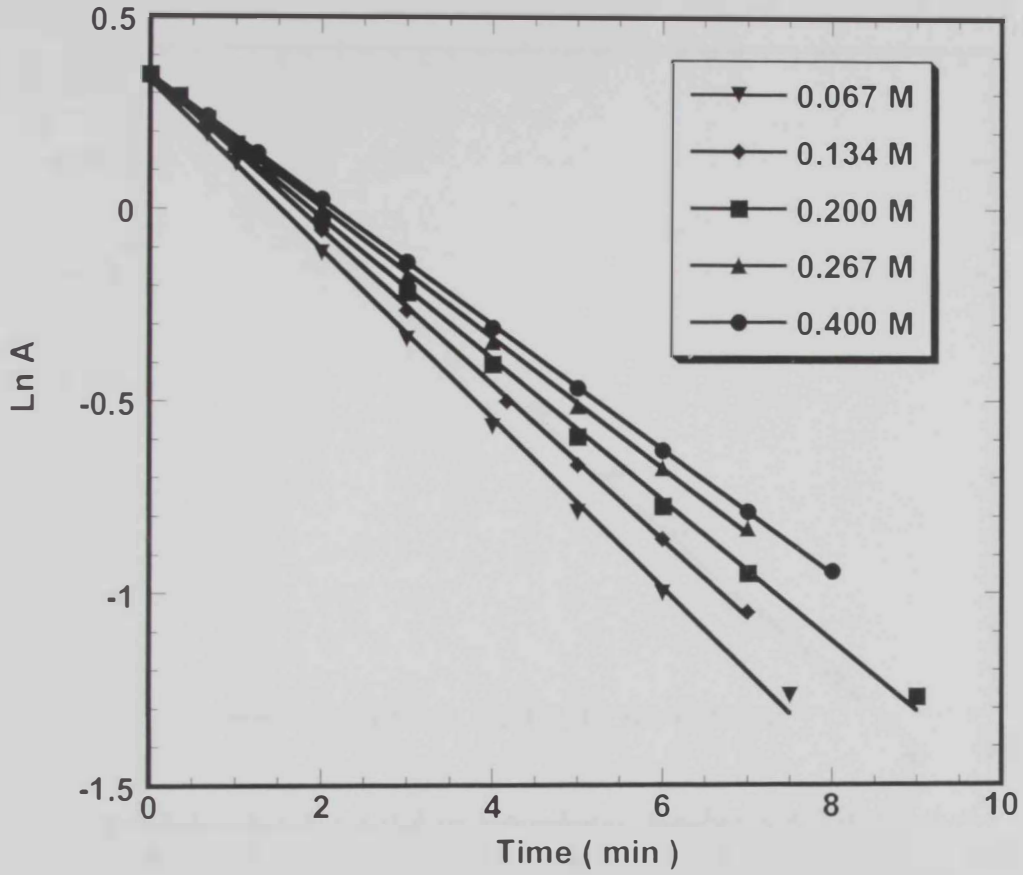

Fig. 3. 29. First order plot for the oxidation of 3.34 X 10^{-5} M of methyl violet with 0.992 M of H_2O_2 at 25°C and pH = 7.0 using different concentrations of chloride ion.

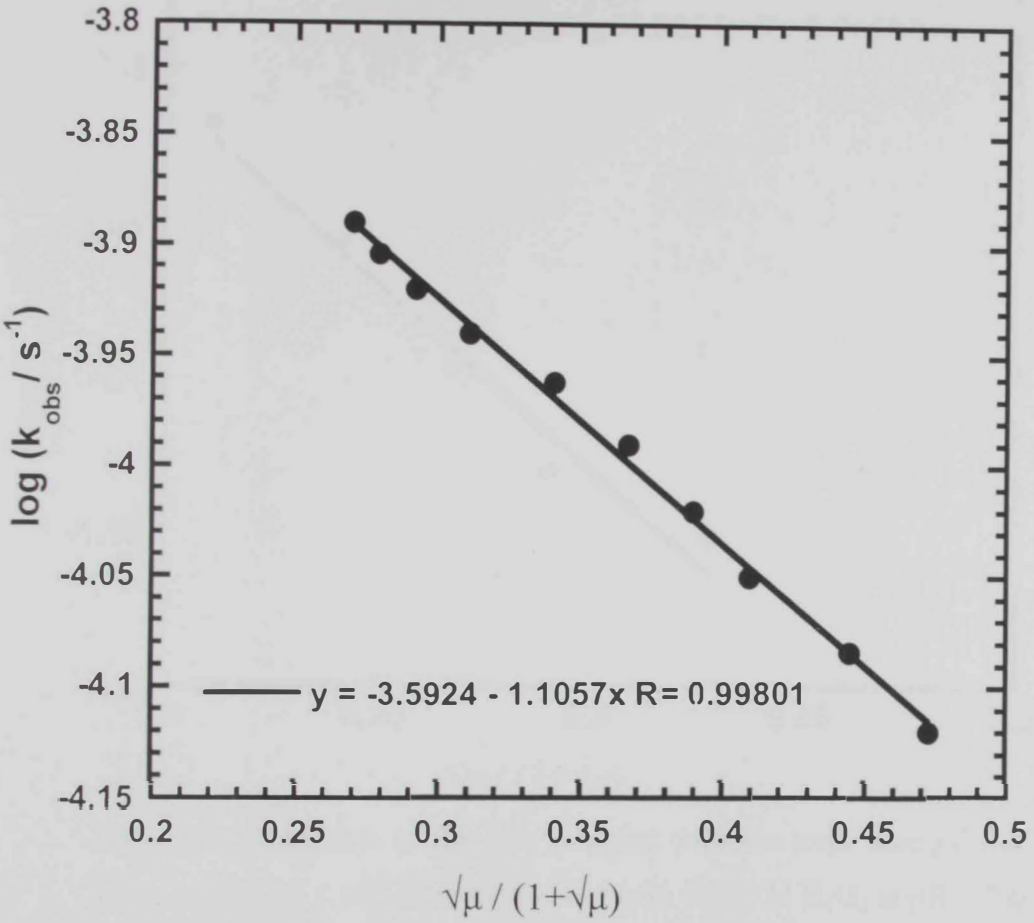

Fig. 3. 30. Variation of the rate constant with the ionic strength for the oxidation reaction of 3.34 x 10^{-5} M thionine with 0.50 M H_2O_2 at pH = 7.0 and 40°C.

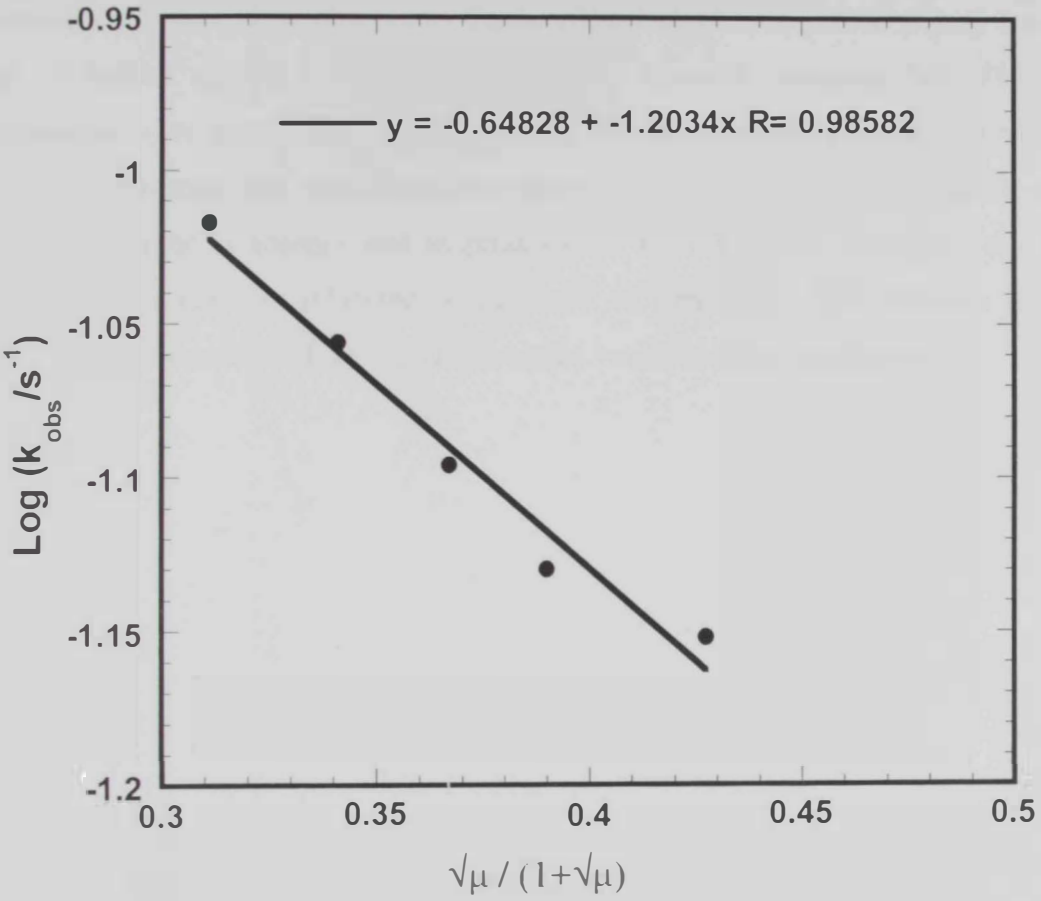

Fig. 3. 31. Variation of the rate constant with the ionic strength for the oxidation reaction of 3.34 x 10^{-5} M methyl violet with 0.992 M H_2O_2 at pH = 7.0 and 25°C.

3. 1. 7. **Detection of free radicals for the copper (II) catalyzed reaction**

The use of a free-radical trapping agent is a useful method for discovering whether or not free radical are implicated in the reaction mechanism [69, 89-91]. The radical species react preferentially with the trap and so a decrease in the rate of the radical reaction should be observed. Tertiary butyl alcohol is known to trap a wide range of radical species and have been used in peroxide reactions [69, 89, 91]. Experiments were carried out in presence of 4% t-butanol as a radical scavenger. Figure 32 represents the decomposition reaction of 0.1 M hydrogen peroxide with 0.20 M Cu^{+2} ions in absence and in presence of 4% t-butanol. It is clear that the reaction rate is strongly inhibited in presence of t-butanol. This submits strong evidence that that catalyzed reaction is proceded via free radical mechanism.

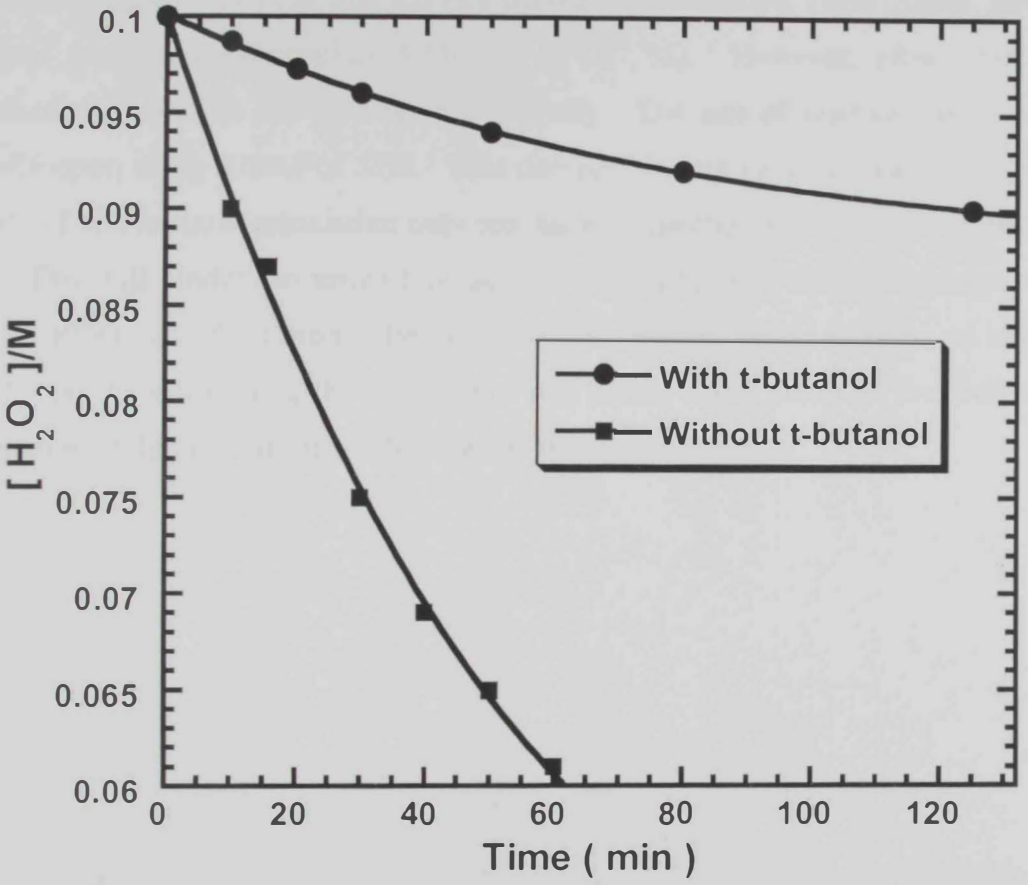

Fig. 3. 32. Decomposition of hydrogen peroxide with copper (II) in absence and in presence of 4% t-butanol at 25°C.

3. 1. 8. **Effect of sodium dodecyl sulfate, SDS**

The effect of anionic surfactants on the reaction rate was examined for degradation of thionine dye. Constant concentrations of 3.34 x 10^{-5} M of the dye was mixed with 0.5 M hydrogen peroxide at variable concentration of sodium dodecyl sulphate, (SDS). Figure 33 shows the absorbance decay with time. The initial reaction rates determined from figure 33 were then plotted versus [SDS], (Figure 34). From this figure it is clear that the rate decreases even at low [SDS] lower than the critical micelles concentration, CMC (3 X 10^{-3} M). However, after CMC was reached, the reaction rate decreased drastically. The rate of reaction decreased by 87.4% upon using 0.03M of SDS. This decrease in rate could be ascribed to some kinds of electrostatic association between anionic micelles and the cationic thionine dye. This will hinder the interaction between the negatively charged hydropeorxide anion, HOO^-, and the cationic dye which is now present inside the core of micelles [92]. On the other hand, the decrease in rate before CMC could be ascribed to the formation of dimers and trimers between SDS molecules [93].

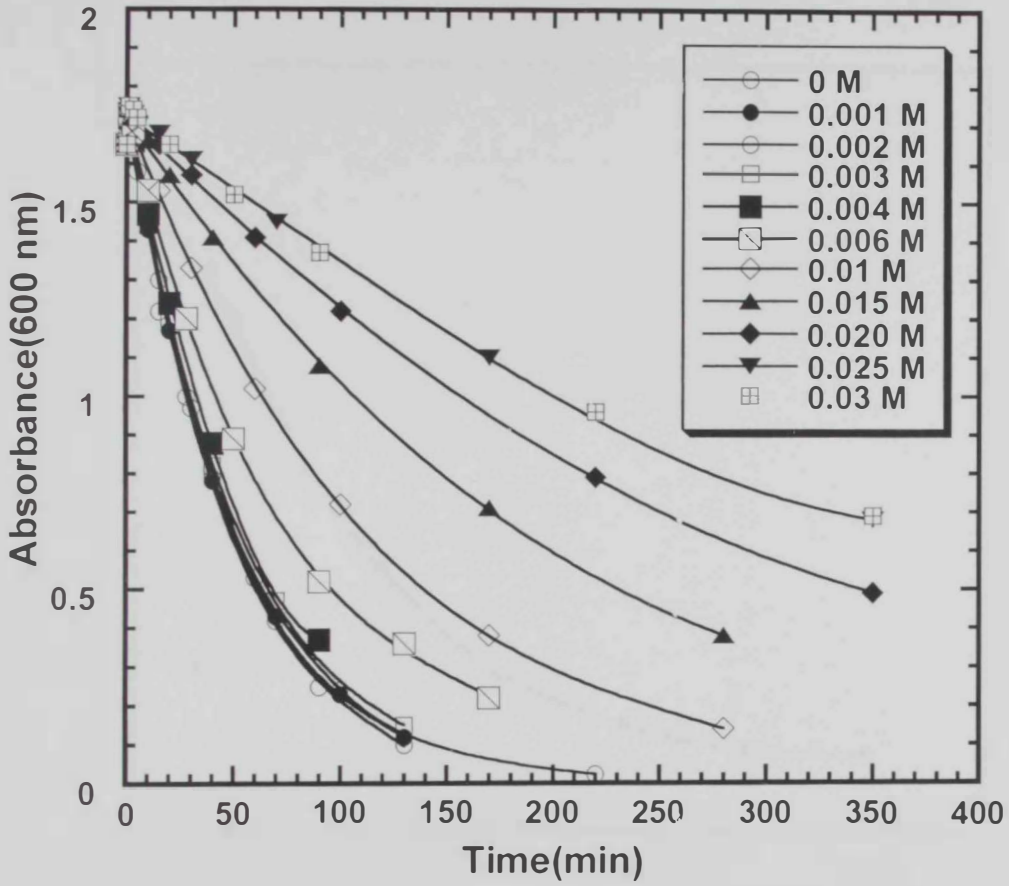

Fig. 3. 33. Absorbance – time curves for the reaction of 3.34 x 10^{-5} M thionine with 0.50 M H_2O_2 with different concentration of SDS at pH = 7.0, 40oC and the presence of 5.50 X 10^{-5} M Cu^{+2}.

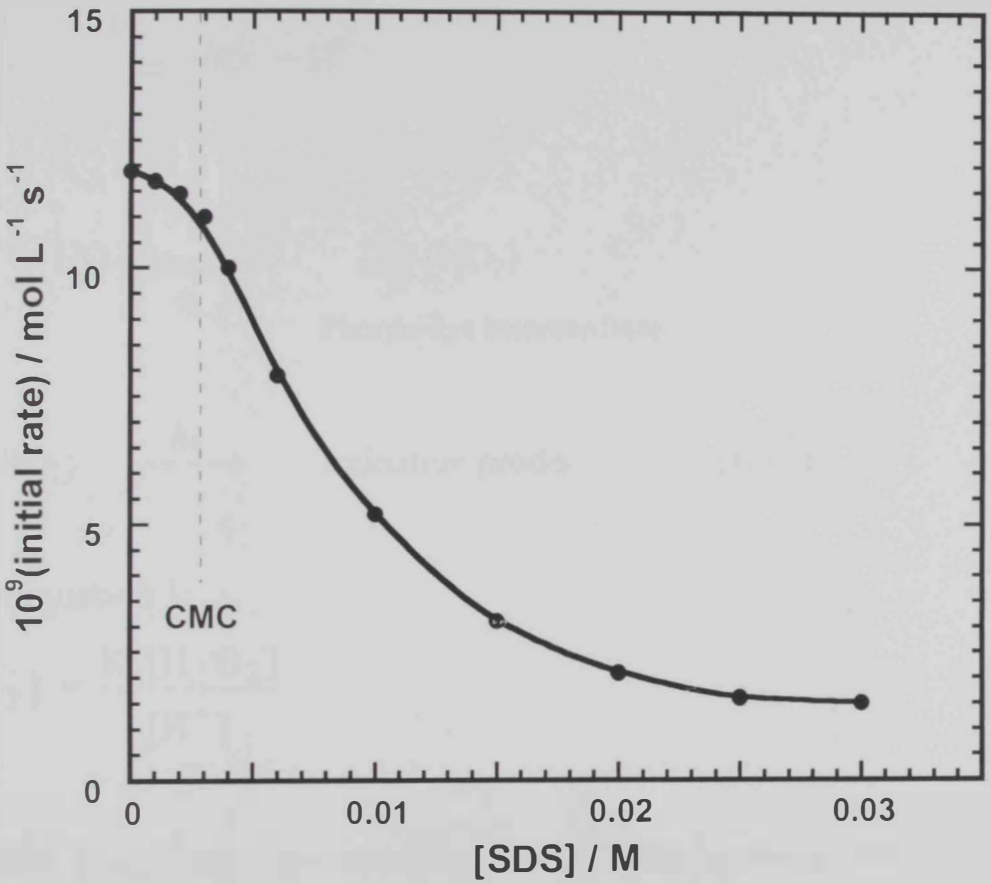

Fig. 3. 34. Variation of the initial reaction rate with different concentrations of SDS for the oxidation of 3.34 x 10^{-5} M thionine with 0.50 M H_2O_2 at pH = 7.0 and 40°C in the presence of 5.50 x 10^{-5} M Cu^{+2}.

3. 1. 9. Proposed reaction mechanism and the rate equation for the non-catalyzed reaction

Based on the results shown in this work, a mechanism that implies the dissociation of H_2O_2 in the first step with the production of hydroperoxide anions, HOO^- is proposed. The latter then attacks the substrate, to give a peroxo-dye intermediate, which in turn decomposes in the rate-determining step to give the final oxidation products according to the following mechanism:.

$$H_2O_2 \overset{k1}{=\!=\!=\!=} HO_2^- + H^+ \qquad (1)$$

$$DH^+ + HO_2^- \underset{k_{-2}}{\overset{k_2}{=\!=\!=\!=}} \underset{\textbf{Peroxo-dye intermediate}}{DH(HO_2)} \qquad (2)$$

$$DH(HO_2) \xrightarrow{k_3} \text{oxidation products} \quad \text{(slow)} \qquad (3)$$

From equation 1:

$$[HO_2^-] = \frac{K_1[H_2O_2]}{[H^+]} \qquad (4)$$

Applying steady state approximation for DH (HO_2) assuming that $k_2 >>> k_{-2}$, therefore:

$$\frac{d[QR(HO_2)^-]}{dt} = k_2[DH^+][HO_2^-] - k_3[DH(HO_2)] = 0$$

$$[DH(HO_2)^-] = \frac{k_2K_1[DH^+][HO_2^-]}{k_3[H^+]} \qquad (5)$$

From equations 3 and 5:

$$\text{Rate} = \frac{k_2 K_1 [DH^+][H_2O_2]}{[H^+]} \qquad (6)$$

Expressing the rate of reaction in terms of the initial concentration of the dye and the oxidant, $[DH^+]_0$ and $[H_2O_2]_o$ respectively, since:

$$[H_2O_2] = [H_2O_2]_o - [DH(HO_2)] \qquad (7)$$

$$[DH^+] = [DH^+]_0 - [DH(HO_2)] \qquad (8)$$

$$[DH^+][H_2O_2] = \frac{k_3[H^+][H_2O_2]_0[DH^+]_0}{k_3[H^+] + k_2K_1[DH^+]_0 + k_2K_1[H_2O_2]_0} \qquad (9)$$

Substituting in equation 6, the initial rate is given by;

$$\text{Rate} = \frac{k_2 k_3 K_1 [H_2O_2]_0 [DH^+]_0}{k_3[H^+] + k_2K_1[DH^+]_0 + k_2K_1[H_2O_2]_0} \qquad (10)$$

According to our experimental conditions, $[DH^+]_0$ is in the range of 10^{-5} and since $K_1 = 3.38 \times 10^{-12}$ mol L^{-1} at 40°C [94-96], therefore, the $k_2K_1[DH^+]_0$ term can be omitted from the denominator. Equation 10 then becomes:

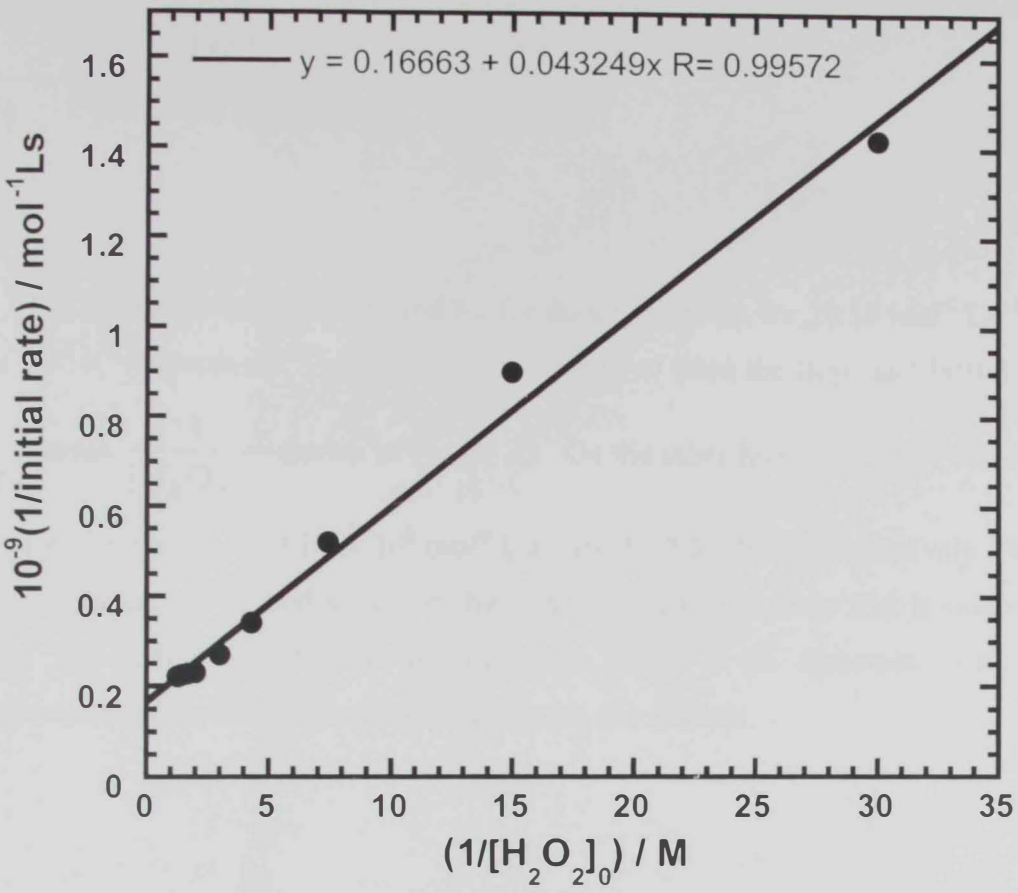

Fig. 3. 35. Reciprocal initial rate versus reciprocal initial hydrogen peroxide concentration for the oxidation of 3.34 x 10^{-5} M thionine at pH = 7.0 according to equation (12) at 40°C.

$$\text{Rate} = \frac{k_2 k_3 K_1 [H_2O_2]_0 [DH^+]_0}{k_3 [H^+] + k_2 K_1 [H_2O_2]_0} \qquad (11)$$

As seen from this equation, the rate of reaction attains a first-order dependence on the substrate, a first-order dependence on hydrogen peroxide only at lower concentrations, and is inversely proportional to $[H^+]$. However, the order of reaction in H_2O_2 decreases with increasing concentration and becomes zero at very high concentrations. Reciprocal of equation 11 gives:

$$\frac{1}{rate} = \frac{[H^+]}{k_2 K_1 [DH]_0 [H_2O_2]} + \frac{1}{k_3 [DH]_0} \qquad (12)$$

The estimated values for k_2 and k_3, for thionine system are 20.56 mol^{-1} L s^{-1} and 1.8 x 10^{-4} s^{-1} respectively. These values are calculated from the slope and intercept of $\frac{1}{\text{rate}}$ versus $\frac{1}{[H_2O_2]_0}$ shown in Figure 35. On the other hand, k_2 and k_3 values for methyl violet system are 3.16 X 10^2 mol^{-1} L s^{-1} and 5.65 X 10^{-2} s^{-1} respectively, Figure 36. Comparing the k_2 and k_3 values for both systems, it is clear that k values are greater for methyl violet than for thionine. This is in agreement with our experimental results and supporting our proposed mechanism.

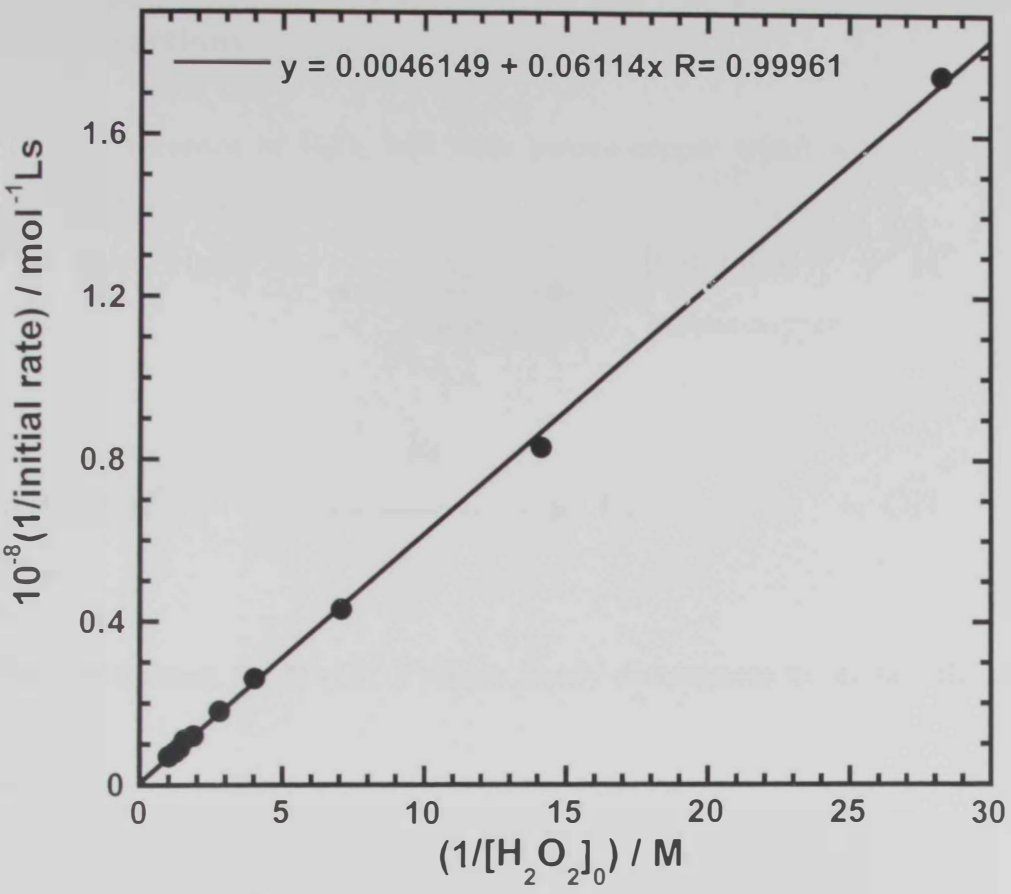

Fig. 3. 36. Reciprocal initial rate versus reciprocal initial hydrogen peroxide concentration for the oxidation of 3.34 x 10^{-5} M methyl violet at pH = 7.0 according to equation (12) at 25°C.

3. 1. 10. Proposed reaction mechanism and rate equation of copper catalyzed reactions

Cu^{2+} in presence of H_2O_2 will form peroxo-copper which will in turn form hydroxy radical as follow:

$$Cu^{2+} + H_2O_2 \underset{\text{Catalyst}}{\overset{k_2}{\longleftrightarrow}} [Cu(OOH)]^+ + H^+ \quad (13)$$

peroxo-copper

$$[Cu(OOH)]^+ \xrightarrow{k_4} Cu^+ + \tfrac{1}{2} O_2 + OH^{\bullet} \quad (14)$$

The $OH^{\bullet}$ Will attack the $D^+(OH^{\bullet})$ Which slowly decomposes to produce the oxidation products

$$DH^+ + OH^{\bullet} \xrightarrow{k_5} D^+(OH^{\bullet}) \quad (15)$$

$$DH^+(OH^{\bullet}) \xrightarrow{k_6,\ \text{slow}} \text{oxidation products} + CO_2 \quad (16)$$

meanwhile, hydroxy radical oxidizes Cu^+ ions to Cu^{2+} ions

$$Cu^+ + HO^{\bullet} \xrightarrow{k_7} Cu^{2+} + OH^- \quad (17)$$

H^+ and OH^- (steps 13, 17) are combining to form H_2O

$$OH^- + H^+ \rightarrow H_2O \quad (18)$$

Applying steady state approximation for $[HO^{\cdot}]$ and $[D^+(OH^{\cdot})]$;

$$\frac{d[HO^{\bullet}]}{dt} = 0 = k_4[Cu^{2+}(OOH)] - k_5[DH^{+}][HO^{\bullet}] - k_7[Cu^{+}][HO^{\bullet}] \quad (19)$$

Since, $[Cu^{+}] = [Cu^{2+}(OOH)]$ (20)

and $[Cu^{2+}(OOH)] = K_2[Cu^{2+}][H_2O_2]/[H^{+}]$ (21)

Therefore,

$$[HO^{\bullet}] = \frac{k_4 k_2[S-Cu^{2+}][H_2O_2]}{k_5[BPB][H^{+}] + k_2 k_7[S-Cu^{2+}][H_2O_2]} \quad (22)$$

and,

$$\frac{d[DH^{+}(OH^{\bullet})]}{dt} = 0 = k_5[DH^{+}][HO^{\bullet}] - k_6[DH^{+}(OH^{\bullet})]$$

Therefore;

$$[D^{+}(OH^{\bullet})] = \frac{k_4 k_5 k_2[D^{+}][Cu^{2+}][H_2O_2]}{k_5 k_6[D^{+}][H^{+}] + k_2 k_6 k_7[Cu^{2+}][H_2O_2]} \quad (23)$$

The rate equation is given from the rate-determining step, equation 16, by;

Rate = $K_6\,[D^{+}(OH^{-})]$

$$Rate = \frac{k_4 k_5 k_2[DH^{+}][Cu^{2+}][H_2O_2]}{k_5[DH^{+}][H^{+}] + k_2 k_7[Cu^{2+}][H_2O_2]} \quad (24)$$

Expressing for the initial concentrations of both Hydrogen peroxide, $[H_2O_2]_o$, and the dye, $[DH^{+}]_o$, since;

$[H_2O_2]_o = [H_2O_2] + [Cu^{2+}(OOH)] + [H\bullet^{\bullet}]$ (25)

Substituting from equations 21 and 22, therefore,

$$[H_2O_2] = \frac{(k_7[H_2O_2]_o - k_4)[H^+]}{k_7[H^+] + k_2k_7[Cu^{2+}]} \quad (26)$$

also,

$[DH^+]_o = [DH^+] + [DH^+(OH^{\bullet})]$

(27)

Substituting from equation 23 and assuming that $k_5k_6[DH^+][H^+] << k_2k_6k_7[Cu^{2+}][H_2O_2]$, therefore;

$$[DH^+] = \frac{k_6k_7[DH^+]_o}{k_6k_7 + k_5k_4} \quad (28)$$

From equations 24, 26 and 28, the rate is given by;

Rate=

$$\frac{k_4k_5k_6k_7k_2[DH^+]_o[Cu^{2+}][H_2O_2]_o}{k_5k_6k_7[DH^+]_o([H^+]+K_2[Cu^{2+}]) + k_2k_7[Cu^{2+}][H_2O_2]_o(K_2k_7k_6+k_4k_5)}$$

Assuming that $k_7k_6K_2 >> k_4k_5$, therefore,

$$\text{Rate} = \frac{k_4k_5K_2[DH^+]_o[Cu^{2+}][H_2O_2]_o}{k_5[DH^+]_o([H^+]+K_2[Cu^{2+}]) + K_2^2k_7[Cu^{2+}][H_2O_2]_o} \quad (29)$$

This equation demonstrates that, at lower $[DH^+]_o$, the first term in the denominator becomes very small compared to the second one and can be neglected. Therefore, the rate attains a first order dependence on $[DH^+]_o$. However, with increasing $[DH^+]_o$, the rate decreases and attains a limiting rate at higher concentrations, (Figure 12). This equation

predicts also that, the rate has a first order dependence on $[H_2O_2]_o$ at low concentrations. With increasing concentration, however, the reaction rate decreases and attains a limiting rate at relatively high concentrations, (Figures 7 and 8). Equation 29 can be written in the reciprocal form;

$$\frac{1}{\text{rate}} = \frac{[H^+] + K_2[Cu^{2+}]}{k_4 K_2 [Cu^{2+}][H_2O_2]_o} + \frac{K_2 k_7}{k_4 k_5 [DH^+]_o} \qquad (30)$$

Plotting 1/rate versus $1/[H_2O_2]_o$ gave straight line, (Figures 37 and 38) for thionine and methyl violet, respectively. From slopes and intercepts, some tentative values for k_7 and k_4 were calculated using an average value for k_2 as 10^{-9} [97]. The produced k_7 values are equal to 5.34 X 10^{10} $M^{-1}s^{-1}$ and 6.89 X 10^{10} $M^{-1}s^{-1}$ for thionine and methyl violet at 40°C and 25°C respectively. The corresponding rate constants for the formation of $HO^{\cdot}$ radicals, k_4, gave values of 2.50 X 10^{-11} and 7.94 X 10^{-10} $mol^{-1}Ls^{-1}$ for thionine and methyl violet at 40°C and 25°C, respectively. Beltran and Gonzales have reported k_5 values in the range 10^8 to 10^{10} $Ml^{-1}Ls^{-1}$ for the overwhelming majority of organic compounds [98]. The value k_5 10^9 $M^{-1}L\ s^{-1}$ was used in our calculations.

3. 1. 11. Rate mechanism at high H_2O_2 concentration:

Equation 29, however, could not explain the decrease in rate at higher $[H_2O_2]_o$. This decrease was ascribed to the fast interaction of hydroxyl radicals with excess hydrogen peroxide or its peroxide anion, HO_2^-,[82, 99, 100]. This leads to the formation of superoxide anion, $O_2^{\bullet}$.

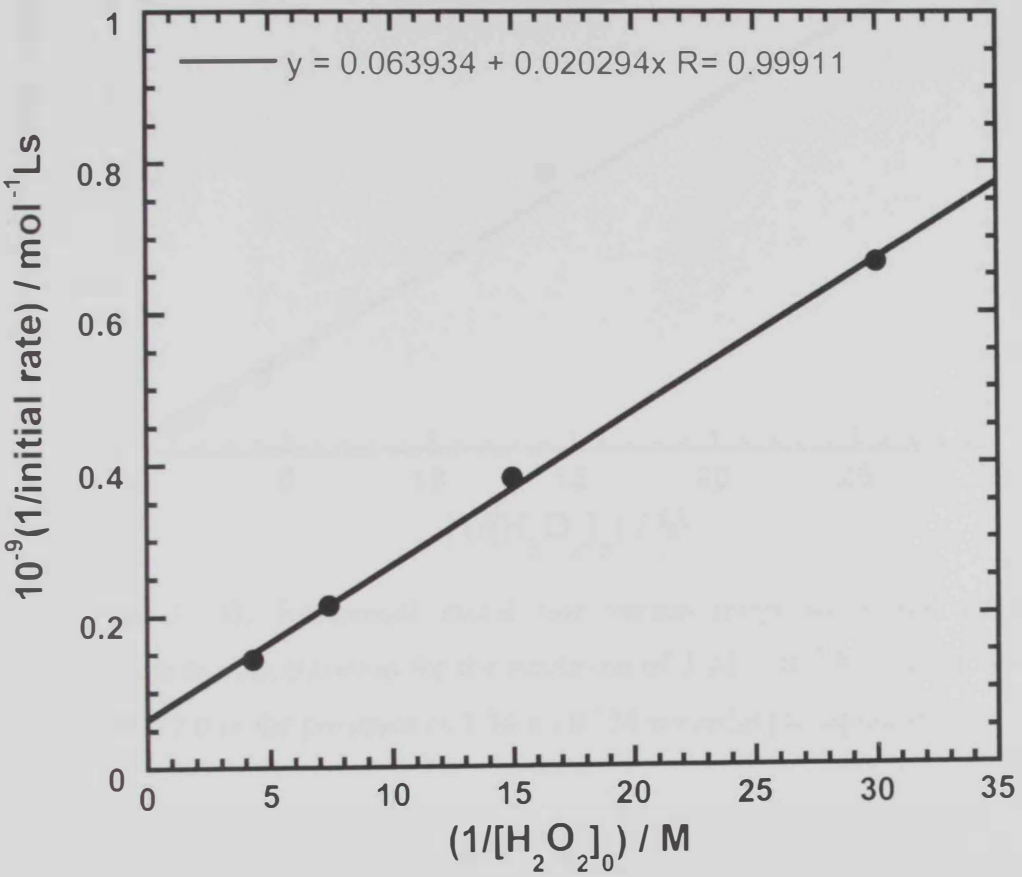

Fig. 3. 37. Reciprocal initial rate versus reciprocal initial hydrogen peroxide concentration for the oxidation of 3.34 x 10^{-5} M thionine at pH = 7.0 in the presence of 2.0 x 10^{-5} M according o equation (30).

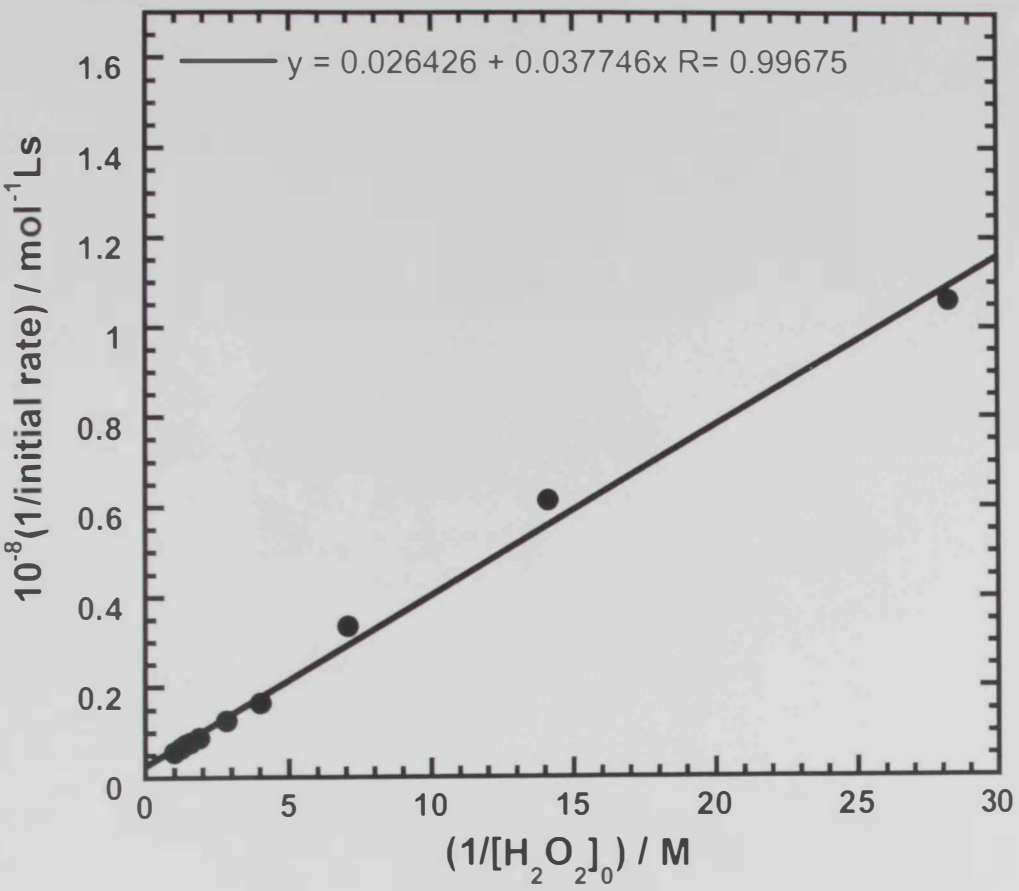

Fig. 3. 38. Reciprocal initial rate versus reciprocal initial hydrogen peroxide concentration for the oxidation of 3.34 x 10^{-5} M methyl violet at pH = 7.0 in the presence of 3.34 x 10^{-5} M according to equation (30).

Or its conjugate acid, $HO_2^{\bullet}$ which are less active than hydroxyl radicals (E^{o} = 0.89 V at pH = 7 for $O_2^{-\bullet}$ and 1.44 V for $HO_2^{\bullet}$ at pH = 0) [101] the following mechanism, could be suggested at high concentration

$$H_2O_2 \xrightleftharpoons{k_1} HO_2^{-} + H^{+} \quad (1)$$

$$Cu^{2+} + HO_2^{-} \xrightleftharpoons{k_3} Cu^{2+}(OOH) \quad (31)$$

$$Cu^{2+}(OOH) \xrightarrow{K_4} Cu^{+} + OH^{\bullet} + \tfrac{1}{2}O_2 \quad (14)$$

$$OH^{\bullet} + HO_2^{-} \xrightarrow{k_8} O_2^{-\bullet} \quad (32)$$

$$O_2^{-\bullet} + DH^{+} \xrightarrow{k_9,\ slow} \text{oxidation products} \quad (33)$$

$$Cu^{+} + O_2^{-\bullet} + H^{+} \xrightarrow{k_{10}} Cu^{2+}OH + \frac{1}{2}O_2 \quad (34)$$

Applying steady state approximation for $HO^{\bullet}$ and $O_2^{-\bullet}$ species;

$$\frac{d[OH^{\bullet}]}{dt} = 0 = k_4[Cu^{2+}(OOH)] - k_8[HO^{\bullet}][HO_2^{-}] \quad (35)$$

$$\frac{d[O_2^{-\bullet}]}{dt} = 0 = k_8[HO^{\bullet}][HO_2^{-}] - k_9[O_2^{-\bullet}][DH^{+}] - k_{10}[O_2^{-\bullet}][Cu^{+}] \quad (36)$$

From equations 4, 35 and 36;

$$[O_2^{-\bullet}] = \frac{k_4k_2[Cu^{2+}][H_2O_2]}{k_9[DH^{+}][H^{+}] + k_2k_{10}[Cu^{2+}][H_2O_2]} \quad (37)$$

According to equation 33,the rate is given by;

Rate = $k_9 [DH^+] [O_2^{-\bullet}]$

$$\text{Rate} = \frac{k_4 k_9 k_2 [Cu^{2+}][DH^+][H_2O_2]}{k_9[DH^+][H^+] + k_2 k_{10}[Cu^{2+}][H_2O_2]} \quad (38)$$

From equations 4 and 35

$$[HO^\bullet] = \frac{k_4 K_3}{k_8} \quad (39)$$

As before, since,

$$[H_2O_2]_o = [H_2O_2] + [Cu^{2+}(OOH)] + [HO^\bullet] + [O_2^{-\bullet}] \quad (40)$$

Substituting from equations, 21,37 and 39 in equation 40 gives;

$$[H_2O_2] = \frac{k_8 k_{10}[H_2O_2]_o[H^+] - k_4(k_{10}K_3 + l_8)[H^+]}{k_8 k_{10}[H^+] + k_8 k_{10} K_2[Cu^{2+}]} \quad (41)$$

From equations 38 and 41, the rate is given by;

$$Rate = \frac{k_4 k_9 [Cu^{2+}][DH^+](k_8 k_{10}[H_2O_2]_o - k_4(k_{10}K_3 + k_8))}{k_8 k_9 k_{10}[D^+][DH^+] + k_8 k_9 k_{10}[DH^+] + k_8 k_{10}^2[H_2O_2]_o - k_4 k_8 k_{10}} \quad (42)$$

k_8 is reported as 7.5×10^9 $mol^{-1} L\ s^{-1}$ [29], assuming that $k_4 >> k_{10}$, therefore, $k_4(k_{10} K_3 + k_8) >> k_8 k_{10}$, and the reaction rate becomes negative. However, with increasing $[H_2O_2]_o$, both the denominator and numerator will be increased, but the increase in numerator will

be significant and the rate of reaction decreases. Within the scope of our experimental results, the rate never reached zero, i.e. $k_8 k_{10}[H_2O_2]_o \neq k_4 (k_{10}K_3 + k_8)$.

Section II

3.2. Analysis of degradation Products

In the following schemes, suggested degradation mechanisms for thionine and methyl violet are presented.

Scheme 1 shows the uncatalytic decomposition mechanism of thionine dye. H_2O_2 ionizes into H^+ and HO_2^- which will attack the S^+ This leads to cracking of the central ring giving rise to two possible cracking modes 1 and 2 as shown in the scheme.

Scheme 2, represents the catalytic decomposition of methyl violet dye. Cu^{2+} reacts with H_2O_2 giving rise to $Cu^{2+}(OOH)$ which will dissociates into Cu^{2+} and OH^- free radicals. Free radicals will attack the N^+ of methyl violet leading to three possible simultaneous bonds cracking. Hence, three degradation products are expected for methyl violet.

3.2.1. Elemental Analysis.

Table 3.1. shows C, H, N and S elemental analysis of pure thionine and methyl violet together with their degradation products. Good correlation between calculated and found values of pure thionine and methyl violet are shown.

A discrepancy between calculated and found values of thionine degradation product is observed. This can be attributed to either incomplete degradation process or to the production of more than one product.

Good agreement between calculated and found values for methyl violet degradation product is shown in table3.1. This may reflect a complete degradation process and/or structurally similar degradation product.

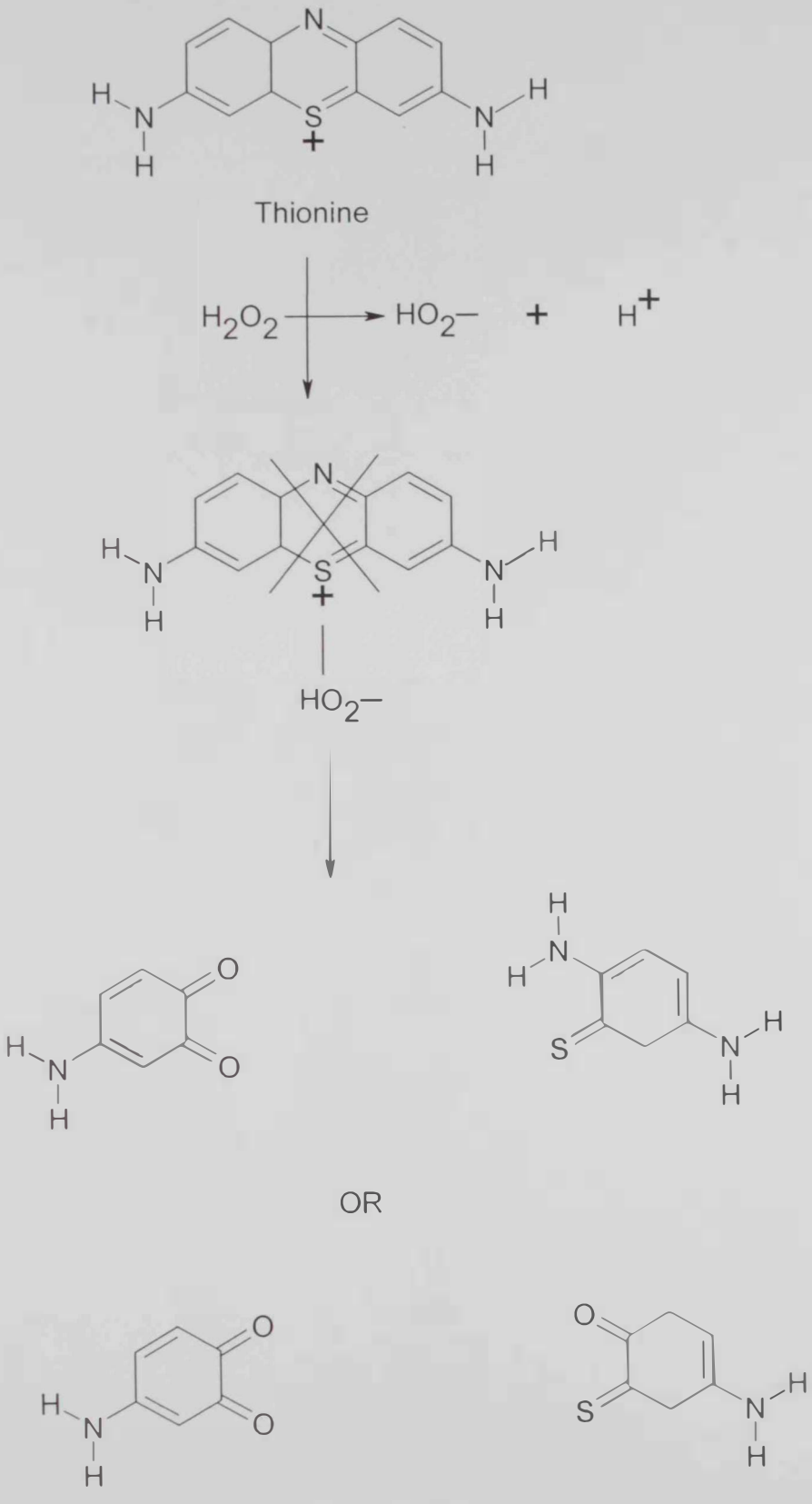

Scheme 1. Suggested mechanism for thionine degradation by H_2O_2.

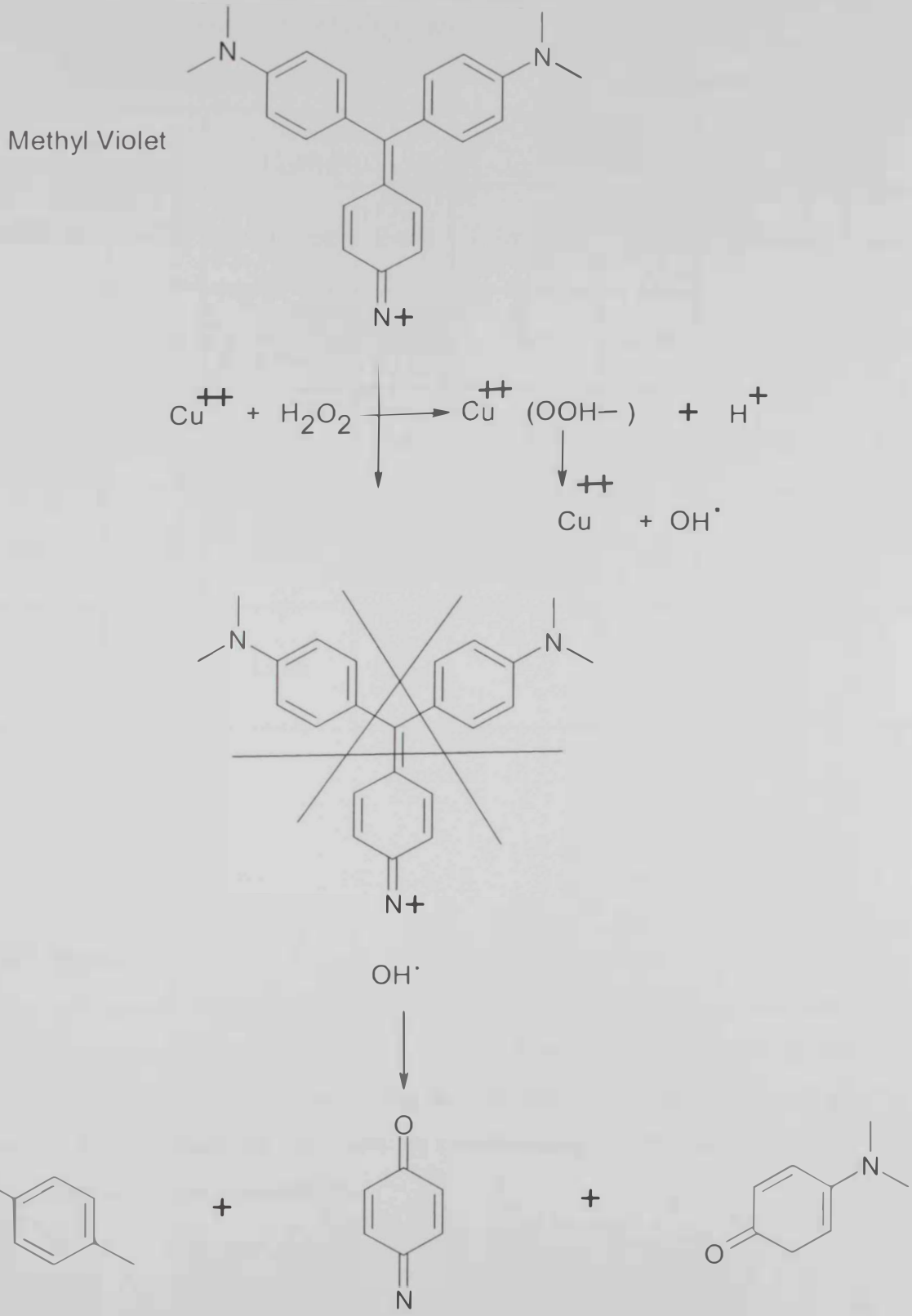

Scheme 2. Suggested mechanism for methyl violet degradation by H_2O_2 in presence of Cu^{2+} ions.

Table 3.1. C, H, N ans S elemental analysis of pure and degradation products of thionine and methyl violet dyes. Degradation was done by H_2O_2 in absence of Cu^{2+} catalyst.

% element	Thionine				Methyl Violet			
	Pure		Product $C_{12}H_{11}N_3OS$		Pure		Product $C_8H_{10}NOCl$	
	calculated	found	calculated	found	calculated	found	calculated	found
C %	58.47	57.82	58.7	47.60	73.1	64.75	55.9	54.05
H %	4.52	4.42	4.49	3.40	7.11	7.02	5.83	4.55
N %	14.62	14.86	17.1	14.00	10.66	9.48	8.16	8.18
S %	11.14	11.51	13.06	12.37	--	--	--	--

3.2.2. IR Spectra

Infra red spectra of pure thionine and methyl violet compounds and their degradation products are shown in Figs 39-40. Fig. 3.39a for pure thionine shows bands at 3421 and 2966 cm^{-1} corresponding to N-H stretching vibration. Bands at 1548 cm^{-1}, 1113 cm^{-1}, 3080 cm^{-1} are possibly corresponding to N=C, S=C, and C-H or $_N$-H bending vibrations, respectively.

Fig. 3.39b for thionine degradation product shows a C=O stretching vibration at 1640 cm^{-1} indicating the formation of a carbonyl compound produced by H_2O_2 oxidation. Disappearance of the band at 1548 cm^{-1} indicates the breakdown of N=C bond as suggested by path one degradation whereas the appearance of strong band at 1640 cm^{-1} indicates the formation of carbonyl compounds.

Fig. 3.40a for pure methyl violet shows IR band at 1584 cm^{-1} corresponds to C=N stretching vibration. The bands at 1475 cm^{-1} (s) corresponds to C=C stretching vibrations. The bands at 1360 (s) and 1168 (s) are corresponding to C-N, $-CH_3$ (γ).

IR spectra for degradation product of methyl violet is shown in Fig. 3.40b. The band at 1584 cm^{-1} is shifted to ~1600 cm-1 indicating the formation of C=O upon oxidation with H_2O_2. New bands at 1517 cm^{-1} corresponds to $=NH_2$ stretching vibration suggesting path one degradation.

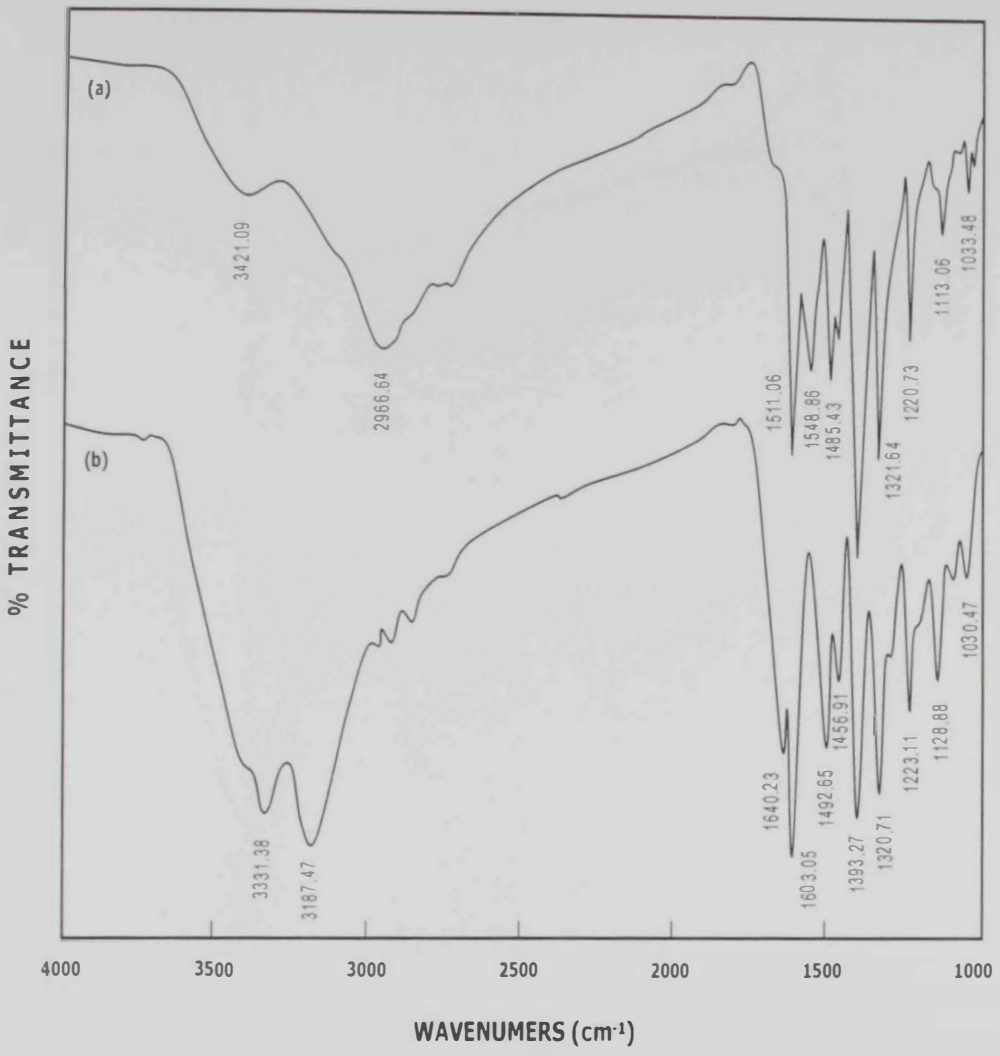

Fig. 3.39. Infrared spectra of thionine (a) and thionine degradation product (b)

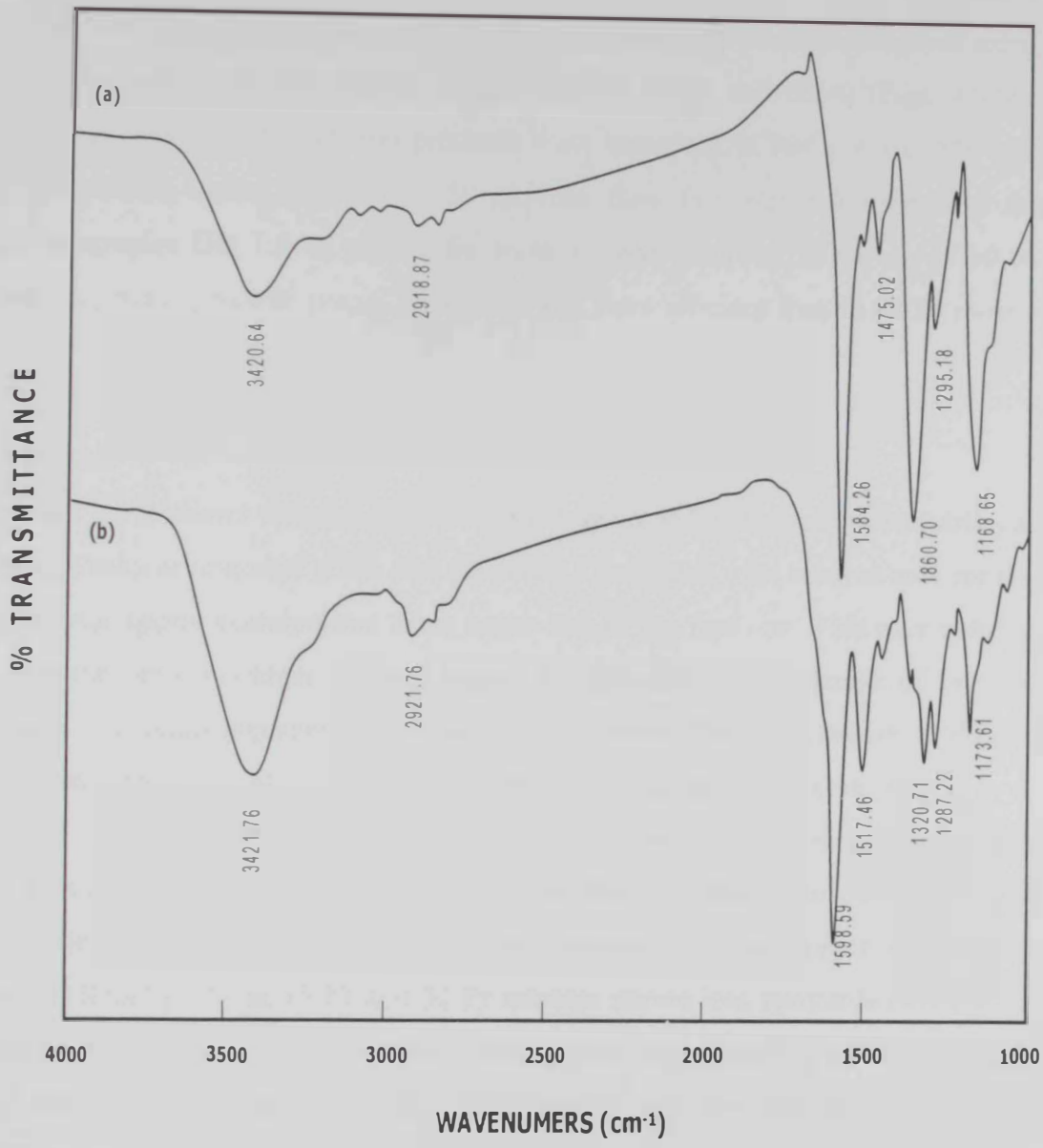

Fig. 3.40. Infrared spectra of methyl violet (a) and methyl violet degradation product (b)

3. 2. 3. High performance liquid chromatography (HPLC)

The two dyes under investigation was measured in reversed phase mode using water-acetonitrile as mobile phases in the ratios of 80:20 and 60:40 (Figs. 41-44). Compounds and their degradation products were measured at 304 nm and 580 nm. Injected volume varied between 10-50 µl. The flow rate was 1.0 ml/minute for thionine samples and 1.5 ml/minute for methyl violet samples. However, in 60:40 (water:acetonitrile) mobile phase, separation was more efficient than in 80:20 mobile phase.

A) Thionine

Fig. 3.41a shows thionine HPLC chromatogram in 80:20 (water:acetonitrile) at 304 nm. Peaks at retention times of 3.83 and 6.37 minutes with relative area for the second peak approximately three times larger that of the first one. This may indicate the dyes themselves contain a second isomer for thionine. At wavelength of 580 nm, the same two peaks appeared at 3.77 and 6.27 minutes. This indicates that thionine can be measured either at 304 or at 580 nm without much difference (Fig. 3.41b).

Fig. 3.42a shows HPLC chromatogram of thionine degradation products at the same previous conditions. At 304 nm, two main peaks at retention times of 19.59 and 31.05 minutes are obtained indicating the existence of two major degradation products. Small peaks at 15.13 and 37.89 minutes shows less favorable degradation products (Scheme 1). At 580 nm, only strong peak corresponding to mobile phase (dead time) were obtained (Fig. 3.42b). This indicated that products have insignificant absorption at 580 nm.

B) Methyl Violet.

Fig. 3.43a shows methyl violet HPLC chromatogram in 60:40 (water:acetonitrile) at 304 nm with flow rate of 1.5 ml/minute. Peaks at retention times of 8.63, 10.42 and 12.90 minutes with third one has larger area than that of the second than of the third. This may indicate the dyes themselves contain three isomers for methyl violet. At wavelength of 580 nm, the same three peaks appeared at 8.23, 10.10 and 12.62 minutes. This indicates that thionine can be measured at either 304 or at 580 nm without much difference (Fig. 3.43b).

Fig. 3.44a shows HPLC chromatogram of methyl violet degradation products at the same previous conditions. At 304 nm, three main peaks at retention times of 5.02, 6.46 and 11.34 minutes are obtained indicating the existence of three major degradation products. (Scheme 2). At 580 nm, strong peak corresponding to mobile phase (dead time) were obtained (Fig. 3.44b). This indicated that products have insignificant absorption at 580 nm (scheme 2).

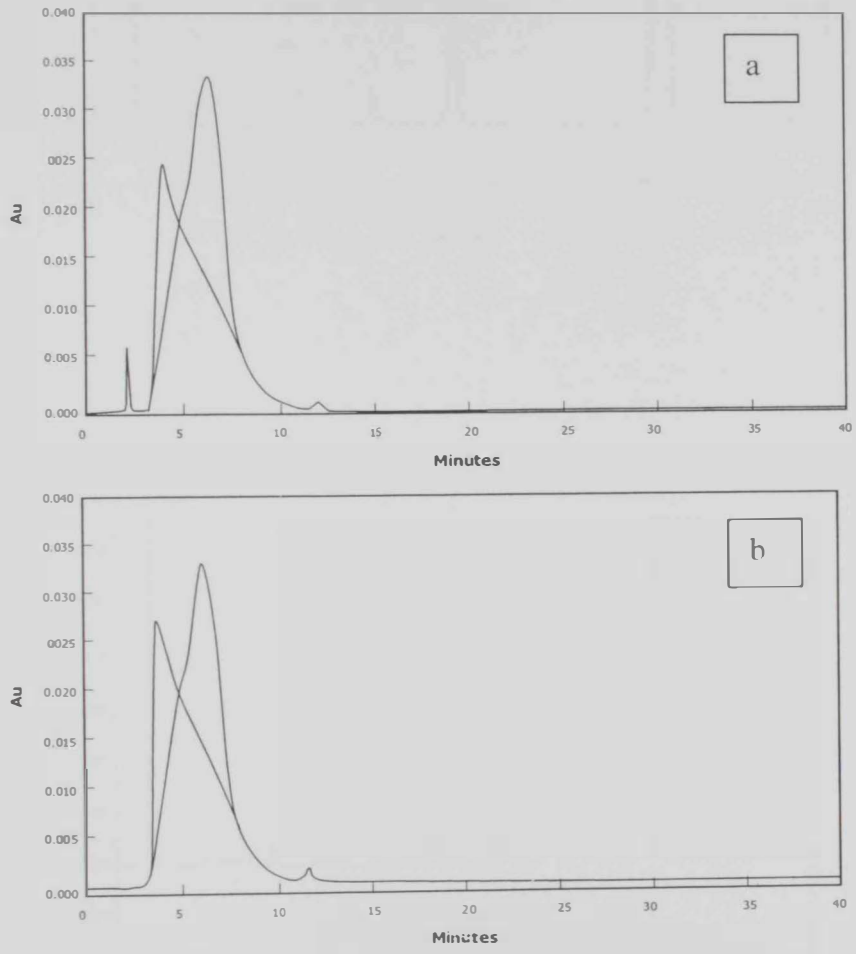

Fig. 3. 41. Reversed phase HPLC chromatograms for thionine using water-acetonitrile as mobile phases in the ratios of 80:20 at 1 ml/minute flow rate. Compounds were measured at 304 nm (a) and at 580 nm (b).

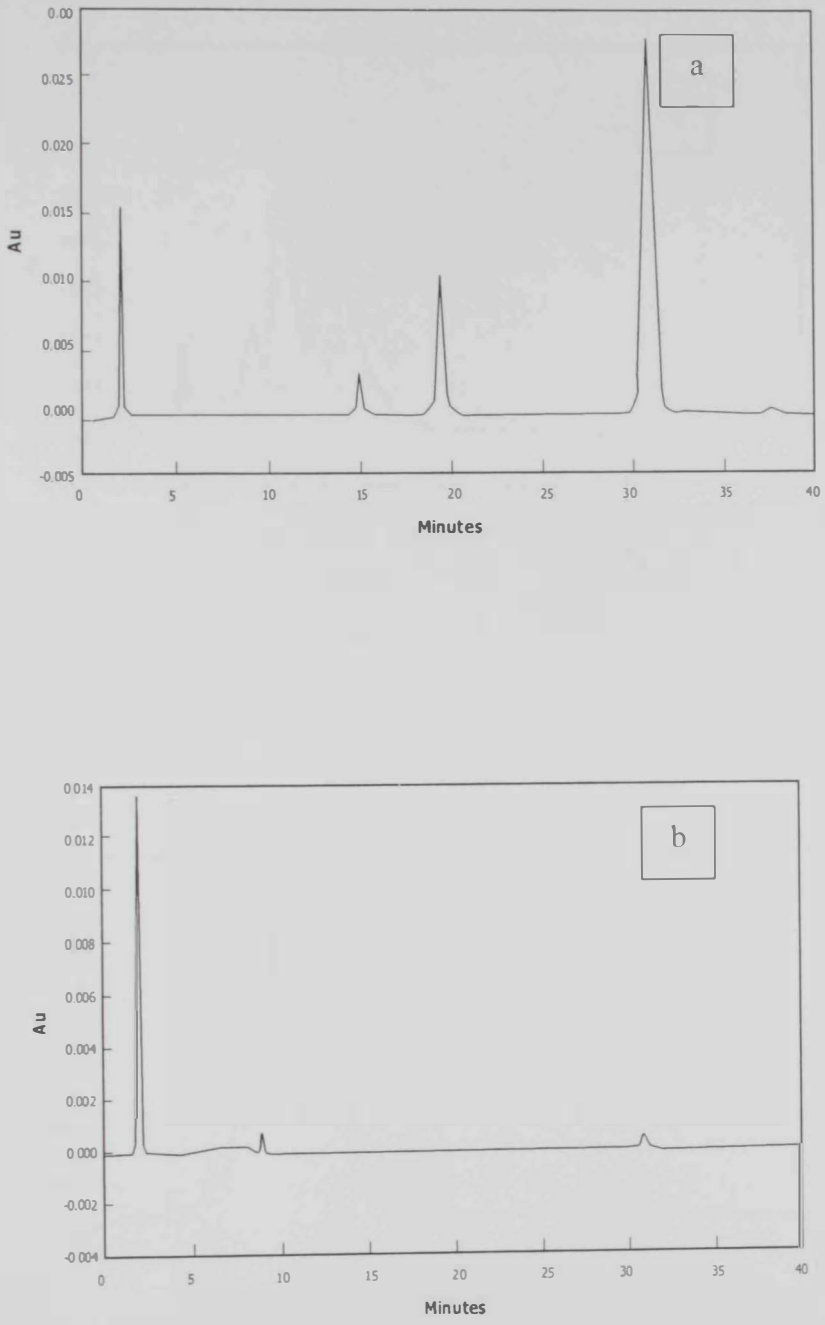

Fig. 3. 42. Reversed phase HPLC chromatograms for thionine degradation products using water-acetonitrile as mobile phases in the ratios of 80:20. Products were measured at 304 nm (a) and at 580 nm (b).

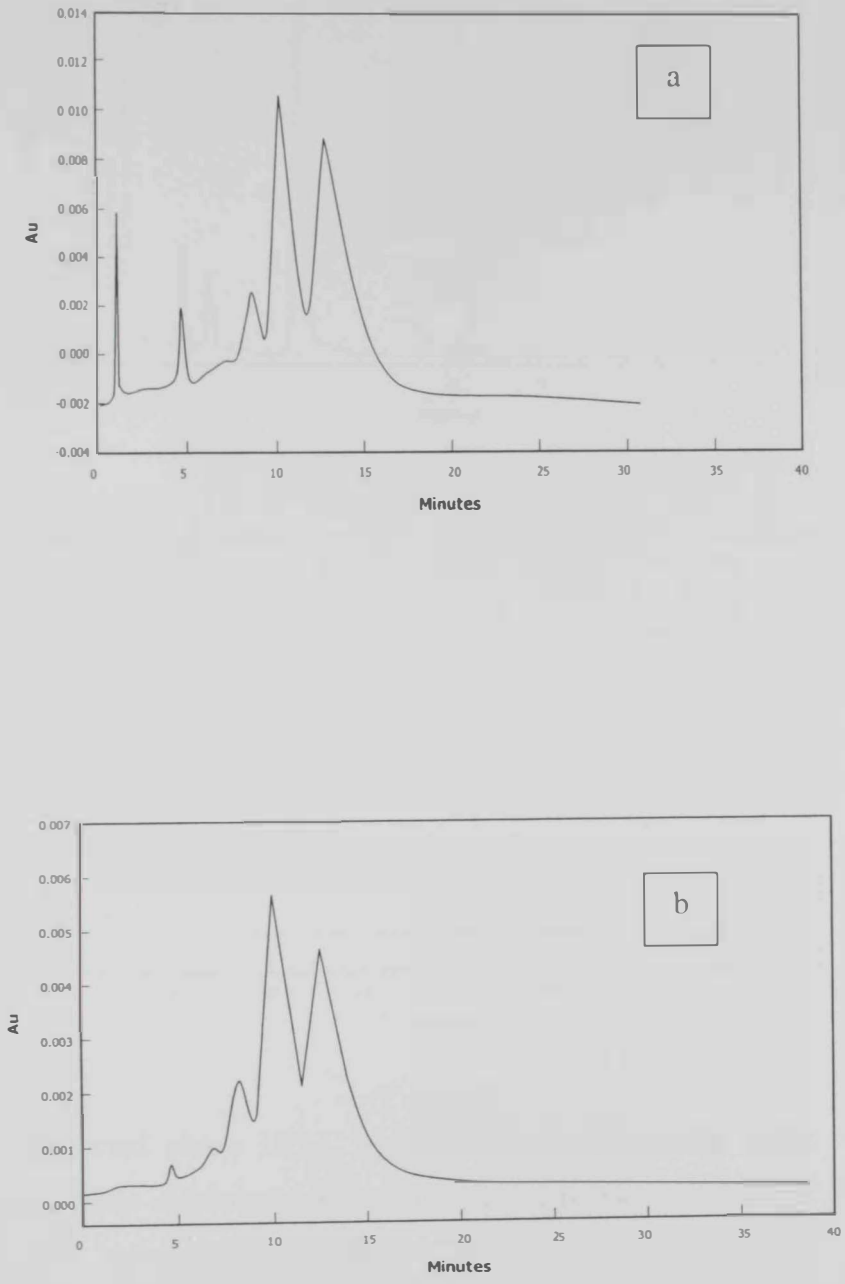

Fig. 3. 43. Reversed phase HPLC chromatograms for methyl violet using water-acetonitrile as mobile phases in the ratios of 60:40 at 1.5 ml/minute flow rate. Compounds were measured at 304 nm (a) and at 580 nm (b).

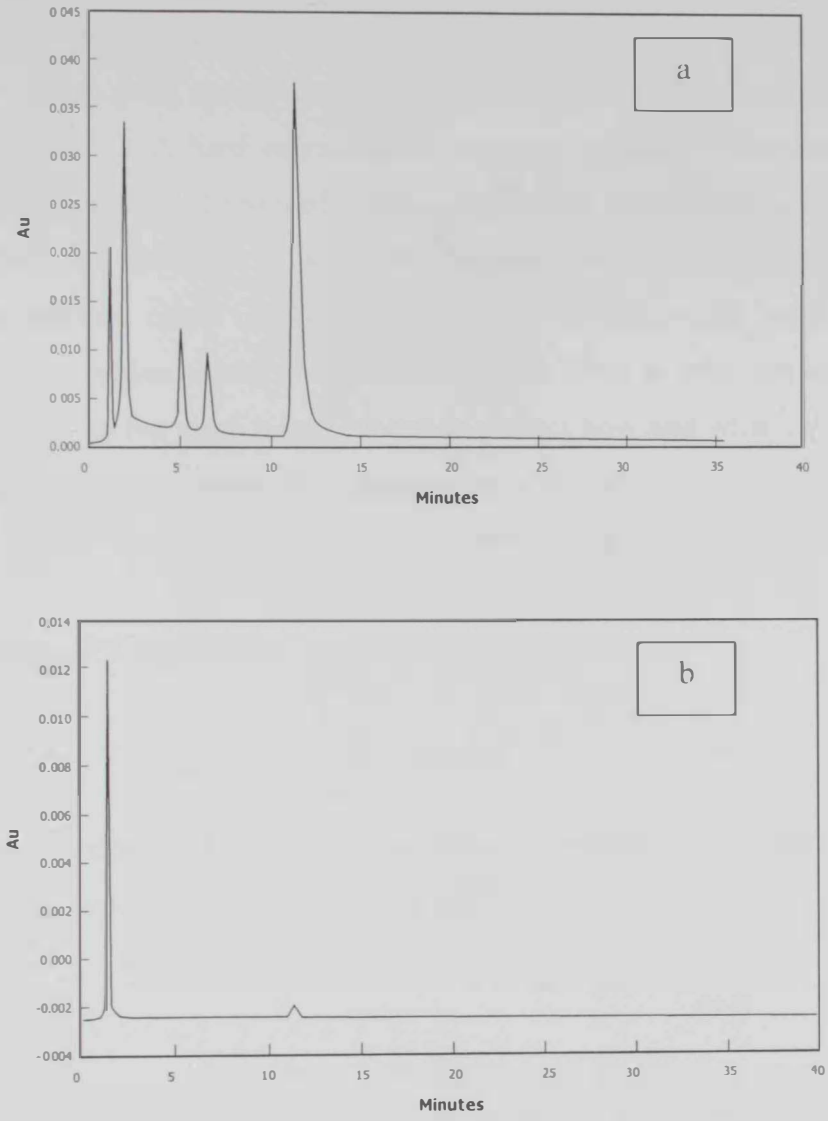

Fig. 3. 44. Reversed phase HPLC chromatograms for methyl violet degradation products using water-acetonitrile as mobile phases in the ratios of 80:20. Products were measured at 304 nm (a) and at 580 nm (b).

3. 3. Computational approach:

The Hartree-Fock-Slater Self-Consistent Field method [102-105] was applied to calculate the single point energy for all the proposed products in the dye degradation, scheme 3.1. and 3.2. A hard experimental evidences could not obtained about the degradation products and the rout of reaction. Therefore, computational methods were used to predict the best rout in which the degradations happened. Products of the degradation reaction could not be separated by chromatography since they have similar structure, physical and chemical properties. That is why molecular orbital calculations will be the most suitable mean to predict how and what are the product being formed. By calculating the single point energies of the proposed product structures, the rout that produces the smaller energies is going to be the most favored one.

The one electron HF hamiltonian can be written as follows .

$$F_{(1)} = -\frac{1}{2}\nabla_1^2 - \sum \frac{Z_\alpha}{r_{1\alpha}} + \sum_{j=1}^{\frac{1}{2}} \left[2J_j(1) - K_j(1)\right] \qquad (43)$$

where J_j and K_j are the coulomb and the exchange operators, respectively.

For polyatomic molecules , the hamiltonian will be

$$H = H_{el} + V_{NN}$$

$$\text{where } H_{el} = -\frac{1}{2}\sum_i \nabla_1^2 - \sum_\alpha \sum_i \frac{Z_\alpha}{r_{1\alpha}} + \sum_j \sum_{i>j} \frac{1}{r_{ij}} \qquad (44)$$

$$\text{and } V_{NN} = \sum_\alpha \sum_{\beta>\alpha} \frac{Z_\alpha Z_\beta}{r_{\alpha\beta}}$$

where the indices i and j represent electrons and α and β represent nuclei.

The HF method is applied on those orbitals ϕi that will minimize the following integral

$$E_{HF} = 2\sum_{i=1}^{\frac{n}{2}} h_i + \sum_i^{\frac{n}{2}} \sum_j^{\frac{n}{2}} (2J_{ij} - K_{ij}) + V_{NN} = \langle D|H|D\rangle \qquad (45)$$

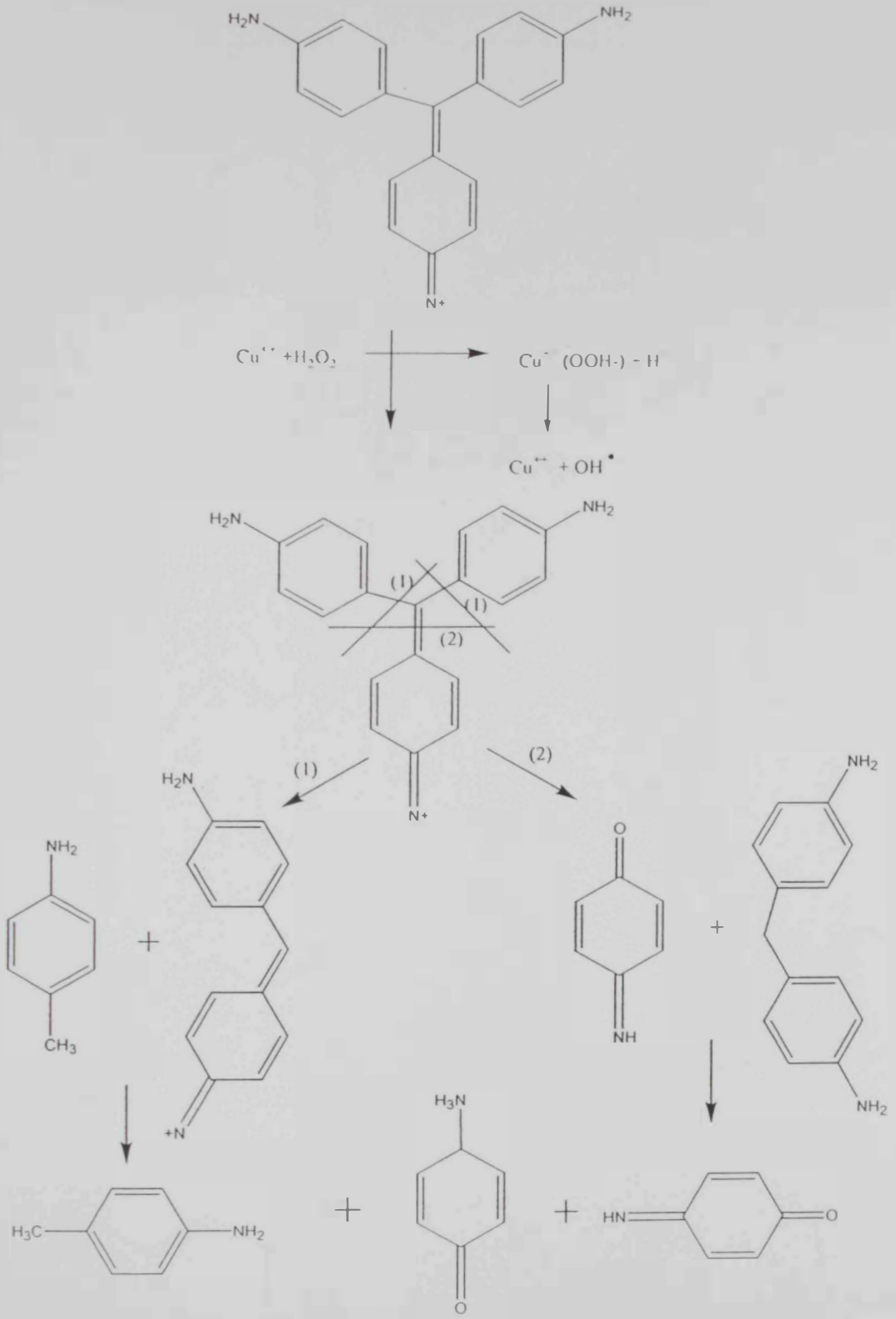

Fig 3 45. The two suggested reactions of the degradation of methyl violet.

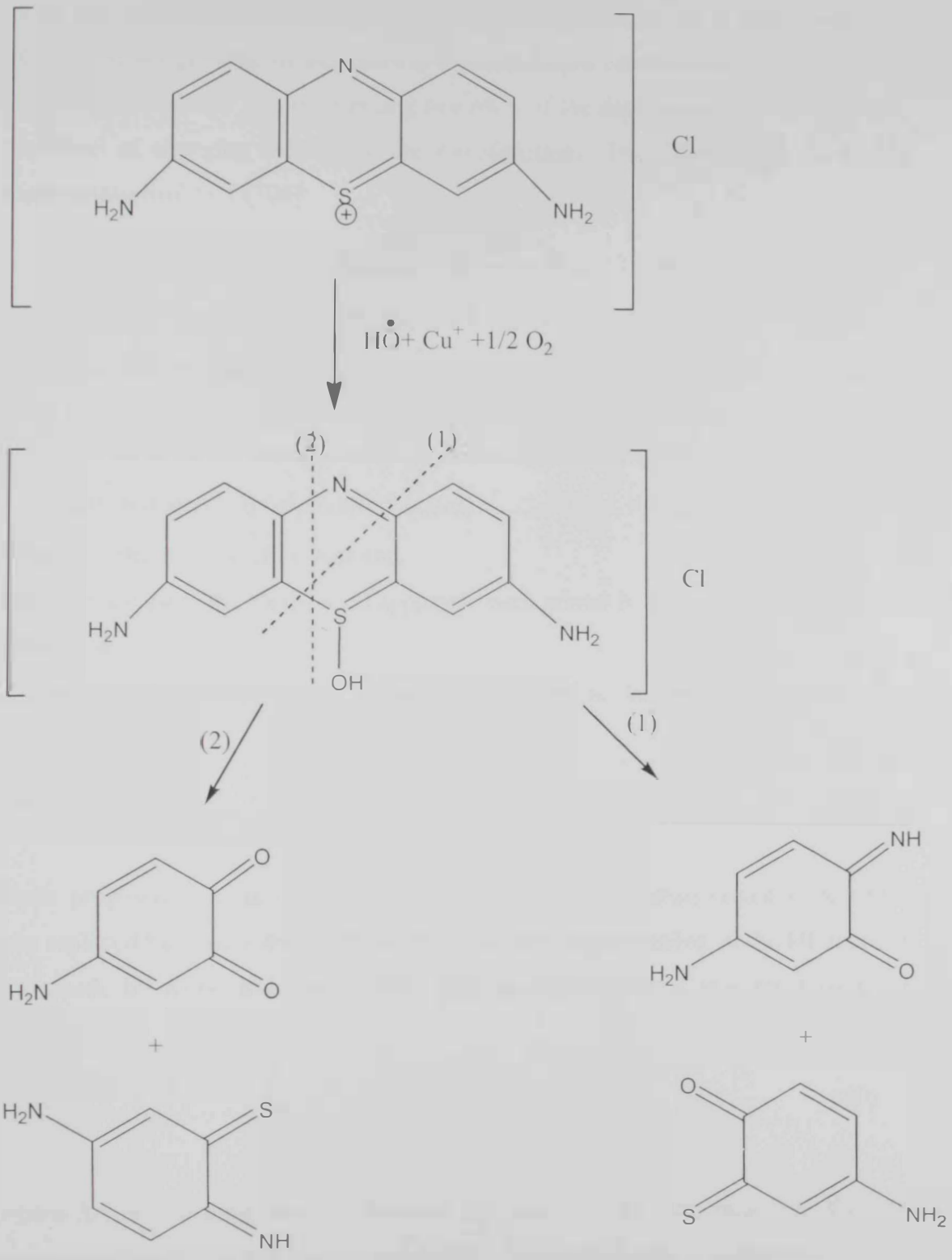

Figure 3. 46. The two suggested reactions of the degradation of thionine.

where D is the overall closed shell wavefunction and can be obtained by defining n/2 molecular orbitals for a system with n electrons. Each row in the D matrix represent all possible assignments of electron i to all orbital-spin combination. Swapping two electrons corresponds to interchanging two rows of the determinant, which will have the effect of changing the sign of the wavefunction. The following is the matrix representation of the D[106]:

$$D=\begin{vmatrix} \phi_1(\vec{r}_1)i(1) & \phi_1(\vec{r}_1)j(1) & \phi_2(\vec{r}_1)i(1)\ \phi_2(\vec{r}_1)j(1) & \cdots\cdots & \phi_{n/2}(\vec{r}_1)i(1)\ \phi_{n/2}(\vec{r}_1)j(1) \\ \phi_1(\vec{r}_2)i(1) & \phi_1(\vec{r}_2)j(1) & \phi_2(\vec{r}_2)i(1)\ \phi_2(\vec{r}_2)j(1) & \cdots\cdots & \phi_{n/2}(\vec{r}_2)i(1)\ \phi_{n/2}(\vec{r}_2)j(1) \\ \phi_1(\vec{r}_3)i(1) & \phi_1(\vec{r}_3)j(1) & \phi_2(\vec{r}_3)i(1)\ \phi_2(\vec{r}_3)j(1) & \cdots\cdots & \phi_{n/2}(\vec{r}_3)i(1)\ \phi_{n/2}(\vec{r}_3)j(1) \\ \cdots & \cdots & \cdots & \cdots & \cdots \\ \cdots & \cdots & \cdots & \cdots & \cdots \\ \phi_1(\vec{r}_n)i(1) & \phi_1(\vec{r}_n)j(1) & \phi_2(\vec{r}_n)i(1)\ \phi_2(\vec{r}_n)j(1) & \cdots\cdots & \phi_{n/2}(\vec{r}_n)i(1)\ \phi_{n/2}(\vec{r}_n)j(1) \end{vmatrix} \quad (46)$$

Where r is the position of the electron.

Since we are using the closed shell approach, each orbital is doubly occupied by i and j electrons.

All these molecular orbitals (ϕi's) were considered to be orthonormal such that

$$\langle \phi_i(1) | \phi_i(1) \rangle = 1 \quad (47)$$

$$\langle \phi_i(1) | \phi_j(1) \rangle = 0 \text{ for } i \neq j \quad (48)$$

Slater proposed a simplification for HF where a weighted mean exchange potential was replaced by a local density function . The next improvement on the HF method was made by Kohn and Sham[104]. The exchange integral was replaced by a function ρ, as:

$$V_{x\alpha} = -3X_\alpha \left(\frac{3\rho}{8\pi}\right)^{\frac{1}{3}} \quad (49)$$

where $X\alpha$ is a scaling constant between 2/3 and 1. The best value for $X\alpha$ was reported by Baerendas and Ros to be 0.7[107]. The spin density ρ is written as:

$$\rho_\mu = \sum f_{\eta\mu} \left| \Phi_{\eta\mu}(r) \right|^2 \quad (50)$$

where f_η is an occupation number and $\Phi\eta\mu$ is an eigenfunction of F.

ϕi's are calculated by solving the HFS equations iteratively. The spatial part was expanded as a summation over a linear combination of a complete set of basis functions Xk, as :

$$\phi_i = \sum_k C_{ki} X_k \tag{51}$$

where the coefficients C_{ki} are known as the molecular orbital expansion coefficients and the X_k are the basis function and are centered on the nuclei and are chosen to be normalized. In this project we used Gaussian type atomic functions as basis functions, which can be expressed in the following from[102]:

$$g(\alpha, r) = cx^{n} y^{m} z^{l} e^{-\alpha r^2} \tag{52}$$

where $\vec{r}$ is composed of x, y, and z and α determine the size (radial extent) of the function.

For a nontrivial solution, we get what is called the Roothaan equation

$$\sum_k C_{ki} (F_{jk} - \varepsilon i S j k) = 0 \tag{53}$$

which is solved by an iterative process that is called the Self-Consistent Field (SCF) method.

The following steps are taken in order to obtain C_{ki}'s and εi's [108]

1. Start with a guess for the occupied MO's, expressed as linear combinations of the basis set.

2. MO's will be used to solve for the eigenfunctions of the HF operator h:

* First the matrix elements are computed

* The secular equations are solved to obtain initial values for the εi's

3. The εi's are used to find an improved set of coefficients for the M.O's.

4. The improved MO's are generate new hi's.

5. The hi's are used to find new, improved ε_i's and so on till we reach self consistency in these values.

3.3.1 Discussion of Molecular Orbital Calculations.

The degradation of methyl violet could have happen through two different routs that lead to the same final products. Upon looking at the results of the calculation, table 2.1 and 2.2, we conclude that the degradation of the dye is more probable to happen through the intermediate step of rout 2. The solvation effect was ignored since we are after the relative values of energies. The total energies calculated from route one and two in the gas phase were –932.30 and -968.70 Hartrees consecutively. The difference in energies is 36.4 Hartrees which is equivalent to 22,684.49 kcal mol^{-1}. Therefore, according the single point energy calculations of the intermediate products, the degradation of methgyl violet could have happened through the suggested mechanism of rout 2.

In the degradation of thionine, the energies produced by the suggested pathways also in the gas phase were -1171.2 and -1171.05 Hartrees respectively. Therefore, the degradation reaction of thionine shell produce the four proposed products suggested by the two different pathways together and at the same time.

However, Tables 2.1, 2.2, 2.3 and 2.4 summarize the results of the calculations:

Table 3. 2: Results of the calculation-assuming path 1 in the degradation of methyl violet.

Structure	**Number of electrons**	**Number of the basis set**	**Energy/HF**
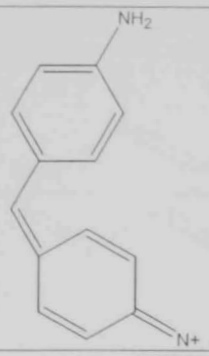	103	247	-607.55
	58	138	-324.75
Total energy			-932.30

Table 3. 3: Results of the calculation-assuming path 2 in the degradation of methyl violet.

Structure	**Number of electrons**	**Number of the basis set**	**Energy/HF**
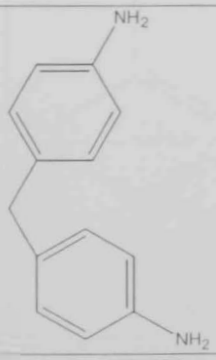	106	253	-609.31
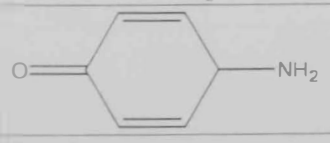	56	130	-359.39
Total energy			-968.70

Table 3. 4: Results of the calculation-assuming path 1 in the degradation of thionine.

Structure	Number of electrons	Number of the basis set	Energy/HF
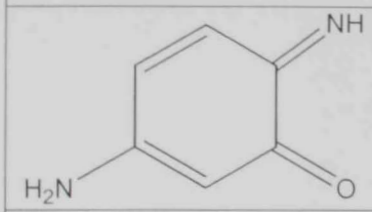	64	147	-414.41
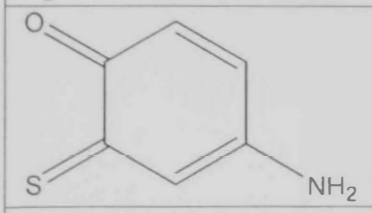	72	149	-756.64
Total energy			-1171.05

Table 3. 5: Results of the calculation-assuming path 2 in the degradation of thionine.

Structure	Number of electrons	Number of the basis set	Energy/HF
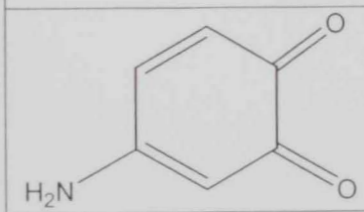	64	147	-434.20
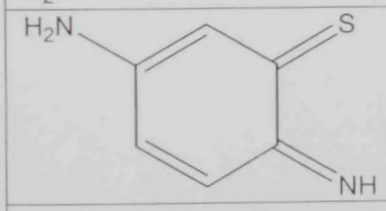	72	151	-737.04
Total energy			-1171.12

4. *References*

References:

1. Hao, O.J., H. Kim, and P.-C. Chiang, Critical Reviews In Environmental Science and Technology, 2000. **30**(4): p. 449.
2. Bajpai, P. and P.K. Pajpai, J. Biotechnol., 1994. **33**(3): p. 211.
3. EPA, *Toxic Release Inventory*, 1995, US Environmnetal Protection Agency: Washington D. C.
4. ECT, *Kirk-Othmer Encyclopedia of Chemical Technology*. 3 rd. 1977, New York: John Wiley.
5. Ingamells, W., *Colour for Textiles, A User's Hand Book*. 1993, West Yorkshire, England: Society of Dyers and Colourists.
6. Wu, J., M.A. Eitman, and S.E. LAw, J. Environ. Eng, ASCE, 1998. **124**(3): p. 2727.
7. Chen, G., et al., J. Membrane Sci, 1997. **127**(1): p. 93.
8. Oehr, K., J. wat. Pollut. Control Fed, 1978. **50**(2): p. 286.
9. Lin, s.H. and C.F. Peng, Wat. Res., 1996. **30**(3): p. 587.
10. Lin, S.H. and C.F. Peng, Wat. Res., 1994. **28**(2): p. 277.
11. Hempholl, L. and R. Rogers, in *Proc 28th Ind. Waste Conf.* 1974. West Lafayette, Purdue University.
12. Pagga, U. and D. Brown, Chemosphere, 1986. **15**(4): p. 479.
13. Uygur, A., J. Sco. Dyers. Colourists, 1997. **113**(7/8): p. 211.
14. P. W. Shepperd, L.W. Becker, and R.J. Cundiff, *U. S. Pat. No.5, 750, 035*. 1990: U.S.A.
15. A. S. shouli, J.K. Bewtra, and N. Biswas, International Journal of Environmental Studies, 1992. **40**(27).
16. Weber, O.W., *U. S. Pat. No. 5, 360,551*. 1994.
17. Klimiuk, E., U. Filipkowska, and A. Korzeniowska, .Pol. J. Environ. Studies, 1999. **8**(73).
18. Klimiuk, E., U. Filipkowska, and Libecki, Pol. J. Environ. Studies, 1999. **8**(81).
19. Cook, M.M., A. Reife, and H.S. Freeman, *Environmental Chemistry of Dyes and Pigments*. First Edition ed. 1996, New York: John Wiley & Sons, Inc. 3-57.
20. Bechtold, T., E. Burtscher, and A. Turcanu, J. Soc. Dyers Color, 2000. **116**: p. 215.

21. Cook, M.M. and J.A. Ulman. 1990: U. S.A. p. 203.
22. Zee, F.P.v.d., G. Lettinga, and J. A. Field. Chemospher, 2001. **44:** p. 1169.
23. Nam, S. and V. Rengathan, Chemosphere, 2000. **40:** p. 351.
24. Nam, S. and P.G. Tratnyek, Wat. Res., 2000. **34:** p. 1837.
25. DeFazio, S.K.A. and A.T. Lemley, J. Environ. Sci. Health, 1999. **34:** p. 217
26. Bechtold, T., E. Burtscher, and A.T. . J. Electranal. Chem., 1999. **465:** p. 80.
27. Bechtold, T., E. Burtscher, and A. Turcanu, J. Chem. Technol. Biotechnol., 2001. **76:** p. 303.
28. Walker, G.M. and L.R. Weatherley, Chem. Eng. J., 2001. **83:** p. 201.
29. Wu, F.C., R.L. Tseng, and R.S. Juang, Environ. Technol., 2001. **22:** p. 205.
30. Barlas, H. and T. Akgun, Fres. Environ. Bull., 2000. **9:** p. 597.
31. Jaung, R.S., F.C. Wu, and R.L. Tseng, J. Coll. Int. Sci., 2000. **227:** p. 437.
32. Walker, G.M. and L.R. Weatherley, Proc.Saft. & Environ. Prot., 2000. **78:** p. 219.
33. L.Nicolet and U. Rott, Wat. Sci. Technol., 1999. **40:** p. 191.
34. Tamai, H., M.S. T. Yoshid, and H. Yasuda, Carbon, 1999. **37:** p. 983.
35. Houas, A., M.K. I. Bakir, and E. Elaloui, J. Chim. Phys. Chim. Biol., 1999. **96:** p. 479.
36. Walker, G.M. and L.R. Weatherley, Separ. Sci. Technol., 2000. **35:** p. 1329.
37. Cione, A.P.P., G.M. Neumann, and F. Gessner, J. Coll. Int. Sci., 1988. **198:** p. 106.
38. Jaung, R.S., F.C. Wu, and R.L. Tseng, Environ. Technol., 1997. **18:** p. 525
39. Wu, F.C., R.L. Tseng, and R.S. Jaung, Environ. Technol., 2001. **22:** p. 721.
40. Harris, R.G., J.D. Wells, and B. B. Johnson, (). Coll. Surf. A, 2001. **180:** p. 131.
41. Kasanava, T., D. Vu, and D.A. Sabatini, Ground Water, 1999. **37:** p. 3.
42. Binkowski, S., T. Jesionowski, and A. Krysztafkiewicz, Dyes Pigments, 2000. **47:** p. 247.
43. Parida, S.K. and B.K. Mishra, Ind. J.Chem., 1998. **37:** p. 618.
44. Davydov, V.Y. and T.D. Khoklova, Russ. J. Phy. Chem., 2000. **74:** p. 1167.
45. R.X.Liu, et al., J. Coll. Int. Sci., 2001. **239:** p. 475.
46. D. A. Sabatini, (). Ground Water, 2000. **38:** p. 651.
47. Mchedlov-Petrossyan, N.O., et al., Chem. Phys. Lett., 2001. **341:** p. 237.
48. Wu, F.C., R.L. Tseng, and R.S. Juang, J. Hazard. Mat., 2001. **81:** p. 167.

49. Khoklova, T.D., A.I. Vilenskii, and B. V. Mchedlishvili, (). Coll. J., 1998. **60:** p. 531.
50. Chen, B.N., C.W. Hui, and G. McKay, Chem. Eng. J., 2001. **84:** p. 77.
51. Sumanji, T. and N. Prasad, Ind. J. Chem. A, 2001. **40:** p. 388.
52. Namasivayam, C., R. Radhika, and S. Suba, Waste Management, 2001. **21:** p. 381.
53. Nicolet, L. and U. Rott, Wat. Sci. Technol., 1999. **40:** p. 191.
54. Liu, R.X., et al., J. Coll. Int. Sci., 2001. **239:** p. 475.
55. Sabatini, D.A., Ground Water, 2000. **38:** p. 651.
56. Soldatkina, L.M. and V. Menchuk, Ads. Sci. Technol., 2001. **19:** p. 267.
57. Bandara, J., J.A. Mielczarski, and J. Kiwi, Langmuir, 1999. **15:** p. 7670.
58. Favre, in *Pat. No. 5*. 1993: U.S.A.
59. Bragg et al., , ( ). in *U.S. Pat. No. 5*. 1991.
60. Postlethwaite, in *U.S. Pat. No. 4,119, 557*. 1978: U.S.A.
61. Ellis Jr. , e.a., *U.S. Pat. No. 4,900,871*. 1990: U.S.A.
62. Uffelman, E.S., *Ph.D. Thesis*, in *chemistry*. 1992, California Institute of Technology: San Fransisco.
63. Collins, T.J. and C.P. Horwitz, *U. S. Pat. No. 5,876,625*. 1999: U.S.A.
64. Collins, T.J. and C.P. Horwitz,). *U. S. Pat. No. 6,099,586*. 2000.
65. Collins, T.J. and C.P. Horwitz, *U. S. Pat. No. 6,136,223*. 2000.
66. Dai, C.-Y., et al., *U. S. Pat. No. 0044402 A1*. 2001: U.S.A.
67. J. Bassett, R.G. Denney, G. H. J. Mendham, *Vogel's Text Book of Quamtitative Inorganic Analysis*, ed. 4. 1978.
68. J. Bassett, R.G. Denney, G. H. J. Mendham, *Vogel's Text Book of Quantitative Inorganic Analysis*, ed. 4. 1978.
69. I. A. Salem and M.S. El-Maazawi, Phys Chem, 2001. **215**: p. 623.
70. I. A. Salem and M.S. El-Maazawi, Phys Chem, 2002. **216**: p. 249.
71. U. Nickel and Y.- H. Chen, J. Chem. Soc. Faraday Trans, 1993. **89**: p. 2479.
72. I. A. Salem, Phys Chem, 2002. **216**: p. 249.
73. I. A. Salem, M. Gaber and D. F. Badr-Eldeen, Transition Met. Chem, 1999. **24**: p. 511.
74. ChemDraw. 1997, Cambridge Soft Coorporation: Cambridge, MA, U.S.A.

75. Abdy, P.R. and M.A.H. Dempster, *Introduction to Optimization Methods*. 1970, New York: Halsted Press.

76. Haming, R.W., *Numerical Methods for Scientists and Engineers*, ed. 2. 1973, New York: McGraw Hill, Inc.

77. Rutishauser, H., *Lectures on Numerical Mathematics*. 1990, Boston: Birkhauser.

78. Press, W.H., et al., *Numerical Recipies in FORTRAN*. secnd ed. 1992, Cambridge: Cambridge University Press.

79. Pople, J.A., et al., *Gaussian*. 1998, Gaussian, Inc: Pittsburgh PA

80. I. A. Salem, Transition Met. Chem, 2000. **25**: p. 599.

81. I. A. Salem and M.S. El-Maazawi, Chemosphere, 2000. **41**: p. 1173.

82. I. A. Salem, Appl. Catal. B, 2000. **28**: p. 153.

83. I. A. Salem, Chemosphere. 2001. **44**: p. 1109.

84. S. F. Dubrow, G. D. Boardman and D. L. Michelsen, *Environmental chemistryof Dyes and Pigments*, 1996. A. Reife and H. S. Freeman, New York: Wiley.

85. Y. Okamoto, K. ohto and T. Imanko, Kagaku kogaku Robunshu, 1993. **19**: p. 863.

86. I. A. Salem, Polyhedron, 1994. **13**: p. 1547.

87. I. A. Salem and M. S. El-Maazawi and A. B. Zaki, Int. J.Chem. Kinet., 2000. **32**: p. 643.

88. J. H. Espenson, *Chemical Kinetics and reaction Mechanism*, ed. 2., , NewYork: McGraw-Hill.

89. O. P. ●liveira, J. G. P. Espinola, W. E. S. Lemus, A. G. Desouza and C. Airoldi, Coll. Surf. A, 1998. **136**: p. 151.

90. J. D. Rush and K.K. M. Yusuff, J. Inorg. Biochem., 1987. **29**: p. 199.

91. I. A. Salem, Montsh. Chem., 2000. **131**: p. 1547.

92. I. A. Salem, Polyhedron, 1994. **13**: p. 1547.

93. J. H. Fendler and E. J. Fendler (1975), *Catalysis in micellar and macromolecular systems*, 1975 , London: Academic Press.

94. P. K. Sen, A. Sanyal and K. K. S. Gupta, Bull. Chem. Soc. Jpn., 1996. **69**: p. 1543.

95. F. A. Cotton and G.Wilkinson, *Advanced Inorganic Chemistry*, ed. 5. 1988, New York : Wiley.

96. A. Maria, C. Ferreira and H. E. Thoma, J. Coord. Chem., 1988. **18**: p. 351.

97. A. Maria, C. Ferreira and H. E. Thoma, J. Coord. Chem., 1988. **18**: p. 351.

98. M. M. Halmann, *Photodegradation of Water Pollutions*, 1996, New York: CRC press.

99. F. J. Beltran, M. Gonzales, F. J. Rivas, P. Alvarez, Water, Air, Soil Pollution, 1998. **105**: p. 685.

100. G. V. Buxton, G. I. Greenstock, W. P. Helman, A. B. Ross, J. Phys. Chem. Ref. Data, 1988. **17**: p. 513.

101. R. E. Huie, P. Neta, *Reactive Oxygen Species in Biological Systems*, New York: Kluwer Academic Publishers, Dordercht, Plenjum Press.

102. I.N. Levine, *Quantum Chemistry*, ed. 5. 2000, Englewood Cliffs, New Jersy: Prentic Hall.

103. R., J. Hoffman, Chem. Phys, 1963. **39**: p. 1397.

104. W. Kohn, and L. Sham, J. Chem. Phys. Rev., 1965. **A1133**: p. 140.

105. A. Hinchliffe, *Computational Quantum Chemistry*. 1988, New York: Wiley.

106. J.B. Foresman, and A. Frisch, *Exploring Chemsitry with Electronic Structure Methods*, ed. 2. 1996, Pittsburg, PA: Gaussian, Inc.

107. E.J. Baerends, and P. Ros, Chem. Phys. lett., 1973. **23**: p. 391.

108. I., Shehadi, in *Department of Chemistry*. 1997, Northeastern University: Boston.

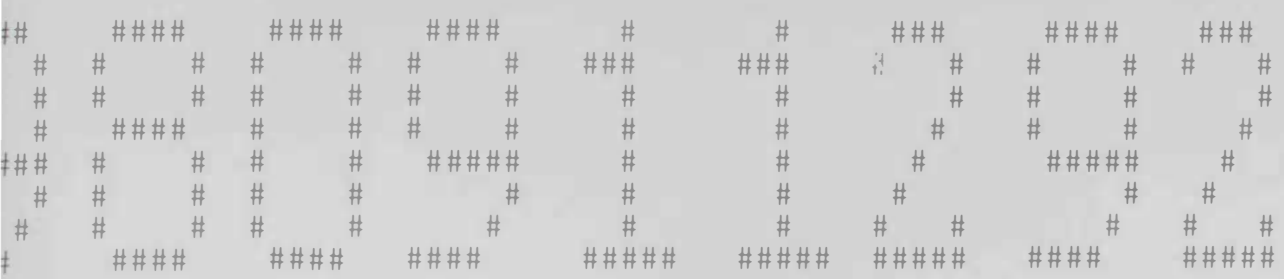

: 111
: 9/16/2003
: 980911292
: 6:38:31 PM

5. *APPENDICES*

Appendix 1

Molecular orbital calculation on thionine degradation products

1. ANALINE-3-O-4-O.PDB

HF/6-31G* Test

Symbolic Z-matrix:

Charge = 0 Multiplicity = 1

```
C
C          1  R2
C          1  R3     2  A3
H          1  R4     2  A4     3  D4     0
C          2  R5     1  A5     3  D5     0
C          3  R6     1  A6     2  D6     0
N          2  R7     1  A7     5  D7     0
H          3  R8     1  A8     6  D8     0
C          5  R9     2  A9     1  D9     0
O          6  R10    3  A10    1  D10    0
H          5  R11    2  A11    9  D11    0
H          7  R12    2  A12    1  D12    0
H          7  R13    2  A13    12 D13    0
O          9  R14    5  A14    2  D14    0
```

Variables:

```
R2          1.45811
R3          1.35003
R4          1.10296
R5          1.36516
R6          1.48299
R7          1.38622
R8          1.10296
R9          1.47271
R10         1.22594
R11         1.10306
R12         1.05003
R13         1.04889
R14         1.22764
A3        121.52309
A4        119.13126
A5        121.31111
A6        120.8244
A7        119.00183
A8        119.84014
A9        120.79492
A10       119.87024
A11       120.03236
A12       119.2726
A13       119.17728
```

A14	119.92286
D4	-179.97896
D5	0.04443
D6	0.00941
D7	-179.99528
D8	179.97544
D9	-0.00211
D10	179.95419
D11	-179.95588
D12	-179.98955
D13	179.98637
D14	179.94376

Z-MATRIX (ANGSTROMS AND DEGREES)

CD	Cent	Atom	N1	Length/X	N2	Alpha/Y	N3	Beta/Z	J
1	1	C							
2	2	C	1	1.458114(1)					
3	3	C	1	1.350025(2)	2	121.523(14)			
4	4	H	1	1.102962(3)	2	119.131(15)	3	-179.979(26)	0
5	5	C	2	1.365156(4)	1	121.311(16)	3	0.044(27)	0
6	6	C	3	1.482993(5)	1	120.824(17)	2	0.009(28)	0
7	7	N	2	1.386216(6)	1	119.002(18)	5	-179.995(29)	0
8	8	H	3	1.102961(7)	1	119.840(19)	6	179.975(30)	0
9	9	C	5	1.472713(8)	2	120.795(20)	1	-0.002(31)	0
10	10	O	6	1.225936(9)	3	119.870(21)	1	179.954(32)	0
11	11	H	5	1.103059(10)	2	120.032(22)	9	-179.956(33)	0
12	12	H	7	1.050032(11)	2	119.273(23)	1	-179.990(34)	0
13	13	H	7	1.048889(12)	2	119.177(24)	12	179.986(35)	0
14	14	O	9	1.227636(13)	5	119.923(25)	2	179.944(36)	0

Z-Matrix orientation:

Center Number	Atomic Number	Atomic Type	Coordinates (Angstroms) X	Y	Z
1	6	0	0.000000	0.000000	0.000000
2	6	0	0.000000	0.000000	1.458114
3	6	0	1.150801	0.000000	-0.705850
4	1	0	-0.963445	0.000354	-0.536935
5	6	0	1.166331	0.000905	2.167565
6	6	0	2.464405	-0.000209	-0.017581
7	7	0	-1.212390	-0.001040	2.130204
8	1	0	1.118409	-0.000253	-1.808336
9	6	0	2.467937	0.001867	1.478576
10	8	0	3.498610	-0.001056	-0.675865
11	1	0	1.141716	0.000185	3.270349
12	1	0	-1.217352	-0.000877	3.180224
13	1	0	-2.103631	-0.001754	1.577160
14	8	0	3.506945	0.003718	2.132448

Distance matrix (angstroms):

		1	2	3	4	5
1	C	0.000000				
2	C	1.458114	0.000000			
3	C	1.350025	2.450936	0.000000		
4	H	1.102962	2.215502	2.120983	0.000000	
5	C	2.461436	1.365156	2.873457	3.442422	0.000000
6	C	2.464468	2.872450	1.482993	3.466971	2.541625
7	N	2.451052	1.386216	3.691595	2.678732	2.379015
8	H	2.126245	3.452612	1.102961	2.439380	3.976190
9	C	2.876960	2.468022	2.550797	3.979531	1.472713
10	O	3.563294	4.098065	2.348000	4.464217	3.677583
11	H	3.463913	2.141894	3.976209	4.350530	1.103059
12	H	3.405257	2.108936	4.550794	3.725821	2.589871
13	H	2.629202	2.106997	3.975358	2.401964	3.327836
14	O	4.104389	3.571191	3.688816	5.206727	2.340878

		6	7	8	9	10
6	C	0.000000				
7	N	4.258145	0.000000			
8	H	2.240203	4.576539	0.000000		
9	C	1.496162	3.737570	3.553170	0.000000	
10	O	1.225936	5.483387	2.635877	2.388286	0.000000
11	H	3.544007	2.615673	5.078738	2.229196	4.596472
12	H	4.876607	1.050032	5.508313	4.059183	6.091775
13	H	4.838404	1.048889	4.673663	4.572632	6.038313
14	O	2.389462	4.719337	4.608134	1.227636	2.808329

		11	12	13	14
11	H	0.000000			
12	H	2.360789	0.000000		
13	H	3.660487	1.831749	0.000000	
14	O	2.624717	4.839095	5.637990	0.000000

Interatomic angles:

C2-C1-C3=121.5231 C2-C1-H4=119.1313 C3-C1-H4=119.3456
C1-C2-C5=121.3111 C1-C3-C6=120.8244 C1-C2-N7=119.0018

C5-C2-N7=119.6871 C1-C3-H8=119.8401 C6-C3-H8=119.3355
C2-C5-C9=120.7949 C3-C6-O10=119.8702 C2-C5-H11=120.0324
C9-C5-H11=119.1727 C2-N7-H12=119.2726 C2-N7-H13=119.1773
H12-N7-H13=121.5501 C5-C9-O14=119.9229

Stoichiometry C6H5NO2
Framework group C1[X(C6H5NO2)]
Deg. of freedom 36
Full point group C1 NOp 1
Largest Abelian subgroup C1 NOp 1
Largest concise Abelian subgroup C1 NOp 1

Standard orientation:

Center Number	Atomic Number	Atomic Type	Coordinates (Angstroms) X	Y	Z
1	6	0	-1.009952	-1.323464	-0.001000
2	6	0	-1.492601	0.052452	0.000007
3	6	0	0.309618	-1.608599	-0.000833
4	1	0	-1.741355	-2.149040	-0.002272
5	6	0	-0.626853	1.107976	0.000255
6	6	0	1.321347	-0.524315	0.000598
7	7	0	-2.859114	0.285342	0.000822
8	1	0	0.643984	-2.659657	-0.001359
9	6	0	0.829439	0.888670	-0.000443
10	8	0	2.515149	-0.803160	0.001579
11	1	0	-1.015113	2.140444	0.001722
12	1	0	-3.211363	1.274527	0.001381
13	1	0	-3.517051	-0.531534	0.000647
14	8	0	1.593439	1.849604	-0.001252

Rotational constants (GHZ): 3.0805447 1.4152800 0.9697520
Isotopes: C-12,C-12,C-12,H-1,C-12,C-12,N-14,H-1,C-12,O-16,H-1,H-1,H-1,O-16
Standard basis: 6-31G(d) (6D, 7F)
There are 145 symmetry adapted basis functions of A symmetry.
Crude estimate of integral set expansion from redundant integrals=1.000.
Integral buffers will be 262144 words long.
Raffenetti 1 integral format.
Two-electron integral symmetry is turned on.
145 basis functions 272 primitive gaussians
32 alpha electrons 32 beta electrons
nuclear repulsion energy 404.6289401557 Hartrees.
One-electron integrals computed using PRISM.
NBasis= 145 RedAO= T NBF= 145
NBsUse= 145 1.00D-04 NBFU= 145
Projected INDO Guess.
Warning! Cutoffs for single-point calculations used.
Requested convergence on RMS density matrix=1.00D-04 within 64 cycles.
Requested convergence on MAX density matrix=1.00D-02.
Requested convergence on energy=5.00D-05.
SCF Done: E(RHF) = -434.238754243 A.U. after 7 cycles
Convg = 0.4429D-04 -V/T = 2.0033
S**2 = 0.0000

2. Out put file for ANALINE-3-S-4-O.PDB

HF/6-31G* Test
Symbolic Z-matrix:
Charge = 0 Multiplicity = 1

C							
C	1	R2					
C	1	R3	2	A3			
H	1	R4	2	A4	3	D4	0
C	2	R5	1	A5	3	D5	0
C	3	R6	1	A6	2	D6	0
O	2	R7	1	A7	5	D7	0
H	3	R8	1	A8	6	D8	0
C	5	R9	2	A9	1	D9	0
N	6	R10	3	A10	1	D10	0
S	5	R11	2	A11	9	D11	0
H	9	R12	5	A12	2	D12	0
H	10	R13	6	A13	3	D13	0
H	10	R14	6	A14	13	D14	0

Variables:

R2	1.49037
R3	1.35794
R4	1.10234
R5	1.48371
R6	1.4377
R7	1.22134
R8	1.1025
R9	1.378
R10	1.33587
R11	1.58429
R12	1.10422
R13	1.04913
R14	1.04925
A3	120.46909
A4	119.57851
A5	118.24554
A6	120.34394
A7	119.15149
A8	119.70775
A9	119.20811
A10	119.41625
A11	121.08382
A12	121.19821
A13	119.16605
A14	119.25465
D4	-179.97526
D5	0.02482
D6	-0.04413

D7	179.86193
D8	-179.92036
D9	-0.0279
D10	-179.94242
D11	-179.81381
D12	179.98775
D13	-0.04249
D14	-179.92932

Z-MATRIX (ANGSTROMS AND DEGREES)

CD	Cent	Atom	N1	Length/X	N2	Alpha/Y	N3	Beta/Z	J
1	1	C							
2	2	C	1	1.490372(1)					
3	3	C	1	1.357939(2)	2	120.469(14)			
4	4	H	1	1.102343(3)	2	119.579(15)	3	-179.975(26)	0
5	5	C	2	1.483709(4)	1	118.246(16)	3	0.025(27)	0
6	6	C	3	1.437699(5)	1	120.344(17)	2	-0.044(28)	0
7	7	O	2	1.221344(6)	1	119.151(18)	5	179.862(29)	0
8	8	H	3	1.102496(7)	1	119.708(19)	6	-179.920(30)	0
9	9	C	5	1.378005(8)	2	119.208(20)	1	-0.028(31)	0
10	10	N	6	1.335869(9)	3	119.416(21)	1	-179.942(32)	0
11	11	S	5	1.584289(10)	2	121.084(22)	9	-179.814(33)	0
12	12	H	9	1.104223(11)	5	121.198(23)	2	179.988(34)	0
13	13	H	10	1.049128(12)	6	119.166(24)	3	-0.042(35)	0
14	14	H	10	1.049250(13)	6	119.255(25)	13	-179.929(36)	0

Z-Matrix orientation:

Center Number	Atomic Number	Atomic Type	Coordinates (Angstroms) X	Y	Z
1	6	0	0.000000	0.000000	0.000000
2	6	0	0.000000	0.000000	1.490372
3	6	0	1.170411	0.000000	-0.688575
4	1	0	-0.958686	0.000414	-0.544134
5	6	0	1.307040	0.000566	2.192539
6	6	0	2.425569	0.000956	0.012535
7	8	0	-1.066640	0.002108	2.085313
8	1	0	1.155762	0.000594	-1.790973
9	6	0	2.468638	0.000484	1.451198
10	7	0	3.565840	0.002108	-0.683401
11	16	0	1.385493	-0.003148	3.774880
12	1	0	3.458940	0.001096	1.939677
13	1	0	3.525004	0.001617	-1.731734
14	1	0	4.480423	0.002354	-0.169142

Distance matrix (angstroms):

		1	2	3	4	5
1	C	0.000000				

2	C	1.490372	0.000000			
3	C	1.357939	2.473392	0.000000		
4	H	1.102343	2.249065	2.133991	0.000000	
5	C	2.552564	1.483709	2.884351	3.552871	0.000000
6	C	2.425602	2.840315	1.437699	3.429733	2.450209
7	O	2.342276	1.221344	3.563545	2.631663	2.376101
8	H	2.131518	3.478938	1.102496	2.454689	3.986384
9	C	2.863590	2.468949	2.502802	3.965842	1.378095
10	N	3.630737	4.176183	2.395435	4.526669	3.656940
11	S	4.021109	2.671812	4.468634	4.914170	1.584289
12	H	3.965679	3.487999	3.484978	5.068011	2.166705
13	H	3.927411	4.775733	2.575324	4.638305	4.507692
14	H	4.483615	4.777884	3.350521	5.452020	3.955742

		6	7	8	9	10
6	C	0.000000				
7	O	4.061027	0.000000			
8	H	2.205687	4.468184	0.000000		
9	C	1.439307	3.591699	3.497902	0.000000	
10	N	1.335869	5.396818	2.652394	2.400076	0.000000
11	S	3.903461	2.977855	5.570593	2.563730	4.962883
12	H	2.186717	4.527922	4.384333	1.104223	2.625256
13	H	2.061852	5.971017	2.369983	3.353650	1.049128
14	H	2.062869	5.987693	3.699150	2.583172	1.049250

		11	12	13	14
11	S	0.000000			
12	H	2.768965	0.000000		
13	H	5.907650	3.672006	0.000000	
14	H	5.013374	2.343191	1.831535	0.000000

Interatomic angles:

C2-C1-C3=120.4691 C2-C1-H4=119.5785 C3-C1-H4=119.9524
C1-C2-C5=118.2455 C1-C3-C6=120.3439 C1-C2-O7=119.1515
C5-C2-O7=122.6028 C1-C3-H8=119.7077 C6-C3-H8=119.9483
C2-C5-C9=119.2081 C3-C6-N10=119.4163 C2-C5-S11=121.0838
C9-C5-S11=119.7078 C5-C9-H12=121.1982 C6-N10-H13=119.166
C6-N10-H14=119.2546 H13-N10-H14=121.5793

Stoichiometry C6H5NOS
Framework group C1[X(C6H5NOS)]
Deg. of freedom 36
Full point group C1 NOp 1
Largest Abelian subgroup C1 NOp 1
Largest concise Abelian subgroup C1 NOp 1

Standard orientation:

Center Number	Atomic Number	Atomic Type	Coordinates (Angstroms) X	Y	Z
1	6	0	0.572550	1.788852	-0.001296
2	6	0	-0.744229	1.090784	-0.000106
3	6	0	1.729126	1.077283	-0.001639
4	1	0	0.604272	2.890739	-0.001486

5	6	0	-0.752412	-0.392902	0.001252
6	6	0	1.697577	-0.360068	0.000098
7	8	0	-1.769471	1.754526	0.002289
8	1	0	2.696261	1.606574	-0.001929
9	6	0	0.446656	-1.071969	0.000783
10	7	0	2.846540	-1.041558	0.000896
11	16	0	-2.113704	-1.203364	-0.001185
12	1	0	0.478916	-2.175720	0.001960
13	1	0	3.753640	-0.514456	-0.000440
14	1	0	2.820557	-2.090486	0.001714

Rotational constants (GHZ): 2.3510539 1.1862065 0.7884174
Isotopes: C-12,C-12,C-12,H-1,C-12,C-12,O-16,H-1,C-12,N-14,S-32,H-1,H-1,H-1
Standard basis: 6-31G(d) (6D, 7F)
There are 149 symmetry adapted basis functions of A symmetry.
Crude estimate of integral set expansion from redundant integrals=1.000.
Integral buffers will be 262144 words long.
Raffenetti 1 integral format.
Two-electron integral symmetry is turned on.
149 basis functions 296 primitive gaussians
36 alpha electrons 36 beta electrons
nuclear repulsion energy 473.3441747019 Hartrees.
One-electron integrals computed using PRISM.
NBasis= 149 RedAO= T NBF= 149
NBsUse= 149 1.00D-04 NBFU= 149
Projected CNDO Guess.
Warning! Cutoffs for single-point calculations used.
Requested convergence on RMS density matrix=1.00D-04 within 64 cycles.
Requested convergence on MAX density matrix=1.00D-02.
Requested convergence on energy=5.00D-05.
SCF Done: E(RHF) = -756.647126209 A.U. after 11 cycles
Convg = 0.6653D-04 -V/T = 2.0011
S**2 = 0.0000

****

Population analysis using the SCF density.

****

Alpha occ. eigenvalues -- -92.11997 -20.46422 -15.56386 -11.30586 -11.26705
Alpha occ. eigenvalues -- -11.25516 -11.24983 -11.23104 -11.22102 -9.12497
Alpha occ. eigenvalues -- -6.80786 -6.80422 -6.80082 -1.32350 -1.22017
Alpha occ. eigenvalues -- -1.16610 -1.06390 -0.97620 -0.90133 -0.81287
Alpha occ. eigenvalues -- -0.78050 -0.69274 -0.68384 -0.63605 -0.60616
Alpha occ. eigenvalues -- -0.59596 -0.57810 -0.57430 -0.53162 -0.51046
Alpha occ. eigenvalues -- -0.50250 -0.48528 -0.38035 -0.36243 -0.33964
Alpha occ. eigenvalues -- -0.20086
Alpha virt. eigenvalues -- -0.13329 0.13301 0.19193 0.20574 0.21058
Alpha virt. eigenvalues -- 0.25419 0.27124 0.30451 0.34458 0.35534

Alpha virt. eigenvalues --	0.36122	0.37198	0.43420	0.47067	0.47496
Alpha virt. eigenvalues --	0.51390	0.54033	0.55824	0.59142	0.61726
Alpha virt. eigenvalues --	0.72292	0.72987	0.75497	0.75946	0.76688
Alpha virt. eigenvalues --	0.81044	0.81881	0.82188	0.84445	0.86079
Alpha virt. eigenvalues --	0.88293	0.89866	0.90940	0.94242	0.95021
Alpha virt. eigenvalues --	0.96299	0.97480	1.02411	1.02957	1.06742
Alpha virt. eigenvalues --	1.08002	1.10030	1.11061	1.14433	1.14924
Alpha virt. eigenvalues --	1.15397	1.17698	1.22508	1.22999	1.25167
Alpha virt. eigenvalues --	1.28364	1.34439	1.37938	1.39066	1.39869
Alpha virt. eigenvalues --	1.47017	1.49611	1.49730	1.55889	1.58214
Alpha virt. eigenvalues --	1.62920	1.68059	1.72550	1.73161	1.74148
Alpha virt. eigenvalues --	1.76470	1.87494	1.90778	1.94120	1.96613
Alpha virt. eigenvalues --	2.02284	2.09022	2.15225	2.15528	2.21395
Alpha virt. eigenvalues --	2.21456	2.23855	2.24673	2.30788	2.39477
Alpha virt. eigenvalues --	2.39537	2.41168	2.42632	2.45789	2.49502
Alpha virt. eigenvalues --	2.58393	2.60517	2.65086	2.65392	2.70689
Alpha virt. eigenvalues --	2.81016	2.84243	2.95289	2.95327	2.98199
Alpha virt. eigenvalues --	3.00483	3.08239	3.12080	3.16093	3.22917
Alpha virt. eigenvalues --	3.35111	3.42833	3.56566	3.71086	4.24874
Alpha virt. eigenvalues --	4.26690	4.39997	4.50629	4.56900	4.72263
Alpha virt. eigenvalues --	4.77230	4.90751	5.18401		

Condensed to atoms (all electrons):

	1	2	3	4	5	6
1 C	5.161559	0.503694	0.489518	0.377840	-0.090106	-0.035540
2 C	0.503694	4.164446	-0.047118	-0.017326	0.326407	-0.018547
3 C	0.489518	-0.047118	5.009748	-0.035854	-0.008356	0.523563
4 H	0.377840	-0.017326	-0.035854	0.450597	0.003332	0.001548
5 C	-0.090106	0.326407	-0.008356	0.003332	5.973639	-0.061935
6 C	-0.035540	-0.018547	0.523563	0.001548	-0.061935	4.497398
7 O	-0.080182	0.545888	0.006020	-0.000073	-0.126557	-0.000025
8 H	-0.018394	0.001201	0.367428	-0.001623	0.000050	-0.033595
9 C	-0.043501	0.005862	-0.035916	0.000346	0.366661	0.631397
10 N	0.003372	0.000427	-0.058193	-0.000081	0.005157	0.212879
11 S	0.007437	-0.033066	-0.001176	-0.000045	0.155705	0.006399
12 H	-0.000086	-0.000412	0.002787	0.000008	-0.053569	-0.018969
13 H	0.000182	-0.000009	-0.000743	-0.000009	-0.000085	-0.032230
14 H	-0.000079	-0.000005	0.002894	0.000002	0.000073	-0.032250

	7	8	9	10	11	12
1 C	-0.080182	-0.018394	-0.043501	0.003372	0.007437	-0.000086
2 C	0.545888	0.001201	0.005862	0.000427	-0.033066	-0.000412
3 C	0.006020	0.367428	-0.035916	-0.058193	-0.001176	0.002787
4 H	-0.000073	-0.001623	0.000346	-0.000081	-0.000045	0.000008
5 C	-0.126557	0.000050	0.366661	0.005157	0.155705	-0.053569
6 C	-0.000025	-0.033595	0.631397	0.212879	0.006399	-0.018969
7 O	8.361538	-0.000053	0.003800	-0.000001	0.013535	-0.000045
8 H	-0.000053	0.484662	0.002482	-0.001739	0.000024	-0.000106
9 C	0.003800	0.002482	5.064147	-0.074648	-0.052139	0.383798
10 N	-0.000001	-0.001739	-0.074648	7.234634	-0.000138	-0.002108
11 S	0.013535	0.000024	-0.052139	-0.000138	15.247900	-0.007508
12 H	-0.000045	-0.000106	0.383798	-0.002108	-0.007508	0.514000

13 H	0.000000	0.004023	0.003025	0.333772	0.000005	-0.000113
14 H	0.000000	-0.000084	-0.001641	0.334361	-0.000009	0.004532

	13	14
1 C	0.000182	-0.000079
2 C	-0.000009	-0.000005
3 C	-0.000743	0.002894
4 H	-0.000009	0.000002
5 C	-0.000085	0.000073
6 C	-0.032230	-0.032250
7 O	0.000000	0.000000
8 H	0.004023	-0.000084
9 C	0.003025	-0.001641
10 N	0.333772	0.334361
11 S	0.000005	-0.000009
12 H	-0.000113	0.004532
13 H	0.323426	-0.014873
14 H	-0.014873	0.331154

Total atomic charges:

	1
1 C	-0.275714
2 C	0.568558
3 C	-0.214603
4 H	0.221338
5 C	-0.490418
6 C	0.359907
7 O	-0.723845
8 H	0.195724
9 C	-0.253673
10 N	-0.987695
11 S	0.663077
12 H	0.177789
13 H	0.383630
14 H	0.375925

Sum of Mulliken charges= 0.00000

Atomic charges with hydrogens summed into heavy atoms:

	1
1 C	-0.054377
2 C	0.568558
3 C	-0.018879
4 H	0.000000
5 C	-0.490418
6 C	0.359907
7 O	-0.723845
8 H	0.000000
9 C	-0.075884
10 N	-0.228141
11 S	0.663077
12 H	0.000000
13 H	0.000000
14 H	0.000000

Sum of Mulliken charges= 0.00000
Electronic spatial extent (au): <R**2>= 1358.6626
Charge= 0.0000 electrons
Dipole moment (Debye):
X= 1.6344 Y= -6.0837 Z= -0.0109 Tot= 6.2994
Quadrupole moment (Debye-Ang):
XX= -47.8014 YY= -54.0904 ZZ= -64.2623
XY= 11.5756 XZ= 0.0116 YZ= -0.0086
Octapole moment (Debye-Ang**2):
XXX= 24.7915 YYY= -30.8718 ZZZ= 0.0078 XYY= 17.9170
XXY= -26.5802 XXZ= -0.0539 XZZ= -5.6093 YZZ= 1.4124
YYZ= -0.0291 XYZ= -0.0063
Hexadecapole moment (Debye-Ang**3):
XXXX= -890.0949 YYYY= -540.8609 ZZZZ= -69.4838 XXXY= 29.6902
XXXZ= -0.0367 YYYX= 21.8125 YYYZ= -0.0314 ZZZX= -0.0129
ZZZY= 0.0289 XXYY= -274.4344 XXZZ= -218.2537 YYZZ= -122.2222
XXYZ= -0.0165 YYXZ= 0.1029 ZZXY= -4.4222
N-N= 4.733441747019D+02 E-N=-2.733513705377D+03 KE= 7.558149137745D+02

Test job not archived.
1|1|UNPC-UNK|SP|RHF|6-31G(d)|C6H5N1O1S1|PCUSER|06-Dec-2002|0||# HF/6-3
1G* TEST||ANALINE-3-S-4-O.PDB||0,1|C|C,1,1.49037177|C,1,1.35793851,2,1
20.46908658|H,1,1.10234341,2,119.57851046,3,-179.97525795,0|C,2,1.4837
092,1,118.2455435,3,0.024819,0|C,3,1.43769886,1,120.34393882,2,-0.0441
2762,0|O,2,1.22134393,1,119.151486,5,179.86193304,0|H,3,1.10249626,1,1
19.70774861,6,-179.92035614,0|C,5,1.37800472,2,119.20810618,1,-0.02790
38,0|N,6,1.33586863,3,119.41625413,1,-179.94241872,0|S,5,1.5842888,2,1
21.08381622,9,-179.81380637,0|H,9,1.10422326,5,121.19820511,2,179.9877
4527,0|H,10,1.04912821,6,119.16604793,3,-0.04249154,0|H,10,1.04924973,
6,119.25464989,13,-179.929321,0||Version=x86-Win32-G98RevA.9|HF=-756.6
471262|RMSD=6.653e-005|Dipole=2.4158773,-0.0051593,0.5529587|PG=C01 [X
(C6H5N1O1S1)]||@

THE MOLECULE ALSO HAS A BODY. WHEN THIS BODY IS HIT, THE
MOLECULE
FEELS HURT ALL OVER -- A. KITAIGORODSKI
Job cpu time: 0 days 0 hours 2 minutes 50.0 seconds.
File lengths (MBytes): RWF= 19 Int= 0 D2E= 0 Chk= 6 Scr= 1
Normal termination of Gaussian 98.

3. DIANALINE.PDB # HF/6-31G* Test

Symbolic Z-matrix:

Charge = 0 Multiplicity = 1

```
C
C              1  R2
C              1  R3     2  A3
H              1  R4     2  A4     3  D4     0
C              2  R5     1  A5     3  D5     0
C              3  R6     1  A6     2  D6     0
N              3  R7     1  A7     6  D7     0
H              2  R8     1  A8     5  D8     0
C              5  R9     2  A9     1  D9     0
O              6  R10    3  A10    1  D10    0
N              5  R11    2  A11    9  D11    0
H              7  R12    3  A12    1  D12    0
H              9  R13    5  A13    2  D13    0
H             11  R14    5  A14    2  D14    0
H             11  R15    5  A15   14  D15    0
```

Variables:

```
R2            1.35175
R3            1.46421
R4            1.10325
R5            1.45982
R6            1.49359
R7            1.27781
R8            1.10266
R9            1.36656
R10           1.22802
R11           1.38672
R12           1.02231
R13           1.10227
R14           1.04928
R15           1.0491
A3          120.76365
A4          119.60878
A5          120.91186
A6          118.92717
A7          120.78981
A8          119.64483
A9          121.75156
A10         120.80886
A11         118.77706
A12         110.1713
A13         120.32801
A14         119.21024
A15         119.09699
D4         -179.91588
D5           -0.05056
```

D6	0.15221
D7	-179.96889
D8	-179.95228
D9	-0.03583
D10	179.90406
D11	179.99194
D12	-179.98356
D13	179.99025
D14	-179.96007
D15	179.92706

Z-MATRIX (ANGSTROMS AND DEGREES)

CD	Cent	Atom	N1	Length/X	N2	Alpha/Y	N3	Beta/Z	J
1	1	C							
2	2	C	1	1.351747(1)					
3	3	C	1	1.464213(2)	2	120.764(15)			
4	4	H	1	1.103249(3)	2	119.609(16)	3	-179.916(28)	0
5	5	C	2	1.459824(4)	1	120.912(17)	3	-0.051(29)	0
6	6	C	3	1.493592(5)	1	118.927(18)	2	0.152(30)	0
7	7	N	3	1.277811(6)	1	120.790(19)	6	-179.969(31)	0
8	8	H	2	1.102665(7)	1	119.645(20)	5	-179.952(32)	0
9	9	C	5	1.366555(8)	2	121.752(21)	1	-0.036(33)	0
10	10	O	6	1.228020(9)	3	120.809(22)	1	179.904(34)	0
11	11	N	5	1.386722(10)	2	118.777(23)	9	179.992(35)	0
12	12	H	7	1.022314(11)	3	110.171(24)	1	-179.984(36)	0
13	13	H	9	1.102273(12)	5	120.328(25)	2	179.990(37)	0
14	14	H	11	1.049280(13)	5	119.210(26)	2	-179.960(38)	0
15	15	H	11	1.049098(14)	5	119.097(27)	14	179.927(39)	0

Z-Matrix orientation:

Center Number	Atomic Number	Atomic Type	Coordinates (Angstroms) X	Y	Z
1	6	0	0.000000	0.000000	0.000000
2	6	0	0.000000	0.000000	1.351747
3	6	0	1.258176	0.000000	-0.748942
4	1	0	-0.959185	0.001408	-0.545088
5	6	0	1.252468	-0.001105	2.101686
6	6	0	2.547614	-0.003473	0.004820
7	7	0	1.258762	0.003512	-2.026748
8	1	0	-0.958335	0.000047	1.897150
9	6	0	2.466411	-0.002903	1.474142
10	8	0	3.622885	-0.005346	-0.588325
11	7	0	1.200812	-0.000128	3.487445
12	1	0	2.218533	0.002634	-2.378834
13	1	0	3.397755	-0.003546	2.063719
14	1	0	2.096951	-0.000275	4.033271
15	1	0	0.265747	0.001905	3.963108

Distance matrix (angstroms):

		1	2	3	4	5
1	C	0.000000				
2	C	1.351747	0.000000			
3	C	1.464213	2.448653	0.000000		
4	H	1.103249	2.125564	2.226712	0.000000	
5	C	2.446582	1.459824	2.850634	3.449178	0.000000
6	C	2.547620	2.881764	1.493592	3.549656	2.464601
7	N	2.385833	3.605374	1.277811	2.667322	4.128441
8	H	2.125460	1.102665	3.451770	2.442238	2.220244
9	C	2.873375	2.469447	2.530205	3.976432	1.366555
10	O	3.670348	4.109648	2.370164	4.582279	3.585395
11	N	3.688391	2.450134	4.236775	4.574594	1.386722
12	H	3.252806	4.340407	1.891782	3.668857	4.583487
13	H	3.975386	3.471550	3.533960	5.078270	2.145625
14	H	4.545819	3.404081	4.855213	5.504665	2.108120
15	H	3.972008	2.624849	4.815426	4.671647	2.106779

		6	7	8	9	10
6	C	0.000000				
7	N	2.405920	0.000000			
8	H	3.984043	4.506939	0.000000		
9	C	1.471564	3.703334	3.450772	0.000000	
10	O	1.228020	2.767348	5.212024	2.364574	0.000000
11	N	3.733974	5.514499	2.681596	2.378053	4.741136
12	H	2.406270	1.022314	5.326962	3.860944	2.275564
13	H	2.227512	4.615979	4.359275	1.102273	2.661583
14	H	4.053582	6.117712	3.727973	2.585662	4.866996
15	H	4.568916	6.071610	2.401367	3.322333	5.655614

		11	12	13	14	15
11	N	0.000000				
12	H	5.953905	0.000000			
13	H	2.617931	4.596398	0.000000		
14	H	1.049280	6.413257	2.360347	0.000000	
15	H	1.049098	6.635781	3.662947	1.832548	0.000000

Interatomic angles:

C2-C1-C3=120.7636 C2-C1-H4=119.6088 C3-C1-H4=119.6275
C1-C2-C5=120.9119 C1-C3-C6=118.9272 C1-C3-N7=120.7898
C6-C3-N7=120.283 C1-C2-H8=119.6448 C5-C2-H8=119.4433
C2-C5-C9=121.7516 C3-C6-O10=120.8089 C2-C5-N11=118.7771
C9-C5-N11=119.4714 C3-N7-H12=110.1713 C5-C9-H13=120.328
C5-N11-H14=119.2102 C5-N11-H15=119.097 H14-N11-H15=121.6927

Stoichiometry C6H6N2O
Framework group C1[X(C6H6N2O)]
Deg. of freedom 39
Full point group C1 NOp 1
Largest Abelian subgroup C1 NOp 1
Largest concise Abelian subgroup C1 NOp 1

Standard orientation:

Center Number	Atomic Number	Atomic Type	Coordinates (Angstroms) X	Y	Z
1	6	0	0.256072	1.623222	-0.001720
2	6	0	-1.060042	1.314898	-0.001188
3	6	0	1.272252	0.569042	0.000003
4	1	0	0.568007	2.681453	-0.002065
5	6	0	-1.504533	-0.075610	0.000011
6	6	0	0.832472	-0.858337	-0.001104
7	7	0	2.516508	0.859935	0.003013
8	1	0	-1.809657	2.123567	-0.002463
9	6	0	-0.616639	-1.114415	-0.000086
10	8	0	1.655244	-1.769973	-0.001486
11	7	0	-2.865545	-0.341397	0.001451
12	1	0	3.078230	0.005773	0.003536
13	1	0	-0.978241	-2.155687	0.000997
14	1	0	-3.192579	-1.338410	0.002957
15	1	0	-3.541951	0.460526	0.002172

Rotational constants (GHZ): 3.1467857 1.4115586 0.9744498
Isotopes: C-12,C-12,C-12,H-1,C-12,C-12,N-14,H-1,C-12,O-16,N-14,H-1,H-1,H-1,H-1
Standard basis: 6-31G(d) (6D, 7F)
There are 147 symmetry adapted basis functions of A symmetry.
Crude estimate of integral set expansion from redundant integrals=1.000.
Integral buffers will be 262144 words long.
Raffenetti 1 integral format.
Two-electron integral symmetry is turned on.
147 basis functions 276 primitive gaussians
32 alpha electrons 32 beta electrons
nuclear repulsion energy 406.1263021577 Hartrees.
One-electron integrals computed using PRISM.
NBasis= 147 RedAO= T NBF= 147
NBsUse= 147 1.00D-04 NBFU= 147
Projected INDO Guess.
Warning! Cutoffs for single-point calculations used.
Requested convergence on RMS density matrix=1.00D-04 within 64 cycles.
Requested convergence on MAX density matrix=1.00D-02.
Requested convergence on energy=5.00D-05.
SCF Done: E(RHF) = -414.414217497 A.U. after 8 cycles
Convg = 0.3202D-04 -V/T = 2.0031
S**2 = 0.0000

4. 1,4-DIANALINE-3-S.PDB # HF/6-31G*

Symbolic Z-matrix:
Charge = 0 Multiplicity = 1

C							
C	1	R2					
C	1	R3	2	A3			
H	1	R4	2	A4	3	D4	0
C	2	R5	1	A5	3	D5	0
C	3	R6	1	A6	2	D6	0
N	3	R7	1	A7	6	D7	0
H	2	R8	1	A8	5	D8	0
C	5	R9	2	A9	1	D9	0
N	5	R10	2	A10	9	D10	0
H	6	R11	3	A11	1	D11	0
H	7	R12	3	A12	1	D12	0
H	7	R13	3	A13	12	D13	0
S	9	R14	5	A14	2	D14	0
H	10	R15	5	A15	2	D15	0

Variables:

R2	1.36151
R3	1.43428
R4	1.10203
R5	1.46647
R6	1.43596
R7	1.34046
R8	1.10257
R9	1.48711
R10	1.27957
R11	1.10382
R12	1.04917
R13	1.04892
R14	1.5831
R15	1.01934
A3	119.75462
A4	119.9935
A5	120.93473
A6	121.17435
A7	119.32354
A8	119.28465
A9	118.86996
A10	117.67217
A11	118.0335
A12	119.24197
A13	119.06904
A14	121.82352
A15	111.60909
D4	-179.98503
D5	-0.0115

D6	-0.05333
D7	179.96051
D8	-179.96351
D9	0.18018
D10	-179.92131
D11	-179.938
D12	-179.99611
D13	-179.96859
D14	179.63266
D15	179.94268

Z-MATRIX (ANGSTROMS AND DEGREES)

CD	Cent	Atom	N1	Length/X	N2	Alpha/Y	N3	Beta/Z	J
1	1	C							
2	2	C	1	1.361511(1)					
3	3	C	1	1.434276(2)	2	119.755(15)			
4	4	H	1	1.102028(3)	2	119.994(16)	3	-179.985(28)	0
5	5	C	2	1.466472(4)	1	120.935(17)	3	-0.011(29)	0
6	6	C	3	1.435958(5)	1	121.174(18)	2	-0.053(30)	0
7	7	N	3	1.340462(6)	1	119.324(19)	6	179.961(31)	0
8	8	H	2	1.102565(7)	1	119.285(20)	5	-179.964(32)	0
9	9	C	5	1.487113(8)	2	118.870(21)	1	0.180(33)	0
10	10	N	5	1.279568(9)	2	117.672(22)	9	-179.921(34)	0
11	11	H	6	1.103823(10)	3	118.034(23)	1	-179.938(35)	0
12	12	H	7	1.049174(11)	3	119.242(24)	1	-179.996(36)	0
13	13	H	7	1.048918(12)	3	119.069(25)	12	-179.969(37)	0
14	14	S	9	1.583105(13)	5	121.824(26)	2	179.633(38)	0
15	15	H	10	1.019339(14)	5	111.609(27)	2	179.943(39)	0

Z-Matrix orientation:

Center Number	Atomic Number	Atomic Type	Coordinates (Angstroms) X	Y	Z
1	6	0	0.000000	0.000000	0.000000
2	6	0	0.000000	0.000000	1.361511
3	6	0	1.245180	0.000000	-0.711812
4	1	0	-0.954446	0.000249	-0.550906
5	6	0	1.257872	-0.000252	2.115368
6	6	0	2.500232	0.001143	-0.014090
7	7	0	1.235095	-0.001893	-2.052235
8	1	0	-0.961658	-0.000420	1.900829
9	6	0	2.543205	0.003585	1.367431
10	7	0	1.185054	-0.005358	3.392851
11	1	0	3.427071	0.002142	-0.613586
12	1	0	2.146685	-0.001953	-2.571628
13	1	0	0.314497	-0.002775	-2.554953
14	16	0	3.941221	0.012185	2.110194
15	1	0	2.109853	-0.006005	3.821569

Distance matrix (angstroms):

		1	2	3	4	5
1	C	0.000000				
2	C	1.361511	0.000000			
3	C	1.434276	2.418500	0.000000		
4	H	1.102028	2.137359	2.205504	0.000000	
5	C	2.461102	1.466472	2.827208	3.464587	0.000000
6	C	2.500272	2.853671	1.435958	3.496137	2.465371
7	N	2.395231	3.630306	1.340462	2.654823	4.167665
8	H	2.130244	1.102565	3.419945	2.451746	2.229874
9	C	2.887520	2.543214	2.451149	3.989184	1.487113
10	N	3.593859	2.351750	4.105107	4.486726	1.279568
11	H	3.481567	3.955481	2.184102	4.381966	3.486061
12	H	3.349856	4.480831	2.066793	3.701397	4.770526
13	H	2.574238	3.929072	2.064787	2.372010	4.764646
14	S	4.470603	4.011720	3.902884	5.572177	2.683383
15	H	4.365307	3.240895	4.615110	5.339336	1.907100

		6	7	8	9	10
6	C	0.000000				
7	N	2.398878	0.000000			
8	H	3.956210	4.522438	0.000000		
9	C	1.382191	3.661324	3.545221	0.000000	
10	N	3.651984	5.445317	2.614293	2.438643	0.000000
11	H	1.103823	2.621924	5.057987	2.169251	4.591104
12	H	2.581861	1.049174	5.446529	3.958970	6.041503
13	H	3.351632	1.048918	4.634929	4.511349	6.011177
14	S	2.566935	4.964789	4.907363	1.583105	3.040061
15	H	3.855480	5.938585	3.622630	2.492124	1.019339

		11	12	13	14	15
11	H	0.000000				
12	H	2.339516	0.000000			
13	H	3.668385	1.832265	0.000000		
14	S	2.771900	5.013982	5.909056	0.000000	
15	H	4.626633	6.393305	6.624451	2.506600	0.000000

Interatomic angles:

C2-C1-C3=119.7546 C2-C1-H4=119.9935 C3-C1-H4=120.2519
C1-C2-C5=120.9347 C1-C3-C6=121.1744 C1-C3-N7=119.3235
C6-C3-N7=119.5021 C1-C2-H8=119.2847 C5-C2-H8=119.7806
C2-C5-C9=118.87 C2-C5-N10=117.6722 C9-C5-N10=123.4578
C3-C6-H11=118.0335 C3-N7-H12=119.242 C3-N7-H13=119.069
H12-N7-H13=121.689 C5-C9-S14=121.8235 C5-N10-H15=111.6091

Stoichiometry C6H6N2S
Framework group C1[X(C6H6N2S)]
Deg. of freedom 39
Full point group C1 NOp 1
Largest Abelian subgroup C1 NOp 1
Largest concise Abelian subgroup C1 NOp 1

Standard orientation:

Center Number	Atomic Number	Atomic Type	Coordinates (Angstroms) X	Y	Z
1	6	0	-1.732667	1.095426	-0.003604
2	6	0	-0.560449	1.787971	-0.003519
3	6	0	-1.712145	-0.338699	0.000310
4	1	0	-2.692464	1.636945	-0.006922
5	6	0	0.728421	1.088446	0.000779
6	6	0	-0.473036	-1.064353	0.003200
7	7	0	-2.871339	-1.011829	0.002087
8	1	0	-0.585268	2.890254	-0.006123
9	6	0	0.738271	-0.398634	0.000981
10	7	0	1.791246	1.800957	0.005733
11	1	0	-0.517739	-2.167270	0.005111
12	1	0	-2.854834	-2.060869	0.005012
13	1	0	-3.772433	-0.474937	0.000011
14	16	0	2.088891	-1.224485	-0.003128
15	1	0	2.630762	1.222812	0.009347

Rotational constants (GHZ): 2.3698062 1.1818014 0.7885593
Isotopes: C-12,C-12,C-12,H-1,C-12,C-12,N-14,H-1,C-12,N-14,H-1,H-1,H-1,S-32,H-1
Standard basis: 6-31G(d) (6D, 7F)
There are 151 symmetry adapted basis functions of A symmetry.
Crude estimate of integral set expansion from redundant integrals=1.000.
Integral buffers will be 262144 words long.
Raffenetti 1 integral format.
Two-electron integral symmetry is turned on.
151 basis functions 300 primitive gaussians
36 alpha electrons 36 beta electrons
nuclear repulsion energy 474.1154975451 Hartrees.
One-electron integrals computed using PRISM.
NBasis= 151 RedAO= T NBF= 151
NBsUse= 151 1.00D-04 NBFU= 151
Projected CNDO Guess.
Warning! Cutoffs for single-point calculations used.
Requested convergence on RMS density matrix=1.00D-04 within 64 cycles.
Requested convergence on MAX density matrix=1.00D-02.
Requested convergence on energy=5.00D-05.
SCF Done: E(RHF) = -737.045937311 A.U. after 8 cycles
Convg = 0.5316D-04 -V/T = 2.0012
S**2 = 0.0000

Appendix 2

Molecular orbital calculation on methyl violet degradation products

1. Output file for 1-oxy emine

Z-matrix:
Charge = 0 Multiplicity = 1

```
C
C          1   1.48507
C          2   1.34937  1   120.63449
C          3   1.46638  2   120.89265  1   -0.01858  0
C          4   1.46546  3   119.02108  2    0.04295  0
C          5   1.34965  4   120.80792  3   -0.04953  0
O          1   1.22648  2   121.06379  3   -179.9688  0
N          4   1.28043  3   120.63902  2   -179.97708  0
H          2   1.10192  1   119.37452  7    0.00527  0
H          3   1.10267  2   119.59355  1    179.99945  0
H          5   1.10294  4   119.83329  3   -179.99436  0
H          6   1.1024   5   119.96692  4   -179.98062  0
H          8   1.02166  4   110.00138  3   -179.96817  0
```

Z-MATRIX (ANGSTROMS AND DEGREES)

CD	Cent	Atom	N1	Length/X	N2	Alpha/Y	N3	Beta/Z	J
1	1	C							
2	2	C	1	1.485071(1)					
3	3	C	2	1.349374(2)	1	120.634(13)			
4	4	C	3	1.466382(3)	2	120.893(14)	1	-0.019(24)	0
5	5	C	4	1.465464(4)	3	119.021(15)	2	0.043(25)	0
6	6	C	5	1.349645(5)	4	120.808(16)	3	-0.050(26)	0
7	7	O	1	1.226477(6)	2	121.064(17)	3	-179.969(27)	0
8	8	N	4	1.280433(7)	3	120.639(18)	2	-179.977(28)	0
9	9	H	2	1.101919(8)	1	119.375(19)	7	0.005(29)	0
10	10	H	3	1.102670(9)	2	119.594(20)	1	179.999(30)	0
11	11	H	5	1.102937(10)	4	119.833(21)	3	-179.994(31)	0
12	12	H	6	1.102402(11)	5	119.967(22)	4	-179.981(32)	0
13	13	H	8	1.021662(12)	4	110.001(23)	3	-179.968(33)	0

Z-Matrix orientation:

Center Number	Atomic Number	Atomic Type	Coordinates (Angstroms) X	Y	Z
1	6	0	0.000000	0.000000	0.000000
2	6	0	0.000000	0.000000	1.485071
3	6	0	1.161049	0.000000	2.172657

4	6	0	2.450062	-0.000408	1.473571
5	6	0	2.464084	0.000141	0.008174
6	6	0	1.311556	0.000008	-0.694122
7	8	0	-1.050592	0.000572	-0.632852
8	7	0	3.548893	-0.000847	2.130898
9	1	0	-0.960247	0.000435	2.025580
10	1	0	1.141017	0.000009	3.275145
11	1	0	3.426062	-0.000250	-0.531333
12	1	0	1.338282	0.000104	-1.796200
13	1	0	4.341632	-0.000549	1.486416

Distance matrix (angstroms):

	1	2	3	4	5
1 C	0.000000				
2 C	1.485071	0.000000			
3 C	2.463428	1.349374	0.000000		
4 C	2.859058	2.450089	1.466382	0.000000	
5 C	2.464097	2.872792	2.526438	1.465464	0.000000
6 C	1.483908	2.543435	2.870727	2.448487	1.349645
7 O	1.226477	2.364179	3.572428	4.085535	3.572655
8 N	4.139489	3.607178	2.388209	1.280433	2.383856
9 H	2.241662	1.101919	2.126389	3.454696	3.974415
10 H	3.468212	2.122802	1.102670	2.226942	3.524714
11 H	3.467018	3.975398	3.527300	2.229847	1.102937
12 H	2.239941	3.543690	3.972813	3.453615	2.126780
13 H	4.589030	4.341632	3.253772	1.891614	2.389641

	6	7	8	9	10
6 C	0.000000				
7 O	2.362942	0.000000			
8 N	3.603667	5.365965	0.000000		
9 H	3.543708	2.659967	4.510370	0.000000	
10 H	3.972929	4.480580	2.665927	2.444734	0.000000
11 H	2.120763	4.477805	2.665064	5.077156	4.439674
12 H	1.102402	2.657085	4.506540	4.459736	5.075181
13 H	3.733110	5.793736	1.021662	5.329224	3.666536

	11	12	13
11 H	0.000000		
12 H	2.441047	0.000000	
13 H	2.215757	4.449233	0.000000

Interatomic angles:

C1-C2-C3=120.6345 C2-C3-C4=120.8926 C3-C4-C5=119.0211
C4-C5-C6=120.8079 C2-C1-O7=121.0638 C3-C4-N8=120.639
C5-C4-N8=120.3399 C1-C2-H9=119.3745 C3-C2-H9=119.991
C2-C3-H10=119.5936 C4-C3-H10=119.5138 C4-C5-H11=119.8333
C6-C5-H11=119.3588 C5-C6-H12=119.9669 C4-N8-H13=110.0014

Stoichiometry C6H5NO
Framework group C1[X(C6H5NO)]
Deg. of freedom 33
Full point group C1 NOp 1
Largest Abelian subgroup C1 NOp 1

Largest concise Abelian subgroup C1 NOp 1
Standard orientation:

Center Number	Atomic Number	Atomic Type	Coordinates (Angstroms) X	Y	Z
1	6	0	1.448954	-0.025996	-0.000252
2	6	0	0.722068	1.269022	-0.000090
3	6	0	-0.626943	1.300324	0.000197
4	6	0	-1.408817	0.059780	-0.000052
5	6	0	-0.703787	-1.224945	0.000340
6	6	0	0.644993	-1.273245	-0.000080
7	8	0	2.674854	-0.063633	0.000059
8	7	0	-2.688761	0.095148	-0.000218
9	1	0	1.294868	2.210364	0.000229
10	1	0	-1.149102	2.271525	0.000323
11	1	0	-1.278587	-2.166261	0.000065
12	1	0	1.161113	-2.247365	-0.000100
13	1	0	-3.064599	-0.854872	0.000154

Rotational constants (GHZ): 5.1597250 1.6731686 1.2634603
Isotopes: C-12,C-12,C-12,C-12,C-12,C-12,O-16,N-14,H-1,H-1,H-1,H-1,H-1
Standard basis: 6-31G(d) (6D, 7F)
There are 130 symmetry adapted basis functions of A symmetry.
Crude estimate of integral set expansion from redundant integrals=1.000.
Integral buffers will be 262144 words long.
Raffenetti 1 integral format.
Two-electron integral symmetry is turned on.
130 basis functions 244 primitive gaussians
28 alpha electrons 28 beta electrons
nuclear repulsion energy 322.9521410673 Hartrees.
One-electron integrals computed using PRISM.
NBasis= 130 RedAO= T NBF= 130
NBsUse= 130 1.00D-04 NBFU= 130
Projected INDO Guess.
Warning! Cutoffs for single-point calculations used.
Requested convergence on RMS density matrix=1.00D-04 within 64 cycles.
Requested convergence on MAX density matrix=1.00D-02.
Requested convergence on energy=5.00D-05.
SCF Done: E(RHF) = -359.386127224 A.U. after 7 cycles
Convg = 0.3364D-04 -V/T = 2.0027
S**2 = 0.0000

2. Out put file for 4-methyl analine

Symbolic Z-matrix:

Charge = 0 Multiplicity = 1

```
C
C              1    1.40331
C              2    1.39505  1    119.94788
C              3    1.4014   2    120.88876  1    -0.09254  0
C              4    1.40055  3    118.71707  2     0.16103  0
C              5    1.39605  4    121.01117  3    -0.16321  0
C              4    1.50813  3    121.29043  2     179.86922  0
N              1    1.39203  2    120.15253  3     179.98444  0
H              2    1.10261  1    120.18388  8    -0.00899  0
H              3    1.10156  2    119.11006  1    -179.97288  0
H              6    1.1013   5    119.91424  4    -179.96284  0
H              5    1.10187  4    119.59616  3     179.89516  0
H              7    1.1139   4    110.0946   3     116.65506  0
H              7    1.11245  4    112.40974  3    -3.5463   0
H              7    1.11403  4    110.35884  3    -123.60621  0
H              8    1.05055  1    118.94308  2     179.97028  0
H              8    1.04828  1    119.08764  2     0.02807  0
```

Z-MATRIX (ANGSTROMS AND DEGREES)

CD	Cent	Atom	N1	Length/X	N2	Alpha/Y	N3	Beta/Z	J
1	1	C							
2	2	C	1	1.403308(1)					
3	3	C	2	1.395046(2)	1	119.948(17)			
4	4	C	3	1.401397(3)	2	120.889(18)	1	-0.093(32)	0
5	5	C	4	1.400552(4)	3	118.717(19)	2	0.161(33)	0
6	6	C	5	1.396047(5)	4	121.011(20)	3	-0.163(34)	0
7	7	C	4	1.508128(6)	3	121.290(21)	2	179.869(35)	0
8	8	N	1	1.392026(7)	2	120.153(22)	3	179.984(36)	0
9	9	H	2	1.102612(8)	1	120.184(23)	8	-0.009(37)	0
10	10	H	3	1.101558(9)	2	119.110(24)	1	-179.973(38)	0
11	11	H	6	1.101300(10)	5	119.914(25)	4	-179.963(39)	0
12	12	H	5	1.101867(11)	4	119.596(26)	3	179.895(40)	0
13	13	H	7	1.113895(12)	4	110.095(27)	3	116.655(41)	0
14	14	H	7	1.112445(13)	4	112.410(28)	3	-3.546(42)	0
15	15	H	7	1.114027(14)	4	110.359(29)	3	-123.606(43)	0
16	16	H	8	1.050545(15)	1	118.943(30)	2	179.970(44)	0
17	17	H	8	1.048279(16)	1	119.088(31)	2	0.028(45)	0

Z-Matrix orientation:

Center Number	Atomic Number	Atomic Type	Coordinates (Angstroms) X	Y	Z
1	6	0	0.000000	0.000000	0.000000
2	6	0	0.000000	0.000000	1.403308

3	6	0	1.208779	0.000000	2.099732
4	6	0	2.432526	-0.001942	1.416830
5	6	0	2.421621	-0.000441	0.016322
6	6	0	1.219552	-0.000486	-0.693592
7	6	0	3.744535	0.000982	2.160520
8	7	0	-1.203673	-0.000327	-0.699220
9	1	0	-0.953116	-0.000109	1.957676
10	1	0	1.192672	-0.000456	3.201172
11	1	0	1.232062	0.000090	-1.794820
12	1	0	3.375459	-0.000182	-0.535316
13	1	0	4.309177	-0.934498	1.944145
14	1	0	3.607285	0.068293	3.262411
15	1	0	4.366501	0.869980	1.845786
16	1	0	-1.181499	0.000156	-1.749531
17	1	0	-2.104478	-0.000123	-0.163087

Distance matrix (angstroms):

	1	2	3	4	5
1 C	0.000000				
2 C	1.403308	0.000000			
3 C	2.422813	1.395046	0.000000		
4 C	2.815066	2.432564	1.401397	0.000000	
5 C	2.421676	2.790695	2.410722	1.400552	0.000000
6 C	1.402989	2.425757	2.793344	2.434171	1.396047
7 C	4.323123	3.820329	2.536484	1.508128	2.519462
8 N	1.392026	2.422695	3.695139	4.207091	3.695234
9 H	2.177366	1.102612	2.166557	3.428569	3.893290
10 H	3.416134	2.157494	1.101558	2.172812	3.413735
11 H	2.177006	3.427244	3.894622	3.428676	2.166861
12 H	3.417644	3.892555	3.411448	2.167949	1.101867
13 H	4.818920	4.442386	3.241907	2.160912	2.855141
14 H	4.864206	4.058748	2.666331	2.188872	3.456533
15 H	4.819764	4.474258	3.285203	2.164373	2.808404
16 H	2.111113	3.366947	4.531032	4.804896	4.012569
17 H	2.110788	2.623437	4.012235	4.804222	4.529654

	6	7	8	9	10
6 C	0.000000				
7 C	3.810708	0.000000			
8 N	2.423231	5.715144	0.000000		
9 H	3.427784	4.702028	2.668684	0.000000	
10 H	3.894856	2.755896	4.577720	2.480058	0.000000
11 H	1.101300	4.685855	2.670795	4.342376	4.996148
12 H	2.161709	2.720983	4.582064	4.995154	4.327343
13 H	4.168431	1.113895	6.184785	5.344622	3.487858
14 H	4.621251	1.112445	6.232539	4.743867	2.416368
15 H	4.136356	1.114027	6.185574	5.391465	3.559202
16 H	2.622986	6.289221	1.050545	3.714234	5.490550
17 H	3.366098	6.293656	1.048279	2.413146	4.710567

	11	12	13	14	15
11 H	0.000000				

```
 12  H    2.486062  0.000000
 13  H    4.931729  2.809360  0.000000
 14  H    5.587659  3.805412  1.798907  0.000000
 15  H    4.882155  2.721946  1.808066  1.796090  0.000000
 16  H    2.413986  4.715950  6.683138  6.932291  6.668073
 17  H    3.714169  5.492565  6.815311  6.660553  6.831268
            16        17
 16  H    0.000000
 17  H    1.835400  0.000000
                Interatomic angles:
  C1-C2-C3=119.9479    C2-C3-C4=120.8888    C3-C4-C5=118.7171
  C4-C5-C6=121.0112    C3-C4-C7=121.2904    C5-C4-C7=119.9919
  C2-C1-N8=120.1525    C1-C2-H9=120.1839    C3-C2-H9=119.8682
 C2-C3-H10=119.1101   C4-C3-H10=120.0011   C5-C6-H11=119.9142
 C4-C5-H12=119.5962   C6-C5-H12=119.3926   C4-C7-H13=110.0946
 C4-C7-H14=112.4097  H13-C7-H14=107.8041   C4-C7-H15=110.3588
H13-C7-H15=108.495   H14-C7-H15=107.549    C1-N8-H16=118.9431
 C1-N8-H17=119.0876  H16-N8-H17=121.9693
Stoichiometry   C7H9N
Framework group  C1[X(C7H9N)]
Deg. of freedom  45
Full point group                 C1     NOp  1
Largest Abelian subgroup         C1     NOp  1
Largest concise Abelian subgroup C1     NOp  1
                Standard orientation:
---------------------------------------------------------------------
Center     Atomic     Atomic              Coordinates (Angstroms)
Number     Number      Type               X           Y           Z
---------------------------------------------------------------------
    1          6          0       -1.426496   -0.002501   -0.000344
    2          6          0       -0.724866    1.212813   -0.000123
    3          6          0        0.670179    1.211571    0.000037
    4          6          0        1.388548    0.008302    0.001922
    5          6          0        0.678874   -1.199135    0.000200
    6          6          0       -0.717105   -1.212931    0.000083
    7          6          0        2.896626   -0.003618   -0.000830
    8          7          0       -2.818517   -0.006235   -0.000178
    9          1          0       -1.273124    2.169456    0.000034
   10          1          0        1.206931    2.173511    0.000665
   11          1          0       -1.256867   -2.172889   -0.000666
   12          1          0        1.229122   -2.153775   -0.000106
   13          1          0        3.277335   -0.473426    0.934640
   14          1          0        3.328698    1.019289   -0.067973
   15          1          0        3.278009   -0.587060   -0.869852
   16          1          0       -3.324451   -0.926927   -0.000825
   17          1          0       -3.330590    0.908462   -0.000335
---------------------------------------------------------------------
Rotational constants (GHZ):     5.3717721     1.4615184     1.1575981
Isotopes: C-12,C-12,C-12,C-12,C-12,C-12,C-12,N-14,H-1,H-1,H-1,H-1,H-1,H-1,H-1,H-
1,H-1
```

Standard basis: 6-31G(d) (6D, 7F)
There are 138 symmetry adapted basis functions of A symmetry.
Crude estimate of integral set expansion from redundant integrals=1.000.
Integral buffers will be 262144 words long.
Raffenetti 1 integral format.
Two-electron integral symmetry is turned on.
138 basis functions 260 primitive gaussians
29 alpha electrons 29 beta electrons
nuclear repulsion energy 341.2445819324 Hartrees.
One-electron integrals computed using PRISM.
NBasis= 138 RedAO= T NBF= 138
NBsUse= 138 1.00D-04 NBFU= 138
Projected INDO Guess.
Warning! Cutoffs for single-point calculations used.
Requested convergence on RMS density matrix=1.00D-04 within 64 cycles.
Requested convergence on MAX density matrix=1.00D-02.
Requested convergence on energy=5.00D-05.
SCF Done: E(RHF) = -324.752514480 A.U. after 6 cycles
Convg = 0.1698D-04 -V/T = 2.0031
S**2 = 0.0000

3. Output for 4-oxy analine

Symbolic Z-matrix:

Charge = 0 Multiplicity = 1

```
C
C          1  1.3551
C          2  1.50346  1  122.98136
C          3  1.51866  2  114.54641  1   0.12749  0
C          4  1.48041  3  119.04395  2  -0.14537  0
C          5  1.35053  4  120.94151  3   0.11509  0
N          1  1.39521  2  120.07479  3   179.9355  0
O          4  1.22666  3  120.30887  2   179.87475  0
H          2  1.10313  1  119.72864  7   0.0176  0
H          3  1.1149  2  108.64686  1  -121.02587  0
H          3  1.11534  2  108.62074  1   121.20937  0
H          6  1.10244  5  119.24535  4   179.98461  0
H          5  1.10277  4  119.162  3  -179.97647  0
H          7  1.04963  1  119.11456  2   179.95102  0
H          7  1.04886  1  119.18617  2   0.06891  0
```

Z-MATRIX (ANGSTROMS AND DEGREES)

CD	Cent	Atom	N1	Length/X	N2	Alpha/Y	N3	Beta/Z	J
1	1	C							
2	2	C	1	1.355103(1)					
3	3	C	2	1.503464(2)	1	122.981(15)			
4	4	C	3	1.518665(3)	2	114.546(16)	1	0.127(28)	0
5	5	C	4	1.480408(4)	3	119.044(17)	2	-0.145(29)	0
6	6	C	5	1.350525(5)	4	120.942(18)	3	0.115(30)	0
7	7	N	1	1.395210(6)	2	120.075(19)	3	179.935(31)	0
8	8	O	4	1.226663(7)	3	120.309(20)	2	179.875(32)	0
9	9	H	2	1.103126(8)	1	119.729(21)	7	0.018(33)	0
10	10	H	3	1.114903(9)	2	108.647(22)	1	-121.026(34)	0
11	11	H	3	1.115337(10)	2	108.621(23)	1	121.209(35)	0
12	12	H	6	1.102445(11)	5	119.245(24)	4	179.985(36)	0
13	13	H	5	1.102765(12)	4	119.162(25)	3	-179.976(37)	0
14	14	H	7	1.049627(13)	1	119.115(26)	2	179.951(38)	0
15	15	H	7	1.048865(14)	1	119.186(27)	2	0.069(39)	0

Z-Matrix orientation:

Center Number	Atomic Number	Atomic Type	Coordinates (Angstroms) X	Y	Z
1	6	0	0.000000	0.000000	0.000000
2	6	0	0.000000	0.000000	1.355103
3	6	0	1.261177	0.000000	2.173538
4	6	0	2.542400	0.003074	1.358184
5	6	0	2.453878	0.002441	-0.119575
6	6	0	1.256093	0.001514	-0.743458

7	7	0	-1.207375	-0.001359	-0.699182
8	8	0	3.633225	0.005663	1.919251
9	1	0	-0.957936	-0.001373	1.902135
10	1	0	1.263805	-0.905247	2.824329
11	1	0	1.261779	0.903990	2.826821
12	1	0	1.222773	0.001320	-1.845400
13	1	0	3.383005	0.004274	-0.713553
14	1	0	-1.189786	-0.000556	-1.748661
15	1	0	-2.108879	-0.001273	-0.163077

Distance matrix (angstroms):

	1	2	3	4	5
1 C	0.000000				
2 C	1.355103	0.000000			
3 C	2.512934	1.503464	0.000000		
4 C	2.882442	2.542404	1.518665	0.000000	
5 C	2.456790	2.862900	2.584745	1.480408	0.000000
6 C	1.459624	2.445758	2.917001	2.464038	1.350525
7 N	1.395210	2.382822	3.787647	4.277100	3.706849
8 O	4.109000	3.676767	2.385645	1.226663	2.355352
9 H	2.129733	1.103126	2.235648	3.542351	3.965829
10 H	3.223897	2.138995	1.114903	2.146959	3.302536
11 H	3.224934	2.138980	1.115337	2.146750	3.303807
12 H	2.213747	3.426134	4.019121	3.464731	2.119926
13 H	3.457441	3.965360	3.582941	2.235780	1.102765
14 H	2.115043	3.323995	4.625026	4.856100	3.991267
15 H	2.115175	2.598508	4.100860	4.893736	4.562966

	6	7	8	9	10
6 C	0.000000				
7 N	2.463868	0.000000			
8 O	3.569424	5.503421	0.000000		
9 H	3.449797	2.613249	4.591198	0.000000	
10 H	3.681220	4.397598	2.695009	2.569740	0.000000
11 H	3.682579	4.398758	2.693405	2.569408	1.809240
12 H	1.102445	2.686902	4.470222	4.335841	4.757091
13 H	2.127124	4.590406	2.644668	5.068098	4.223132
14 H	2.644383	1.049627	6.059294	3.658151	5.267904
15 H	3.414658	1.048865	6.108019	2.364270	4.595298

	11	12	13	14	15
11 H	0.000000				
12 H	4.758779	0.000000			
13 H	4.224138	2.438788	0.000000		
14 H	5.269099	2.414499	4.688485	0.000000	
15 H	4.595685	3.732308	5.519406	1.832705	0.000000

Interatomic angles:

C1-C2-C3=122.9814	C2-C3-C4=114.5464	C3-C4-C5=119.044
C4-C5-C6=120.9415	C2-C1-N7=120.0748	C3-C4-O8=120.3089
C5-C4-O8=120.6472	C1-C2-H9=119.7286	C3-C2-H9=117.2899
C2-C3-H10=108.6469	C4-C3-H10=108.243	C2-C3-H11=108.6207
C4-C3-H11=108.2024	H10-C3-H11=108.4328	C5-C6-H12=119.2453

C4-C5-H13=119.162 C6-C5-H13=119.8964 C1-N7-H14=119.1146
C1-N7-H15=119.1862 H14-N7-H15=121.6992
Stoichiometry C6H7NO
Framework group C1[X(C6H7NO)]
Deg. of freedom 39
Full point group C1 NOp 1
Largest Abelian subgroup C1 NOp 1
Largest concise Abelian subgroup C1 NOp 1
Standard orientation:

Center Number	Atomic Number	Atomic Type	Coordinates (Angstroms) X	Y	Z
1	6	0	1.349021	-0.003683	-0.000115
2	6	0	0.693112	-1.189468	-0.000389
3	6	0	-0.806629	-1.295196	0.001164
4	6	0	-1.533113	0.038432	0.000000
5	6	0	-0.740372	1.288700	0.000810
6	6	0	0.609729	1.254868	0.000231
7	7	0	2.743962	0.023733	-0.000260
8	8	0	-2.759216	0.075462	-0.001217
9	1	0	1.266577	-2.131819	-0.000431
10	1	0	-1.122940	-1.864156	0.906283
11	1	0	-1.124353	-1.865806	-0.902956
12	1	0	1.172257	2.202996	0.000602
13	1	0	-1.265906	2.258187	0.000362
14	1	0	3.236548	0.950596	-0.000828
15	1	0	3.273334	-0.881740	-0.001682

Rotational constants (GHZ): 5.0041429 1.5232688 1.1767621
Isotopes: C-12,C-12,C-12,C-12,C-12,C-12,N-14,O-16,H-1,H-1,H-1,H-1,H-1,H-1,H-1
Standard basis: 6-31G(d) (6D, 7F)
There are 134 symmetry adapted basis functions of A symmetry.
Crude estimate of integral set expansion from redundant integrals=1.000.
Integral buffers will be 262144 words long.
Raffenetti 1 integral format.
Two-electron integral symmetry is turned on.
134 basis functions 252 primitive gaussians
29 alpha electrons 29 beta electrons
nuclear repulsion energy 341.5618202187 Hartrees.
One-electron integrals computed using PRISM.
NBasis= 134 RedAO= T NBF= 134
NBsUse= 134 1.00D-04 NBFU= 134
Projected INDO Guess.
Warning! Cutoffs for single-point calculations used.
Requested convergence on RMS density matrix=1.00D-04 within 64 cycles.
Requested convergence on MAX density matrix=1.00D-02.
Requested convergence on energy=5.00D-05.
SCF Done: E(RHF) = -360.547039707 A.U. after 7 cycles
Convg = 0.3016D-04 -V/T = 2.0031

S**2 = 0.0000

4. Output for intermediate 1

Title Card Required

Symbolic Z-matrix:
Charge = 0 Multiplicity = 2

```
C
C            1   1.40553
C            2   1.39402  1   119.82329
C            3   1.40487  2   120.99269  1   -1.73481  0
C            4   1.40382  3   118.56729  2    4.45902  0
C            5   1.39455  4   120.84441  3   -4.47037  0
C            4   1.47286  3   118.93646  2   177.45033  0
C            7   1.36436  4   126.78488  3   144.58612  0
C            8   1.46814  7   118.86465  4   176.30612  0
C            9   1.35243  8   121.29683  7  -178.45186  0
C           10   1.46179  9   120.27024  8    -1.37901  0
C           11   1.46242 10   118.8675   9    -3.60251  0
C           12   1.35249 11   120.3767  10     3.6309   0
N            1   1.3892   2   120.12054  3  -179.70844  0
N           11   1.28603 10   120.70775  9   178.57479  0
H            3   1.10288  2   118.88709  1   178.87647  0
H            5   1.10229  4   120.6548   3   173.01338  0
H            7   1.10354  4   115.52238  3   -33.78155  0
H            2   1.10156  1   120.2226  14    -0.32993  0
H            9   1.10229  8   120.14694  7     0.52827  0
H           13   1.10034 12   117.88893 11  -176.04585  0
H            6   1.10287  5   119.89517  4  -179.88931  0
H           10   1.10213  9   119.96902  8   178.98962  0
H           12   1.10306 11   119.83037 10  -173.92938  0
H           14   1.04948  1   119.04792  2   179.31196  0
H           14   1.04976  1   119.03487  2    -0.69861  0
```

Z-MATRIX (ANGSTROMS AND DEGREES)

CD	Cent	Atom	N1	Length/X	N2	Alpha/Y	N3	Beta/Z	J
1	1	C							
2	2	C	1	1.405533(1)					
3	3	C	2	1.394023(2)	1	119.823(26)			
4	4	C	3	1.404865(3)	2	120.993(27)	1	-1.735(50)	0
5	5	C	4	1.403816(4)	3	118.567(28)	2	4.459(51)	0
6	6	C	5	1.394553(5)	4	120.844(29)	3	-4.470(52)	0
7	7	C	4	1.472859(6)	3	118.936(30)	2	177.450(53)	0
8	8	C	7	1.364364(7)	4	126.785(31)	3	144.586(54)	0
9	9	C	8	1.468140(8)	7	118.865(32)	4	176.306(55)	0
10	10	C	9	1.352429(9)	8	121.297(33)	7	-178.452(56)	0
11	11	C	10	1.461794(10)	9	120.270(34)	8	-1.379(57)	0
12	12	C	11	1.462423(11)	10	118.868(35)	9	-3.603(58)	0

13	13	C	12	1.352490(12)	11	120.377(36)	10	3.631(59)	0
14	14	N	1	1.389202(13)	2	120.121(37)	3	-179.708(60)	0
15	15	N	11	1.286033(14)	10	120.708(38)	9	178.575(61)	0
16	16	H	3	1.102881(15)	2	118.887(39)	1	178.876(62)	0
17	17	H	5	1.102285(16)	4	120.655(40)	3	173.013(63)	0
18	18	H	7	1.103538(17)	4	115.522(41)	3	-33.782(64)	0
19	19	H	2	1.101564(18)	1	120.223(42)	14	-0.330(65)	0
20	20	H	9	1.102291(19)	8	120.147(43)	7	0.528(66)	0
21	21	H	13	1.100336(20)	12	117.889(44)	11	-176.046(67)	0
22	22	H	6	1.102874(21)	5	119.895(45)	4	-179.889(68)	0
23	23	H	10	1.102128(22)	9	119.969(46)	8	178.990(69)	0
24	24	H	12	1.103063(23)	11	119.830(47)	10	-173.929(70)	0
25	25	H	14	1.049477(24)	1	119.048(48)	2	179.312(71)	0
26	26	H	14	1.049757(25)	1	119.035(49)	2	-0.699(72)	0

Z-Matrix orientation:

Center Number	Atomic Number	Atomic Type	Coordinates (Angstroms) X	Y	Z
1	6	0	0.000000	0.000000	0.000000
2	6	0	0.000000	0.000000	1.405533
3	6	0	1.209403	0.000000	2.098818
4	6	0	2.435658	-0.036458	1.414262
5	6	0	2.423535	0.022770	0.011748
6	6	0	1.220470	0.022517	-0.693527
7	6	0	3.686604	0.022436	2.189490
8	6	0	4.854764	-0.622833	1.905728
9	6	0	6.025768	-0.375372	2.755991
10	6	0	7.216138	-0.964553	2.501140
11	6	0	7.354091	-1.892262	1.379905
12	6	0	6.168522	-2.230298	0.593242
13	6	0	4.981992	-1.636142	0.854689
14	7	0	-1.201605	0.006115	-0.697131
15	7	0	8.488519	-2.436243	1.113376
16	1	0	1.191475	0.018935	3.201391
17	1	0	3.364637	0.112129	-0.555150
18	1	0	3.649872	0.636828	3.105443
19	1	0	-0.951779	0.010324	1.960017
20	1	0	5.952133	0.314595	3.612477
21	1	0	4.102765	-1.968685	0.282750
22	1	0	1.229257	0.067661	-1.795441
23	1	0	8.085335	-0.750261	3.143995
24	1	0	6.232545	-3.003168	-0.191182
25	1	0	-1.181936	0.017032	-1.746366
26	1	0	-2.102896	-0.000490	-0.158968

Distance matrix (angstroms):

		1	2	3	4	5
1	C	0.000000				

2	C	1.405533	0.000000			
3	C	2.422332	1.394023	0.000000		
4	C	2.816717	2.435946	1.404865	0.000000	
5	C	2.423670	2.795832	2.414641	1.403816	0.000000
6	C	1.403935	2.428190	2.792457	2.433707	1.394553
7	C	4.287822	3.769104	2.478961	1.472859	2.517519
8	C	5.252471	4.920045	3.703222	2.537213	3.148783
9	C	6.636737	6.186641	4.875464	3.847596	4.545929
10	C	7.697968	7.362294	6.096974	4.989555	5.490075
11	C	7.717995	7.593679	6.469519	5.257012	5.463477
12	C	6.586109	6.609441	5.642149	4.406959	4.409011
13	C	5.312975	5.272631	4.296189	3.058746	3.163580
14	N	1.389202	2.421794	3.691927	4.205885	3.693836
15	N	8.901115	8.836040	7.738986	6.518177	6.636593
16	H	3.415973	2.155244	1.102881	2.178276	3.419328
17	H	3.411971	3.895848	3.420695	2.182582	1.102285
18	H	4.834345	4.076372	2.715646	2.188087	3.384068
19	H	2.178912	1.101564	2.165660	3.431438	3.897262
20	H	6.969709	6.355899	4.988348	4.161849	5.049892
21	H	4.559424	4.687114	3.942761	2.791606	2.618997
22	H	2.176984	3.429561	3.894898	3.430516	2.166622
23	H	8.707482	8.304082	6.995264	5.951499	6.516481
24	H	6.920995	7.100220	6.284510	5.078894	4.868884
25	H	2.108805	3.366264	4.528160	4.804104	4.011287
26	H	2.108896	2.621037	4.008606	4.803625	4.529709

		6	7	8	9	10
6	C	0.000000				
7	C	3.793890	0.000000			
8	C	4.514498	1.364364	0.000000		
9	C	5.928607	2.439439	1.468140	0.000000	
10	C	6.865002	3.678164	2.459142	1.352429	0.000000
11	C	6.751800	4.215680	2.852118	2.441108	1.461794
12	C	5.586964	3.712511	2.456120	2.852825	2.517873
13	C	4.392855	2.492109	1.465492	2.508776	2.855389
14	N	2.422133	5.676921	6.621937	8.019009	9.057016
15	N	7.882572	5.501047	4.137688	3.607009	2.389710
16	H	3.895027	2.692512	3.938310	4.870754	6.144442
17	H	2.150495	2.764915	2.969271	4.275855	5.033311
18	H	4.550993	1.103538	2.116087	2.606060	3.955737
19	H	3.429302	4.644072	5.841214	7.033385	8.242669
20	H	6.404343	2.691258	2.235169	1.102291	2.114001
21	H	3.636705	2.788084	2.238499	3.514756	3.952547
22	H	1.102874	4.681909	5.226828	6.627091	7.441023
23	H	7.902540	4.566944	3.462100	2.129062	1.102128
24	H	5.876054	4.615592	3.458512	3.953972	3.517386
25	H	2.622986	6.260485	7.084417	8.507421	9.462160
26	H	3.366162	6.247727	7.284182	8.643651	9.739096

		11	12	13	14	15
11	C	0.000000				
12	C	1.462423	0.000000			

13	C	2.443011	1.352490	0.000000		
14	N	9.006544	7.809313	6.583466	0.000000	
15	N	1.286033	2.386491	3.605941	10.155863	0.000000
16	H	6.704350	6.052477	4.755450	4.574436	7.977127
17	H	4.865981	3.829823	2.767659	4.569678	5.960902
18	H	4.805727	4.568934	3.465087	6.196304	6.068328
19	H	8.540717	7.588620	6.256376	2.668870	9.788857
20	H	3.438034	3.954628	3.514533	8.357263	4.499541
21	H	3.432304	2.105279	1.100336	5.744244	4.488139
22	H	7.172009	5.948341	4.899914	2.668176	8.211433
23	H	2.225061	3.517246	3.956823	10.078373	2.669927
24	H	2.227172	1.103063	2.127554	8.036065	2.666964
25	H	9.288850	8.034519	6.891479	1.049477	10.378554
26	H	9.766347	8.599664	7.341560	1.049757	10.942113

		16	17	18	19	20
16	H	0.000000				
17	H	4.340843	0.000000			
18	H	2.536673	3.708990	0.000000		
19	H	2.476817	4.996787	4.783273	0.000000	
20	H	4.787512	4.909709	2.379353	7.105435	0.000000
21	H	4.576538	2.361503	3.867997	5.681384	4.440790
22	H	4.997212	2.469847	5.495634	4.343233	7.184157
23	H	6.936876	6.059075	4.647454	9.146023	2.429804
24	H	6.786386	4.249993	5.548648	8.082283	5.055097
25	H	5.487566	4.700996	6.875360	3.713529	8.927524
26	H	4.705876	5.483025	6.645065	2.411490	8.899807

		21	22	23	24	25
21	H	0.000000				
22	H	4.089331	0.000000			
23	H	5.052934	8.489572	0.000000		
24	H	2.414690	6.085764	4.430782	0.000000	
25	H	5.999037	2.412224	10.506507	8.155656	0.000000
26	H	6.525269	3.712942	10.736469	8.859836	1.835296

		26
26	H	0.000000

Interatomic angles:

C1-C2-C3=119.8233 C2-C3-C4=120.9927 C3-C4-C5=118.5673
C4-C5-C6=120.8444 C3-C4-C7=118.9365 C5-C4-C7=122.1069
C4-C7-C8=126.7849 C7-C8-C9=118.8647 C8-C9-C10=121.2968
C9-C10-C11=120.2702 C10-C11-C12=118.8675 C11-C12-C13=120.3767
C2-C1-N14=120.1205 C10-C11-N15=120.7077 C12-C11-N15=120.3886
C2-C3-H16=118.8871 C4-C3-H16=120.1174 C4-C5-H17=120.6548
C6-C5-H17=118.4544 C4-C7-H18=115.5224 C8-C7-H18=117.6738
C1-C2-H19=120.2226 C3-C2-H19=119.9512 C8-C9-H20=120.1469
C10-C9-H20=118.5486 C12-C13-H21=117.8889 C5-C6-H22=119.8952
C9-C10-H23=119.969 C11-C10-H23=119.7597 C11-C12-H24=119.8304
C13-C12-H24=119.7482 C1-N14-H25=119.0479 C1-N14-H26=119.0349
H25-N14-H26=121.9172

Stoichiometry C13H11N2(2)
Framework group C1[X(C13H11N2)]

Deg. of freedom 72
Full point group C1 NOp 1
Largest Abelian subgroup C1 NOp 1
Largest concise Abelian subgroup C1 NOp 1
Standard orientation:

Center Number	Atomic Number	Atomic Type	Coordinates (Angstroms) X	Y	Z
1	6	0	3.754359	-0.392524	-0.019979
2	6	0	3.476963	0.883891	-0.538960
3	6	0	2.185452	1.401517	-0.453156
4	6	0	1.141672	0.651431	0.113888
5	6	0	1.443222	-0.596936	0.680763
6	6	0	2.730992	-1.126141	0.600954
7	6	0	-0.192573	1.263673	0.233316
8	6	0	-1.395427	0.634357	0.096960
9	6	0	-2.626206	1.399136	0.333030
10	6	0	-3.843494	0.816920	0.241932
11	6	0	-3.960301	-0.592879	-0.126394
12	6	0	-2.748318	-1.335536	-0.470253
13	6	0	-1.534892	-0.745654	-0.376101
14	7	0	5.040543	-0.911868	-0.096746
15	7	0	-5.111818	-1.162067	-0.188974
16	1	0	1.989178	2.412194	-0.848574
17	1	0	0.676462	-1.162401	1.235164
18	1	0	-0.201594	2.349747	0.428661
19	1	0	4.278544	1.479772	-1.003542
20	1	0	-2.571445	2.465481	0.606812
21	1	0	-0.656546	-1.319432	-0.707805
22	1	0	2.950119	-2.109210	1.050276
23	1	0	-4.752565	1.407744	0.439926
24	1	0	-2.826567	-2.369399	-0.846755
25	1	0	5.231270	-1.862080	0.305899
26	1	0	5.793376	-0.342395	-0.556021

Rotational constants (GHZ): 2.0462076 0.2557983 0.2338403
Isotopes: C-12,C-12,C-12,C-12,C-12,C-12,C-12,C-12,C-12,C-12,C-12,C-12,N-14,
N-14,H-1,H-1,H-1,H-1,H-1,H-1,H-1,H-1,H-1,H-1,H-1
Standard basis: 6-31G(d) (6D, 7F)
There are 247 symmetry adapted basis functions of A symmetry.
Crude estimate of integral set expansion from redundant integrals=1.000.
Integral buffers will be 262144 words long.
Raffenetti 2 integral format.
Two-electron integral symmetry is turned on.
247 basis functions 464 primitive gaussians
52 alpha electrons 51 beta electrons
nuclear repulsion energy 835.2774756736 Hartrees.
One-electron integrals computed using PRISM.
NBasis= 247 RedAO= T NBF= 247

```
NBsUse=   247 1.00D-04 NBFU=   247
Projected INDO Guess
<S**2> of initial guess= 1.1820
Warning!  Cutoffs for single-point calculations used.
Requested convergence on RMS density matrix=1.00D-04 within  64 cycles.
Requested convergence on MAX density matrix=1.00D-02.
Requested convergence on                energy=5.00D-05.
Convergence on energy, delta-E=2.86D-06
SCF Done:  E(UHF) =  -607.551860555     A.U. after   14 cycles
           Conv =    0.1044D-03          -V/T =  2.0018
           S**2 =    2.6452
Annihilation of the first spin contaminant:
S**2 before annihilation    2.6452,  after    6.0165
```

5. Output for intermediate 2

```
----------
# HF/6-31G*
--------------------
Symbolic Z-matrix:
Charge =  0 Multiplicity = 1
C
C              1    1.40383
C              2    1.3953   1    119.92409
C              3    1.40162  2    120.89587  1     0.09554  0
C              4    1.39925  3    118.67693  2    -0.13094  0
C              5    1.39501  4    121.0743   3     0.071    0
C              4    1.51113  3    121.12057  2   -179.58703  0
C              7    1.50968  4    109.98368  3    110.39918  0
C              8    1.40165  7    121.16331  4    110.84026  0
C              9    1.39527  8    120.94525  7   -179.65004  0
C              10   1.4032   9    119.93814  8     0.17685  0
C              11   1.40289  10   119.58048  9    -0.03743  0
C              12   1.39506  11   119.86973  10   -0.09784  0
N              1    1.39193  2    120.12984  3    179.88748  0
N              11   1.39158  10   120.20621  9     179.8509  0
H              3    1.10103  2    119.11441  1   -179.61607  0
H              5    1.10276  4    119.67169  3   -179.72334  0
H              7    1.11468  4    111.40961  3   -10.47765  0
H              7    1.11323  4    108.88399  3   -127.18514  0
H              2    1.10239  1    120.18688  14    0.02525  0
H              9    1.10142  8    119.97949  7     0.16792  0
H              13   1.10249  12   119.30426  11    179.83569  0
H              12   1.10204  11   120.23718  10    179.84327  0
H              6    1.10266  5    119.91031  4   -179.8169  0
H              10   1.10201  9    119.89405  8    179.95325  0
H              14   1.04995  1    118.97793  2   -179.9161  0
H              14   1.04896  1    119.06839  2     0.12187  0
```

H 15 1.04952 11 119.0302 10 -179.95341 0
H 15 1.04973 11 119.03136 10 0.11323 0

Z-MATRIX (ANGSTROMS AND DEGREES)

CD	Cent	Atom	N1	Length/X	N2	Alpha/Y	N3	Beta/Z	J
1	1	C							
2	2	C	1	1.403827(1)					
3	3	C	2	1.395298(2)	1	119.924(29)			
4	4	C	3	1.401620(3)	2	120.896(30)	1	0.096(56)	0
5	5	C	4	1.399246(4)	3	118.677(31)	2	-0.131(57)	0
6	6	C	5	1.395012(5)	4	121.074(32)	3	0.071(58)	0
7	7	C	4	1.511126(6)	3	121.121(33)	2	-179.587(59)	0
8	8	C	7	1.509679(7)	4	109.984(34)	3	110.399(60)	0
9	9	C	8	1.401649(8)	7	121.163(35)	4	110.840(61)	0
10	10	C	9	1.395273(9)	8	120.945(36)	7	-179.650(62)	0
11	11	C	10	1.403197(10)	9	119.938(37)	8	0.177(63)	0
12	12	C	11	1.402893(11)	10	119.580(38)	9	-0.037(64)	0
13	13	C	12	1.395063(12)	11	119.870(39)	10	-0.098(65)	0
14	14	N	1	1.391930(13)	2	120.130(40)	3	179.887(66)	0
15	15	N	11	1.391578(14)	10	120.206(41)	9	179.851(67)	0
16	16	H	3	1.101034(15)	2	119.114(42)	1	-179.616(68)	0
17	17	H	5	1.102758(16)	4	119.672(43)	3	-179.723(69)	0
18	18	H	7	1.114683(17)	4	111.410(44)	3	-10.478(70)	0
19	19	H	7	1.113232(18)	4	108.884(45)	3	-127.185(71)	0
20	20	H	2	1.102389(19)	1	120.187(46)	14	0.025(72)	0
21	21	H	9	1.101418(20)	8	119.979(47)	7	0.168(73)	0
22	22	H	13	1.102486(21)	12	119.304(48)	11	179.836(74)	0
23	23	H	12	1.102044(22)	11	120.237(49)	10	179.843(75)	0
24	24	H	6	1.102658(23)	5	119.910(50)	4	-179.817(76)	0
25	25	H	10	1.102009(24)	9	119.894(51)	8	179.953(77)	0
26	26	H	14	1.049951(25)	1	118.978(52)	2	-179.916(78)	0
27	27	H	14	1.048957(26)	1	119.068(53)	2	0.122(79)	0
28	28	H	15	1.049521(27)	11	119.030(54)	10	-179.953(80)	0
29	29	H	15	1.049733(28)	11	119.031(55)	10	0.113(81)	0

Z-Matrix orientation:

Center Number	Atomic Number	Atomic Type	Coordinates (Angstroms) X	Y	Z
1	6	0	0.000000	0.000000	0.000000
2	6	0	0.000000	0.000000	1.403827
3	6	0	1.209287	0.000000	2.099874
4	6	0	2.433029	0.002006	1.416508
5	6	0	2.420746	0.001212	0.017316
6	6	0	1.219645	-0.000035	-0.692201
7	6	0	3.745640	-0.007309	2.165152
8	6	0	4.435247	-1.337582	1.980911

9	6	0	5.611658	-1.446425	1.226703
10	6	0	6.241289	-2.679430	1.053355
11	6	0	5.694315	-3.833040	1.635561
12	6	0	4.515567	-3.735751	2.390013
13	6	0	3.898179	-2.495998	2.557482
14	7	0	-1.203864	-0.002364	-0.698695
15	7	0	6.315955	-5.066129	1.463675
16	1	0	1.193739	-0.006446	3.200780
17	1	0	3.374073	-0.001864	-0.536970
18	1	0	3.594000	0.173394	3.254588
19	1	0	4.376272	0.833036	1.797171
20	1	0	-0.952891	-0.002291	1.958132
21	1	0	6.050053	-0.551052	0.758472
22	1	0	2.970699	-2.430698	3.149927
23	1	0	4.075193	-4.635226	2.849922
24	1	0	1.232365	-0.003699	-1.794779
25	1	0	7.165168	-2.745226	0.456243
26	1	0	-1.182755	-0.003668	-1.748433
27	1	0	-2.104861	-0.002183	-0.161558
28	1	0	5.890504	-5.917131	1.906710
29	1	0	7.197189	-5.117581	0.895592

Distance matrix (angstroms):

		1	2	3	4	5
1	C	0.000000				
2	C	1.403827	0.000000			
3	C	2.423189	1.395298	0.000000		
4	C	2.815338	2.433063	1.401620	0.000000	
5	C	2.420808	2.789699	2.409291	1.399246	0.000000
6	C	1.402382	2.425050	2.792094	2.432891	1.395012
7	C	4.326402	3.822236	2.537204	1.511126	2.523612
8	C	5.038308	4.668358	3.494295	2.474252	3.115492
9	C	5.923483	5.797777	4.715447	3.498236	3.706776
10	C	6.873325	6.801167	5.796171	4.671704	4.780771
11	C	7.056378	6.868123	5.918045	5.039002	5.294946
12	C	6.329166	5.942957	4.997150	4.388109	4.897230
13	C	5.288338	4.770401	3.697236	3.112637	3.856334
14	N	1.391930	2.422786	3.695307	4.207267	3.694656
15	N	8.227957	8.096945	7.221389	6.384772	6.553056
16	H	3.416145	2.157335	1.101034	2.172450	3.411751
17	H	3.416534	3.892437	3.411634	2.168330	1.102758
18	H	4.851725	4.046259	2.655237	2.180771	3.447622
19	H	4.803699	4.472183	3.288673	2.147489	2.771984
20	H	2.177680	1.102389	2.166820	3.428969	3.892069
21	H	6.122261	6.109278	5.053319	3.717761	3.745154
22	H	4.965419	4.216895	3.180169	3.035107	4.003734
23	H	6.798130	6.339062	5.501028	5.123992	5.679560
24	H	2.177147	3.427801	3.894724	3.428410	2.167017
25	H	7.686615	7.731353	6.760940	5.555405	5.499556
26	H	2.110910	3.366848	4.531153	4.805286	4.012868

27	H	2.111053	2.623142	4.012188	4.804451	4.529141
28	H	8.564229	8.364411	7.547420	6.872453	7.115885
29	H	8.876443	8.845760	7.968369	7.012756	7.056048

		6	7	8	9	10
6	C	0.000000				
7	C	3.813813	0.000000			
8	C	4.390291	1.509679	0.000000		
9	C	5.006397	2.536487	1.401649	0.000000	
10	C	5.953405	3.821595	2.433661	1.395273	0.000000
11	C	6.335066	4.325970	2.816350	2.422794	1.403197
12	C	5.858218	3.813743	2.434138	2.792082	2.424992
13	C	4.895387	2.524038	1.401001	2.410101	2.790379
14	N	2.423519	5.718324	6.384565	7.227988	8.103497
15	N	7.502364	5.717539	4.207927	3.695192	2.422864
16	H	3.893072	2.754038	3.710442	5.048616	6.101971
17	H	2.160013	2.727555	3.041375	3.194383	4.233134
18	H	4.609205	1.114683	2.147789	3.287411	4.471260
19	H	4.105517	1.113232	2.179180	2.654723	4.045858
20	H	3.426979	4.703092	5.551176	6.761199	7.729290
21	H	5.073550	2.754038	2.172691	1.101418	2.157201
22	H	4.871987	2.728210	2.169424	3.412074	3.892846
23	H	6.495058	4.689897	3.429179	3.894101	3.427064
24	H	1.102658	4.690162	5.127722	5.512623	6.353009
25	H	6.648627	4.702099	3.429073	2.166538	1.102009
26	H	2.624340	6.293269	6.873811	7.556257	8.374135
27	H	3.366589	6.296186	7.010454	7.972312	8.848835
28	H	7.973913	6.292316	4.805783	4.530715	3.366597
29	H	8.027540	6.296019	4.805688	4.012597	2.623588

		11	12	13	14	15
11	C	0.000000				
12	C	1.402893	0.000000			
13	C	2.421512	1.395063	0.000000		
14	N	8.228469	7.496011	6.546124	0.000000	
15	N	1.391578	2.422685	3.694269	9.320152	0.000000
16	H	6.111294	5.059605	3.731716	4.577600	7.406418
17	H	4.978084	4.879769	4.008868	4.580792	6.189024
18	H	4.804589	4.108307	2.775632	6.219231	6.170008
19	H	4.851352	4.609195	3.448060	6.169696	6.218821
20	H	7.678804	6.635456	5.487320	2.668655	8.872601
21	H	3.415739	3.893440	3.413182	7.419145	4.577546
22	H	3.417302	2.160383	1.102486	6.175408	4.580358
23	H	2.177092	1.102044	2.166368	7.869214	2.669901
24	H	6.807354	6.497700	5.679815	2.671445	7.879631
25	H	2.176589	3.426513	3.892369	8.882447	2.668834
26	H	8.567939	7.970323	7.111153	1.049951	9.600874
27	H	8.873118	8.017487	7.046189	1.048957	9.959671
28	H	2.110794	2.623443	4.012109	9.597013	1.049521
29	H	2.110979	3.366578	4.529685	9.964180	1.049733

		16	17	18	19	20
16	H	0.000000				

17	H	4.327199	0.000000			
18	H	2.407590	3.801972	0.000000		
19	H	3.578179	2.673888	1.780770	0.000000	
20	H	2.480365	4.994813	4.731372	5.396634	0.000000
21	H	5.463081	3.023350	3.575977	2.407517	7.126117
22	H	3.006188	4.433413	2.679692	3.802308	4.765720
23	H	5.463651	5.781924	4.849549	5.576811	6.894998
24	H	4.995709	2.483747	5.577166	4.846274	4.342775
25	H	7.119787	4.783817	5.394656	4.730749	8.699555
26	H	5.490213	4.715116	6.919461	6.646364	3.713686
27	H	4.710211	5.491780	6.646645	6.821971	2.412493
28	H	7.659662	6.877091	6.647195	6.918790	9.045443
29	H	8.214561	6.545152	6.822188	6.646824	9.680857

		21	22	23	24	25
21	H	0.000000				
22	H	4.328342	0.000000			
23	H	4.995469	2.483919	0.000000		
24	H	5.479854	5.776006	7.148843	0.000000	
25	H	2.479762	4.994841	4.341630	6.912396	0.000000
26	H	7.674484	6.865535	8.381062	2.415565	9.058948
27	H	8.224982	6.528776	8.290184	3.715440	9.687073
28	H	5.489873	4.714454	2.414184	8.388561	3.713436
29	H	4.710404	5.492230	3.714692	8.304758	2.412908

		26	27	28	29
26	H	0.000000			
27	H	1.835335	0.000000		
28	H	9.917666	10.158258	0.000000	
29	H	10.166928	10.668317	1.835502	0.000000

Interatomic angles:

C1-C2-C3=119.9241 C2-C3-C4=120.8959 C3-C4-C5=118.6769
C4-C5-C6=121.0743 C3-C4-C7=121.1206 C5-C4-C7=120.2003
C4-C7-C8=109.9837 C7-C8-C9=121.1633 C8-C9-C10=120.9453
C9-C10-C11=119.9381 C10-C11-C12=119.5805 C11-C12-C13=119.8697
C2-C1-N14=120.1298 C10-C11-N15=120.2062 C12-C11-N15=120.2132
C2-C3-H16=119.1144 C4-C3-H16=119.9891 C4-C5-H17=119.6717
C6-C5-H17=119.2537 C4-C7-H18=111.4096 C8-C7-H18=108.9209
C4-C7-H19=108.884 C8-C7-H19=111.4726 H18-C7-H19=106.1264
C1-C2-H20=120.1869 C3-C2-H20=119.8889 C8-C9-H21=119.9795
C10-C9-H21=119.075 C12-C13-H22=119.3043 C11-C12-H23=120.2372
C13-C12-H23=119.8931 C5-C6-H24=119.9103 C9-C10-H25=119.8941
C11-C10-H25=120.1674 C1-N14-H26=118.9779 C1-N14-H27=119.0684
H26-N14-H27=121.9537 C11-N15-H28=119.0302 C11-N15-H29=119.0314
H28-N15-H29=121.9384

Stoichiometry C13H14N2
Framework group C1[X(C13H14N2)]
Deg. of freedom 81
Full point group C1 NOp 1
Largest Abelian subgroup C1 NOp 1
Largest concise Abelian subgroup C1 NOp 1

Standard orientation:

Center Number	Atomic Number	Atomic Type	Coordinates (Angstroms) X	Y	Z
1	6	0	-3.526924	-0.666723	-0.104921
2	6	0	-3.231785	0.070149	1.052941
3	6	0	-2.094779	0.877906	1.092965
4	6	0	-1.237006	0.968435	-0.011829
5	6	0	-1.540809	0.228892	-1.160162
6	6	0	-2.673276	-0.583899	-1.214471
7	6	0	0.000673	1.834441	0.029233
8	6	0	1.236651	0.967656	0.042432
9	6	0	2.099899	0.918495	-1.060748
10	6	0	3.237135	0.110241	-1.046423
11	6	0	3.526959	-0.670847	0.082677
12	6	0	2.668013	-0.631292	1.191169
13	6	0	1.535970	0.183542	1.164205
14	7	0	-4.658783	-1.475702	-0.148689
15	7	0	4.658001	-1.481321	0.101766
16	1	0	-1.872624	1.445132	2.010122
17	1	0	-0.874717	0.284342	-2.037272
18	1	0	0.009073	2.489688	0.930953
19	1	0	-0.008435	2.517826	-0.849509
20	1	0	-3.894653	0.010743	1.931769
21	1	0	1.882870	1.521222	-1.956705
22	1	0	0.865874	0.205398	2.039402
23	1	0	2.883859	-1.242264	2.082586
24	1	0	-2.892705	-1.160807	-2.128190
25	1	0	3.903564	0.084237	-1.923703
26	1	0	-4.861489	-2.019991	-1.023364
27	1	0	-5.284066	-1.523235	0.692188
28	1	0	4.856663	-2.058439	0.955560
29	1	0	5.287945	-1.496666	-0.737802

Rotational constants (GHZ): 1.4162000 0.2736057 0.2680968
Isotopes: C-12,C-12,C-12,C-12,C-12,C-12,C-12,C-12,C-12,C-12,C-12,C-12,N-14,
N-14,H-1,H-1,H-1,H-1,H-1,H-1,H-1,H-1,H-1,H-1,H-1,H-1,H-1
Standard basis: 6-31G(d) (6D, 7F)
There are 253 symmetry adapted basis functions of A symmetry.
Crude estimate of integral set expansion from redundant integrals=1.000.
Integral buffers will be 262144 words long.
Raffenetti 1 integral format.
Two-electron integral symmetry is turned on.
253 basis functions 476 primitive gaussians
53 alpha electrons 53 beta electrons
nuclear repulsion energy 888.1524672184 Hartrees.
One-electron integrals computed using PRISM.
NBasis= 253 RedAO= T NBF= 253
NBsUse= 253 1.00D-04 NBFU= 253
Projected INDO Guess.

Warning! Cutoffs for single-point calculations used.
Requested convergence on RMS density matrix=1.00D-04 within 64 cycles.
Requested convergence on MAX density matrix=1.00D-02.
Requested convergence on energy=5.00D-05.
SCF Done: E(RHF) = -609.310584822 A.U. after 6 cycles
Convg = 0.2016D-04 -V/T = 2.0029
S**2 = 0.0000

الملخص العربي

الملخص العربي

تحتل الألوان الصناعية مكانه هامة في حياتنا المعاصرة ، فهي تدخل في أغلب الصناعات الحديثة إلى جانب الغذائية منها. نتيجة لذلك أصبحت الملونات الصبغيه المصاحبة لعمليات التصنيع ، والناتجة بكميات ضخمه تشكل عبئا كبيرا على البيئة الطبيعية، وذلك عند التخلص منها بالطرق التقليدية كطرحها في مجاري المياه والأنهار. بناء على ما سبق, تركز البحث العلمي في مجال البيئة إلى كيفية التوصل لأفضل الطرق العملية لمعالجة المحاليل الملوثة بالأصباغ وذلك في مواقع استخدامها بغرض إعادة استخدام المحاليل الحاوية لها مرة أخرى أو تخفيض درجة السمية لمستوى يسمح بطرحها إلى البيئة الطبيعية دون ضرر سيلحق بها أو بمحيطها الحيوي لاحقا.

تتنوع طرق المعالجات الصبغيه وذلك نظرا لاختلاف الخواص الطبيعة والكيميائية للأصباغ المستعملة في الصناعة و يمكن تقسيم الصبغات الرئيسية إلى ستة أنواع هي: الحامضيه والقاعدية والمباشرة والفعالة والمنتشرة وأخيرا صبغات المعقدات المعدنية . وباختلاف هذه الأنواع تختلف أيضا طرق معالجة المحاليل أو المياه الملوثة التي تحويها، ولهذا فهناك ثلاث أساليب شائعة لمعالجتها . هذه الأساليب هي المعالجة الطبيعية والكهروكيميائيه والكيميائية الصرفة .

تندرج طريقة استخدام فوق أكسيد الهيدروجين تحت المعالجة الكيميائية الصرفة ، وهي طريقة تتميز بفعاليتها في التخلص الآمن من الصبغات إضافة وذلك بتحويلها إلى عناصر غير ضاره بالبيئة.

في هذه الرسالة تمت دراسة تأثير استخدام فوق أكسيد الهيدروجين في التخلص الآمن من نوعين شائعين من الصبغات الصناعية هما (الثايونين وأزرق الميثايل) وذلك عن طرقة تفسير آلية التفاعلات الكيميائية الحاصلة من ناحية و تحليل نواتج هذه التفاعلات من ناحية أخرى. تمت دراسة تأثير استخدام فوق أكسيد الهيدروجين وذلك في حالتين هما أولا: عند استخدام محلول فوق أكسيد الهيدروجين النقي وثانيا : عند استخدام محلول فوق أكسيد الهيدروجين بوجود عامل حفاز هو أيون النحاس الثنائي .

وفي ما يلي عرض موجز لمحتويات هذه الرسالة :

1. الفصل الأول ويتضمن مقدمة تشرح أنواع الصبغات المستخدمة في الصناعة والطرق المختلفة للتخلص من ملوثاتها وآخر ما تم إنجازه من بحوث بهذا الشأن .
2. الفصل الثاني ويحوي القسم التجريبي حيث يتضمن وصفا للأجهزة المستخدمة وطرق تحضير المحاليل القياسية المختلفة والمحاليل المنظمة ، كما يتضمن وصفا لطرق إجراء التجارب العملية والقياسات المتعلقة بها .
3. الفصل الثالث ويحتوي مناقشة النتائج المتحصل عليها من الجزء العملي .

ويمكن تلخيص ما جاء في هذا الفصل كما يلي :

1 . يمكن تسريع تفاعل أكسدة الصبغة مع اختفاء اللون بفعل فوق أكسيد الهيدروجين بشكل كبير عن طريق إضافة أيونات النحاس كمادة محفزة وذلك نتيجة لتولد الجذور الحرة النشطة في وسط التفاعل ، والتي تتولد من تفاعل فوق أكسيد الهيدروجين مع أيونات النحاس, حيث تم إثبات ذلك باستخدام عامل ماص للجذور الحرة .

2 . تمت دراسة تأثير تركيزات المتفاعلات وظروف التفاعل من حيث درجة الحرارة وتغير المحاليل المنظمة وذلك بتثبيت جميع العوامل الأخرى عدا العامل المدروس .

3 . تبين من دراسة تأثير هذه العوامل على تفاعل الأكسدة ما يلي :

أ) **تأثير تركيز فوق أكسيد الهيدروجين:** تتزايد سرعة التفاعل طرديا مع ازدياد تركيزات فوق أكسيد الهيدروجين حتى تصل سرعة التفاعل لقيمتها العظمى عند التراكيز العالية أي أن رتبة التفاعل تتغير من الرتبة الأولى إلى الرتبة الصفرية عند التركيزات العالية لفوق أكسيد الهيدروجين. أما في وجود أيونات النحاس كعامل محفز في وسط التفاعل فان سرعة التفاعل تتزايد إلى قيمتها العظمى ثم تبدأ بالتناقص ويفسر ذلك بتولد مركبات وسطية معيقة لسير التفاعل الأساسي ناتجة عن تفاعل كاتيونات النحاس مع فوق أكسيد الهيدروجين . وبمقارنة التفاعلين فان سرعة التفاعل بوجود عامل التحفيز أعلى بكثير عنه في حالة غيابه لكلا الصبغتين .

ب) **تأثير تركيز الصبغات** : التفاعل من الرتبة الأولى ويتناسب طرديا مع زيادة تركيز كلا الصبغتين وفي حالة ازرق الميثايل فان التركيز العالي يخفض سير التفاعل . كما يصعب دراسة تأثير التركيزات العالية من الثايونين لارتفاع قيمة معامل الامتصاص لها.

ج) **تأثير تركيز أيون النحاس كمحفز** : تزداد سرعة تفاعل الأكسدة لكلا الصبغتين حتى تصل إلى قيمها العظمى ثم تبدأ بالانخفاض في حالة التركيزات العالية ويفسر ذلك بتولد مركبات وسطية معيقة لسير التفاعل الأساسي.

د) **تأثير الرقم الهيدروجيني** : تزداد معدل سرعة تفاعل الأكسدة مع ازدياد الرقم الهيدروجيني لكلا الصبغتين وخاصة في مدى القيم من (9-11) , ويمكن تعليل هذا السلوك بأن الشكل القاعدي لفوق أكسيد الهيدروجين -HOO , والجزء الكاتيوني للصبغة هما طرفي التفاعل.

ه) **تأثير القوى الأيونيه** : تم استخدام تراكيز متدرجة لمحاليل كلوريد الصوديوم مع تثبيت تراكيز المواد المتفاعلة والرقم الهيدروجيني وذلك لدراسة طبيعة الشحنات على الجزيئات المتفاعلة التي بينت ا لدراسة أن هناك تفاعل بين أيونين مختلفين في الشحنة وهذا ما يفسر زيادة سرعة التفاعل مع زيادة الرقم الهيدروجيني .

و) **تأثير SDS (موادالتصبن)** : تمت دراسة تأثير تراكيز متدرجة من SDS على سرعة تفاعل أكسدة للثايونين فوجد أن معدل سرعة التفاعل تبدأ بالانخفاض حتى قبل الوصول إلى التركيز الحرج للأيون الغروي والتي بعدها ينخفض معدل التفاعل بشكل كبير . وهذا يفسر بالاعاقه التي توجدها مادة SDS بين الجزيئات المتفاعلة .

لقداستخدمت طرق تحليلية مختلفة وذلك لأجل التعرف على نواتج تفاعل أكسدة الصبغتين بفعل فوق أكسيد الهيدروجين. فقد تم إجراء تحليل عنصري لعناصر(C N S H) و دراسة طيف الأشعة تحت الحمراء إضافة إلى HPLC.

ولقد دل التحليل العنصري للصبغتين وهما في الحالة النقية ولنواتج تفاعلهما مع فوق أكسيد الهيدروجين على وجود تطابق عالي بين النتائج المحسوبة نظريا والمتحصل عليها عمليا وذلك

لكلا الصبغتين. أما في ما يخص التحليل العنصري لنواتج أكسدة الصبغتين فقد وجد انه فى حالة صبغة أزرق الميثايل فان النتائج النظرية والعملية جدا متقاربة بما يفسر بتكسر كامل للصبغة أو تشكل نواتج لها نفس الشكل التركيبي للصبغة الأصلية. أما في حالة الثايونين فان التطابق بين النتائج المحسوبة نظريا والمتحصل عليها عمليا للمواد الناتجة ليس كبيرا مما يفسر على عدم حصول تكسير كامل للصبغة أو تشكل أكثر من مركب واحد لتفاعل الأكسدة.

كما بين تحليل الأشعة تحت الحمراء على ظهور قمة عند $1640cm^{-1}$ تعبر عن تردد امتطاطي لمجموعة C=O مما يدلل على نواتج أكسدة كلا الصبغتين حاوية لمجموعة الكربونيل. كما بين تحليل HPLC لنواتج تفاعل الأكسدة لكلا الصبغتين على وجود ناتجين أساسيين لتفاعل أكسدة الثايونين عند التردد 304nm وثلاثة نواتج لأزرق الميثيل عند نفس التردد.

ونظرا لصعوبة فصل نواتج تفاعلات الأكسدة الناتجة فقد تم الاستعانة بالحاسب الآلي وذلك بغرض استخدام الطرق الحسابية لتوقع أفضل مسارات تفاعلات الأكسدة على الصبغات من حيث الطاقة و من ثم توقع نواتج تفاعلات الأكسدة نظريا. ولقد تنبأت هذه الحسابات النظرية باحتمالية تكون أربعة نواتج أكسدة لكلا الصبغتين.

بسم الله الرحمن الرحيم

جامعة الإمارات العربية المتحدة
كلية العلوم
قسم الكيمياء

عنوان الرسالة دراسات حركية وتحليلية على الأكسدة التكسيرية الحفزية و غير الحفزية لبعض الصبغات العضوية باستخدام فوق أكسيد الهيدروجين.

.

اسم الطالب : سالم حمود سالم العامري .

لجنة الإشراف

الاسم	الوظيفة	التوقيع
المشرف الرئيس د . علاء الدين سالم	أستاذ مشارك الكيمياء التحليلية قسم الكيمياء كلية العلوم جامعة الإمارات العربية المتحدة	.....
المشرفون المساعدون د . إبراهيم سالم	أستاذ مشارك الكيمياء الفيزيانية قسم الكيمياء كلية العلوم جامعة الإمارات العربية المتحدة	.....
د . إحسان شحادة	أستاذ مساعد الكيمياء الفيزيانية قسم الكيمياء كلية العلوم جامعة الإمارات العربية المتحدة	.....

جامعة الإمارات العربية المتحدة
كلية العلوم

دراسات حركية وتحليلية على الأكسدة التكسيرية الحفزية وغير الحفزية لبعض الصبغات العضوية باستخدام فوق أكسيد الهيدروجين

رسالة مقدمة من الطالب

سالم حمود سالم العامري

بكالوريوس في العلوم تخصص كيمياء / فيزياء
كلية العلوم – جامعة الإمارات العربية المتحدة

استكمالا لمتطلبات الحصول على درجة الماجستير في العلوم
(علوم البيئة)

جامعة الإمارات العربية المتحدة

سبتمبر 2003